# Stellar Interior

- A star has a stable configuration.

  ✓ That is, there is a certain structure (mass distribution) to allow for such a force balance.

  Inward = gravity
  Outward = gas pressure (gradient)
  $\qquad$ (ideal gas, degenerate electron/neutron gas)
  $\qquad$ + magnetic pressure ($P_{\mathrm{mag}} = B^2/8\pi$)
  $\qquad$ + radiation pressure ($P_{\mathrm{rad}} = 4\sigma T^4/3c$)
  $\qquad$ + turbulence pressure ($P_{\mathrm{tur}} = \rho\, v^2/2$)

- How is the pressure sustained?  Energy→ thermal pressure

  ✓ How is the energy generated?
  ✓ How is the energy transported?

# Structure Equations

$$\frac{dm(r)}{dr} = 4\pi r^2 \rho(r)$$ Mass continuity (distribution)

$$\frac{dP(r)}{dr} = -\frac{G\,m(r)\rho(r)}{r^2}$$ Hydrostatic equilibrium

$$\frac{dL(r)}{dr} = 4\pi r^2 \rho(r)\,q(r)$$ Energy conservation

$$\frac{dT(r)}{dr} = -\frac{3\kappa\rho L(r)}{4ac\,4\pi r^2 T^3}$$ by radiation

Energy transport

$$\frac{dT(r)}{dr} = \frac{\gamma-1}{\gamma}\frac{T}{P}\frac{dP(r)}{dr}$$ by convection

$$P = P(\rho, T, \mu)$$

Equation of state

$$\kappa = \kappa(\rho, T, \mu)$$

Opacity

$$q = q(\rho, T, \mu)$$

Nuclear reaction rate

Boundary conditions: $m(r) \to 0$ and $L(r) \to 0$ as $r \to 0$
$T(r) \to 0$, $P(r) \to 0$, and $\rho(r) \to 0$ as $r \to R_*$

*Variables:* $m, r, \rho, T, P, \kappa, L, \mu,$ *and* $q$

## Vogt-Russell "theorem"

Given hydrostatic and thermal equilibrium with energy produced by nuclear reactions, the internal structure of a star, and its subsequent evolution, is uniquely determined by the mass and chemical composition of the star.

In fact, … <u>by any two variables</u> above (e.g., $L$ and $T_{\text{eff}}$ give the HRD. It is not really a "theorem" in the mathematical sense, i.e., not strictly valid. It is a "rule of thumb". There are other factors, too, such as magnetic field or rotation, though these usually have little effect.

# Hydrostatic equilibrium
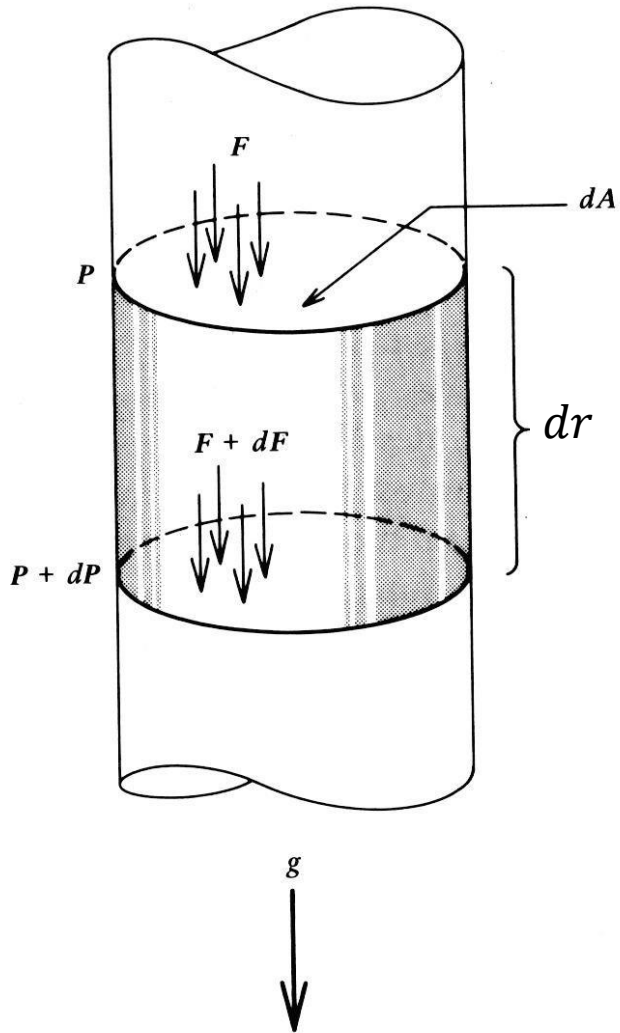


In general, the equation of motion is

$$\ddot{r} = -\frac{Gm}{r^2} - \frac{1}{\rho}\frac{\partial P}{\partial r} = -\frac{Gm}{r^2} - 4\pi r^2 \frac{\partial P}{\partial m}$$

The LHS is usually null, unless there is free fall or explosion.

$$\text{Force} = \text{mass} \cdot \text{acceleration}$$

$$-dP\,dA = \rho(r)\,dA\,dr \cdot g(r)$$

$$\frac{dP}{dr} = -\rho(r)\,g(r) = -\rho(r)\frac{GM(r)}{r^2}$$

Hydrostatic equilibrium

$$\frac{dP(r)}{dr} = -\frac{G\,m(r)}{r^2}\rho(r) = -g(r)\,\rho(r) \ldots (1)$$

Mass continuity

$$\frac{dm(r)}{dr} = 4\pi r^2 \rho(\mathrm{r}) \ldots (2)$$

- ✓ $m(r)$: total mass inside radius $r$
- ✓ $P_{\text{total}} = P_{\text{gas}} + P_{\text{e}} + P_{\text{rad}} + \ldots$

$(1)/(2)$

$(1) \longrightarrow \dfrac{dP(r)}{dm} = -\dfrac{Gm(r)}{4\pi r^4}$

*Using mass as the independent variable, $r = r(m)$, is preferred because mass is usually given and fixed (but $r$ is not.)*

$(2) \longrightarrow \dfrac{dr}{dm} = \dfrac{1}{4\pi r^2 \rho(r)}$

Boundary conditions (1) at $m = 0, r = 0,$ (2) at $m = M$ or $r = R, P = 0.$

# The set of stellar structure equations then becomes

$$\frac{dP(m)}{dm} = -\frac{G\,m}{4\pi r^4}$$

$$\frac{dr}{dm} = \frac{1}{4\pi r^2\,\rho}$$

$$\frac{dL(m)}{dm} = q(r)$$

$$\frac{dT(m)}{dm} = -\frac{3\kappa L(r)}{4ac\,(4\pi r^2)^2 T^3}$$

$$P = \frac{\rho}{\mu m_H}kT + P_e + \frac{1}{3}\,aT^4$$

$$\kappa = \kappa_0\,\rho^a\,T^b$$

$$q = q_0\,\rho^m\,T^n$$

Prianik

8

A polytropic (thermodynamic) process obeys

$$PV^{\alpha} = \text{const}$$

$\alpha$ is the polytropic index

✓ $\alpha = 0, P = \text{const}$ → isobaric process

For an ideal gas

✓ $\alpha = 1$ → isothermal process

✓ $\alpha = \gamma = c_p/c_v$ → isentropic (= adiabatic and reversible) process

✓ $\alpha \rightarrow \infty$ → isochoric (= isovolumetric) process

Recall that the internal energy $\boxed{u = \frac{n}{2} kT}$, $n$: degree of freedom

The specific heat capacity $c_v = \left(\frac{\partial u}{\partial T}\right)_v = \frac{n}{2} k$,

$$c_p - c_v = k$$

$$\gamma = \frac{c_p}{c_v} = \frac{\frac{n}{2} k + k}{\frac{n}{2} k} = 1 + \frac{2}{n} = \frac{n + 2}{n}$$

For an ideal gas, $n = 3$, so $\gamma = 5/3 \approx 1.66$

For a diatomic gas, $n = 5$, so $\gamma = 7/5 \approx 1.40$

For a photon gas, $n = 6$, so $\gamma = 4/3 \approx 1.33$

From hydrostatic equilibrium and mass distribution,

$$(1) \quad \frac{dP}{dr} = -\frac{G\,m(r)}{r^2}\rho \longrightarrow m(r) = -\frac{r^2}{G\rho}\frac{dP}{dr} \qquad \frac{dm(r)}{dr} = 4\pi r^2 \rho(\mathrm{r})$$

Plug into (2)

$$\frac{d}{dr}\left(-\frac{r^2}{G\rho}\frac{dP}{dr}\right) = 4\pi r^2 \rho$$

Rearrange to yield

$$\frac{1}{r^2}\frac{d}{dr}\left(\frac{r^2}{\rho}\frac{dP}{dr}\right) = -4\pi G\rho \;...\;(3)$$

Cf. the general Laplace eq. and Poisson eq.

## Poisson equation

$\nabla^2 \varphi = f$  (if $f = 0 \to$ **Laplace eq.**)

$$\text{or } \left( \frac{\partial^2}{\partial x^2} + \frac{\partial^2}{\partial y^2} + \frac{\partial^2}{\partial z^2} \right) \varphi(x, y, z) = f(x, y, z)$$

(1) Gravity

$\nabla \cdot \vec{g} = -4\pi G \rho,$ but $\vec{g} = -\nabla\varphi \implies \nabla^2 \varphi = 4\pi G \rho$

Solution $\varphi(r) = -\frac{GM}{r}$ (gravitational potential)

(2) Electrostatics

Gauss's law, $\nabla \cdot \vec{D} = \rho_{\text{free}}, \vec{D} = \epsilon\vec{E}, \vec{E} = -\nabla\varphi, \nabla^2 \varphi = -\rho/\epsilon$

Solution $\varphi(r) = -\frac{Q}{4\pi\varepsilon r}$

Assume a polytrope; i.e., a spherical fluid with $P$ and $\rho$ being related by

$$P \equiv K\rho^{1+\frac{1}{n}} = K(\rho_c\theta^n)^{1+\frac{1}{n}}$$

Then (3) becomes  $\frac{1}{r^2}\frac{d}{dr}\left(\frac{r^2}{\rho}\frac{dP}{dr}\right) = -4\pi G\rho$

$$\frac{1}{r^2}\frac{d}{dr}\left[\frac{r^2}{\rho_c\theta^n}K\rho_c^{1+\frac{1}{n}}(n+1)\theta^n\frac{d\theta}{dr}\right] = -4\pi G\,\rho_c\theta^n$$

After rearranging

$$\left[\underbrace{\frac{n+1}{4\pi G}K\,\rho_c^{\frac{1}{n}-1}}_{\alpha^2}\right]\frac{1}{r^2}\frac{d}{dr}\left(r^2\frac{d\theta}{dr}\right) = -\theta^n$$

Letting $r = \alpha\xi$, we get

$$\frac{1}{\xi^2}\frac{d}{d\xi}\left(\xi^2\frac{d\theta}{d\xi}\right) = -\theta^n$$

... in essence describes how density varies with radius.

This is the **Lane-Emden equation** of index $n$, after J. H. Lane and R. Emden.

Compared to (3), a given $n$
→ a solution with different $K$, and $\rho_0$
→ a family of solutions

The structure of the polytrope depends on $n$.



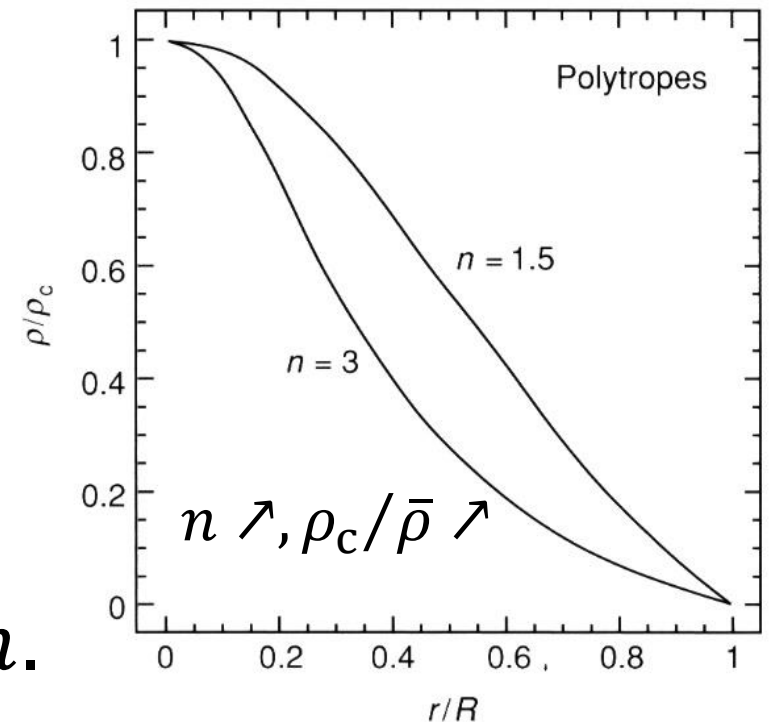$n \nearrow, \rho_c/\bar{\rho} \nearrow$

**Figure 5.1** Normalized polytropes for $n = 1.5$ and $n = 3$.

The Lane-Emden equation has the boundary conditions of $\theta = 1$ and $\frac{d\theta}{d\xi} = 0$ at $\xi = 0$, and can be integrated from $\xi = 0$.

For $n = 0, 1, 5$, analytic solutions are available; otherwise the integration is done numerically.

$$n = 0, \quad \theta_0 = 1 - \xi^2/6 \qquad \theta_0 = 1 - \xi^2/6 = 0 \Longrightarrow \xi_1 = \sqrt{6}$$
$$n = 1, \quad \theta_1 = \sin\xi/\xi \qquad \theta_1 = \sin\xi/\xi = 0 \Longrightarrow \xi_1 = \pi$$
$$n = 5, \quad \theta_5 = (1 + \xi^2/3)^{-1/2} \qquad \theta_5 = (1 + \xi^2/3)^{-1/2} \Longrightarrow \xi_1 = \infty$$

For $n = 0$ and $n = 1$, solution $\to 0$ at some point ($\rho \to 0$); this defines the boundary of the star, i.e., $\xi$ at first zero ($\xi_1$=radius). Solve $\theta_n(\xi_1) = 0$.

For $n = 0$, $\rho = \rho_c\theta^0$ =const; for $n = 5$, solution never goes to 0.
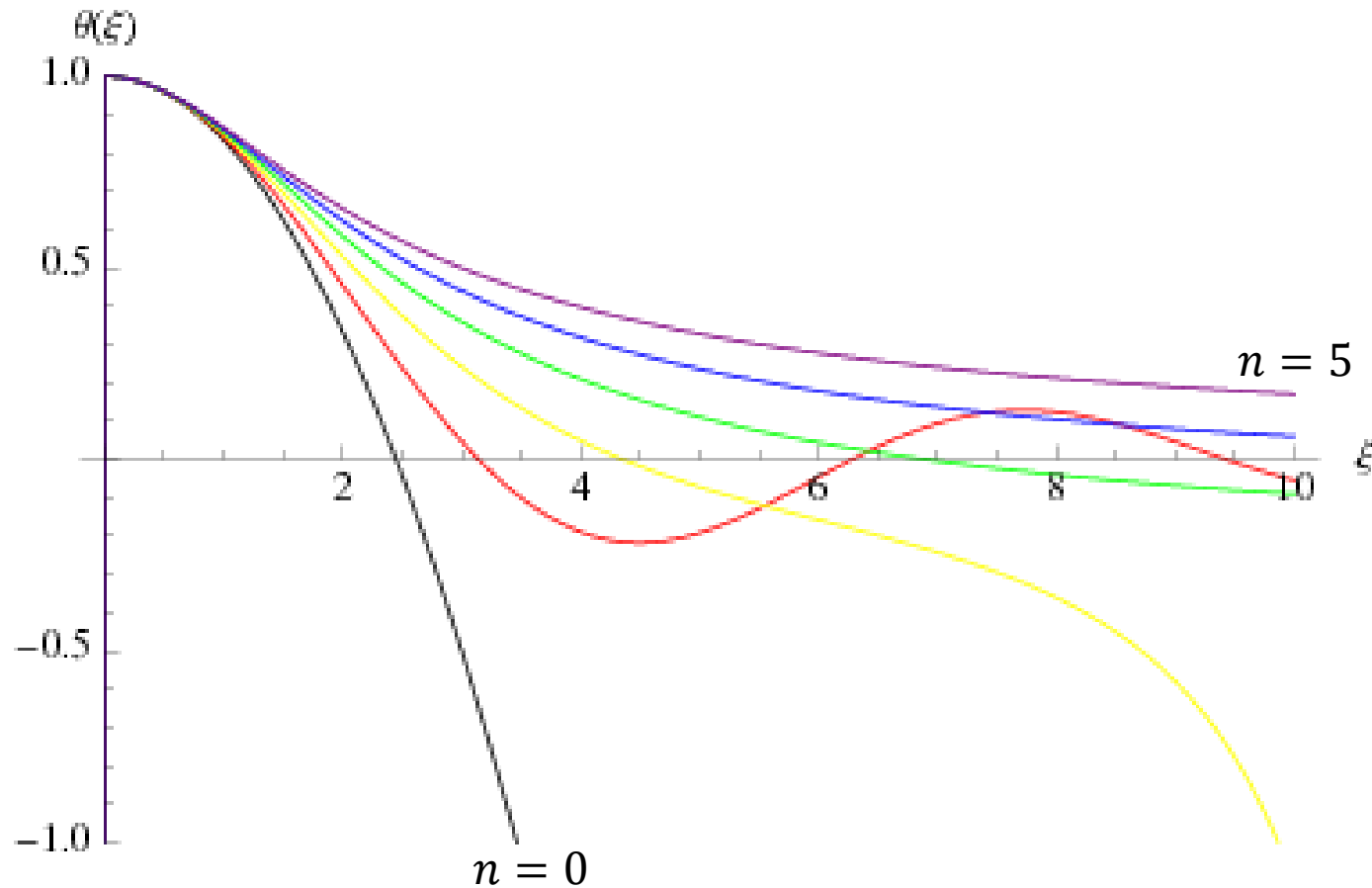
$n = 0$, a constant
density sphere;
$\xi_1 = \sqrt{6}$; $P = P_c\theta$

$n = 1$, solution a
sync function;
$\xi_1 = \pi$; $\rho = \rho_c\theta$; $P = P_c\theta^2$

$n = 5$, finite density, but
infinite radius;
$\xi_1 \rightarrow \infty$

Weisstein, Eric W. "Lane-Emden Differential Equation." From *MathWorld*--A Wolfram Web
Resource. http://mathworld.wolfram.com/Lane-EmdenDifferentialEquation.html

The Lane-Emden equation is integrated often numerically to the first zero. The overall stellar properties can then be computed.

Mass

$$M(\xi) = \int_0^{\alpha\xi} 4\pi\rho r^2 dr = 4\,\pi\alpha^3\rho_c \left[ -\xi^2\,\frac{d\theta}{d\xi} \right]_{\xi=\xi_1}$$

Radius

$$R = \alpha\xi_1$$

Central pressure

$$P_c = \frac{GM^2}{R^4} \left[ 4\,\pi(n+1) \left( \frac{d\theta}{d\xi} \right)_{\xi=\xi_1}^2 \right]^{-1}$$

Mean density

$$\bar{\rho} = \rho_c \left[ -\frac{3}{\xi}\,\frac{d\theta}{d\xi} \right]_{\xi=\xi_1}$$

Bower & Deeming

## Gravitational binding energy

$$\Omega = -\frac{3}{5-n}\frac{GM^2}{R}$$

$$\gamma = \frac{c_p}{c_v} = \frac{\frac{n}{2}k + k}{\frac{n}{2}k} = 1 + \frac{2}{n}$$

For $n = 5$, $\Omega \to -\infty$. For any $n > 5$ (i.e., $\gamma < 6/5$), $\Omega > 0$, the system is not gravitationally bound; no stable configuration

Given a solution $\theta(\xi)$, i.e., $\rho(r)$, the density and pressure profiles can be derived.

# TABLE 4

## THE CONSTANTS OF THE LANE-EMDEN FUNCTIONS*

| $n$ | $\xi_1$ | $-\xi_1^2\left(\dfrac{d\theta_n}{d\xi}\right)_{\xi=\xi_1}$ | $\rho_c/\bar{\rho}$ | $\omega_n = -\xi_1^{\frac{n+1}{n-1}}\left(\dfrac{d\theta_n}{d\xi}\right)_{\xi=\xi_1}$ | $N_n$ | $W_n$ | $-\dfrac{1}{(n+1)\xi_1\left(\frac{d\theta_n}{d\xi}\right)_{\xi=\xi_1}}$ |
|---|---|---|---|---|---|---|---|
| 0 | 2.4494 | 4.8988 | 1.0000 | 0.33333 | ............ | 0.119366 | -0.5 |
| 0.5 | 2.7528 | 3.7871 | 1.8361 | 0.02156 | 2.270 | 0.26227 | 0.53847 |
| 1.0 | 3.14159 | 3.14159 | 3.28987 | ............... | 0.63662 | 0.392699 | 0.5 |
| 1.5 | 3.65375 | 2.71406 | 5.99071 | 132.3843 | 0.42422 | 0.770140 | 0.53849 |
| 2.0 | 4.35287 | 2.41105 | 11.40254 | 10.4950 | 0.36475 | 1.63818 | 0.60180 |
| 2.5 | 5.35528 | 2.18720 | 23.40646 | 3.82662 | 0.35150 | 3.90906 | 0.69956 |
| 3.0 | 6.89685 | 2.01824 | 54.1825 | 2.01824 | 0.36394 | 11.05066 | 0.85432 |
| 3.25 | 8.01894 | 1.94980 | 88.153 | 1.54716 | 0.37898 | 20.365 | 0.96769 |
| 3.5 | 9.53581 | 1.89056 | 152.884 | 1.20426 | 0.40104 | 40.9098 | 1.12087 |
| 4.0 | 14.97155 | 1.79723 | 622.408 | 0.729202 | 0.47720 | 247.558 | 1.66606 |
| 4.5 | 31.83646 | 1.73780 | 6189.47 | 0.394356 | 0.65798 | 4922.125 | 3.33100 |
| 4.9 | 169.47 | 1.7355 | 934800 | 0.14239 | 1.340 | $3.693\times10^6$ | 16.550 |
| 5.0 | $\infty$ | 1.73205 | $\infty$ | 0 | $\infty$ | $\infty$ | $\infty$ |

*The values for $n = 0.5$ and $4.9$ are computed from Emden's integrations of $\theta_n$; for $n = 3.25$ an unpublished integration by Chandrasekhar has been used. $n = 5$ corresponds to the Schuster-Emden integral. For the other values of $n$ the *British Association Tables*, Vol. II, has been used.

$$N_n = \frac{(4\pi)^{1/n}}{n+1}\left[-\xi_1^{\,n+1/n-1}\left(\frac{d\theta}{d\xi}\right)_{\xi=\xi_1}\right]^{1-n}$$

$$W_n = \frac{1}{4\pi(n+1)\left[\left(\frac{d\theta}{d\xi}\right)_{\xi=\xi_1}\right]^{-2}}$$

Chandrasekhar p.96

19

**Table 2-5   Constants of the Lane-Emden functions†**

| $n$ | $\xi_1$ | $-\xi_1{}^2\left(\dfrac{d\phi}{d\xi}\right)_{\xi=\xi_1}$ | $\dfrac{\rho_c}{\bar{\rho}}$ |
|---|---|---|---|
| 0 | 2.4494 | 4.8988 | 1.0000 |
| 0.5 | 2.7528 | 3.7871 | 1.8361 |
| 1.0 | 3.14159 | 3.14159 | 3.28987 |
| 1.5 | 3.65375 | 2.71406 | 5.99071 |
| 2.0 | 4.35287 | 2.41105 | 11.40254 |
| 2.5 | 5.35528 | 2.18720 | 23.40646 |
| 3.0 | 6.89685 | 2.01824 | 54.1825 |
| 3.25 | 8.01894 | 1.94980 | 88.153 |
| 3.5 | 9.53581 | 1.89056 | 152.884 |
| 4.0 | 14.97155 | 1.79723 | 622.408 |
| 4.5 | 31.83646 | 1.73780 | 6,189.47 |
| 4.9 | 169.47 | 1.7355 | 934,800 |
| 5.0 | $\infty$ | 1.73205 | $\infty$ |

The case for $n = 0$, $\rho = \rho_c \theta^0 = $ const.

$$\frac{1}{\xi^2}\frac{d}{d\xi}\left(\xi^2 \frac{d\theta}{d\xi}\right) = -\theta^n$$

$$\frac{d}{d\xi}\left(\xi^2 \frac{d\theta}{d\xi}\right) = -\xi^2$$

$$\xi^2 \frac{d\theta}{d\xi} = -\frac{1}{3}\xi^3 + c_1$$

$$\frac{d\theta}{d\xi} = -\frac{1}{3}\xi + \frac{c_1}{\xi^2}$$

$$\theta = -\frac{1}{6}\xi^2 - \frac{c_1}{\xi} + c_2$$

For the integration constants, $c_1$ must be zero to avoid singularity at origin.

Because $\rho = \rho_c$ at $\theta = 1$, $c_2 = 1$

$$\rightarrow \theta(\xi) = 1 - \frac{1}{6}\xi^2$$

$$\xi_1 = \xi(\theta = 0) = \sqrt{6}$$

Recall $\rho = \rho_c \theta^n$, and $r = \alpha \xi$,

$$M = \int_0^R 4\pi r^2 \rho \, dr = 4\,\pi\alpha^3\rho_c \int_0^{\xi_1} \xi^2 \theta^n \, d\xi$$

(from Lane-Emden eq.)

$$= 4\,\pi\alpha^3\rho_c \int_0^{\xi_1} \left[ -\frac{d}{d\xi}\left( \xi^2 \frac{d\theta}{d\xi} \right) \right] d\xi$$

For the derivations of some solutions, see
https://en.wikipedia.org/wiki/Lane%E2%80%93Emden_equation

# Star Formation in a Nutshell

◆ Stars are formed in groups out of dense molecular cloud cores. Planets are formed in young circumstellar disks.
(*Jeans criteria*)

◆ Initial gravitational contraction leads to a decrease of luminosity, while surface temperature remains almost unchanged.
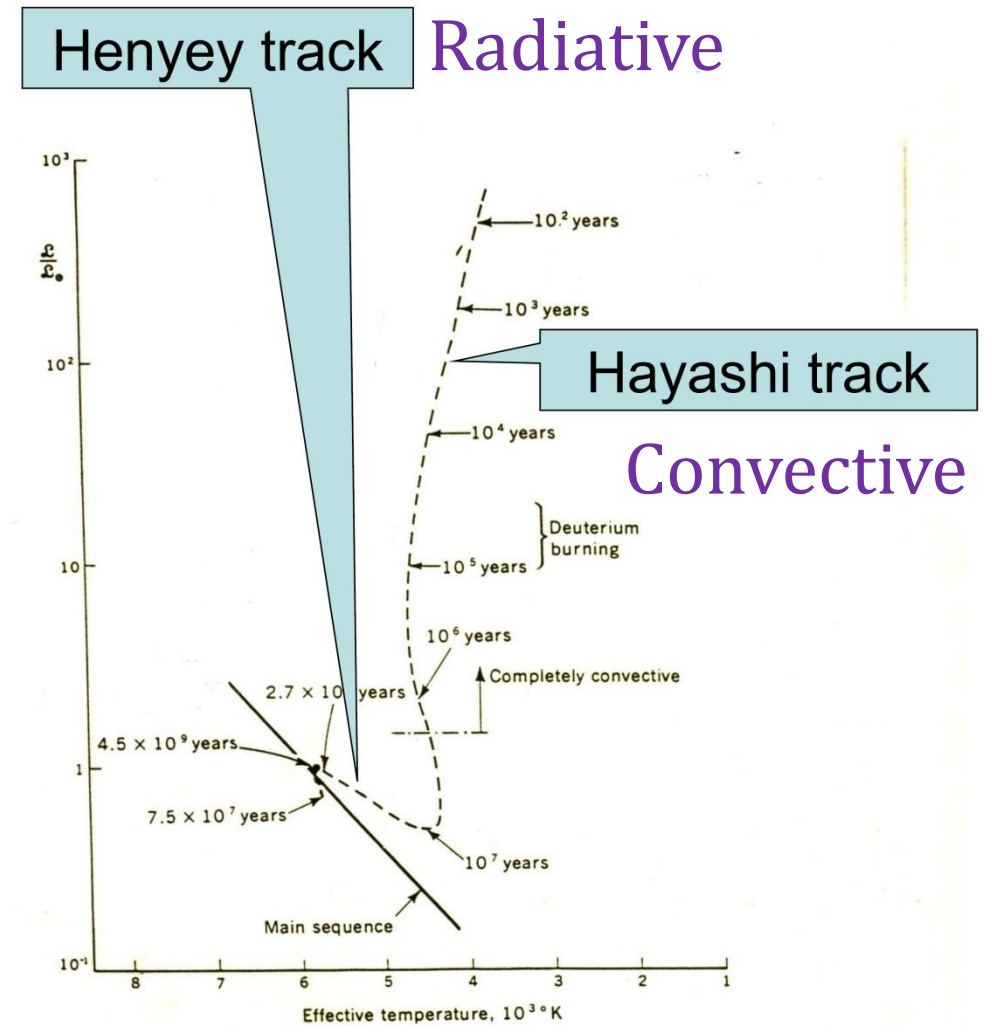(*Pre-main sequence Hayashi track*)



Henyey track  Radiative

Hayashi track

Convective

Deuterium burning

Completely convective

$2.7 \times 10$ years

$4.5 \times 10^9$ years

$7.5 \times 10^7$ years

Main sequence

$10^2$ years
$10^3$ years
$10^4$ years
$10^5$ years
$10^6$ years
$10^7$ years

Effective temperature, $10^3$ °K

**Fig. 5-1** The path on the H-R diagram of the contraction of the sun to the main sequence. The interior has become sufficiently hot to burn deuterium after about $10^5$ years. The contraction ceases near the main sequence when the core has become hot enough to replenish the solar luminosity with the thermonuclear power generated by the fusion of hydrogen into helium. [After D. Ezer and A. G. W. Cameron, *The Contraction Phase of Stellar Evolution*, in R. F. Stein and A. G. W. Cameron (eds.), "Stellar Evolution," Plenum Press, New York, 1966.]

# STELLAR EVOLUTION. I. THE APPROACH TO THE MAIN SEQUENCE*

ICKO IBEN, JR.

California Institute of Technology, Pasadena, California

Received August 18, 1964; revised November 23, 1964

### ABSTRACT

The manner in which nuclear reactions replace gravitational contraction as the major source of stellar luminosity is investigated for model stars of population I composition in the mass range $0.5 < M/M_\odot < 15.0$. By following in detail the depletion of $C^{12}$ from high initial values down to values corresponding to equilibrium with $N^{14}$ in the C-N cycle, the approach to the main sequence in the Hertzsprung-Russell diagram and the time to reach the main sequence, for stars with $M \geq 1.25 M_\odot$, are found to differ significantly from data reported previously.

**Zero-age main sequence (ZAMS):** the locus in the HRD of stars of different masses first reaching the main sequence (i.e., starting steady core H fusion)
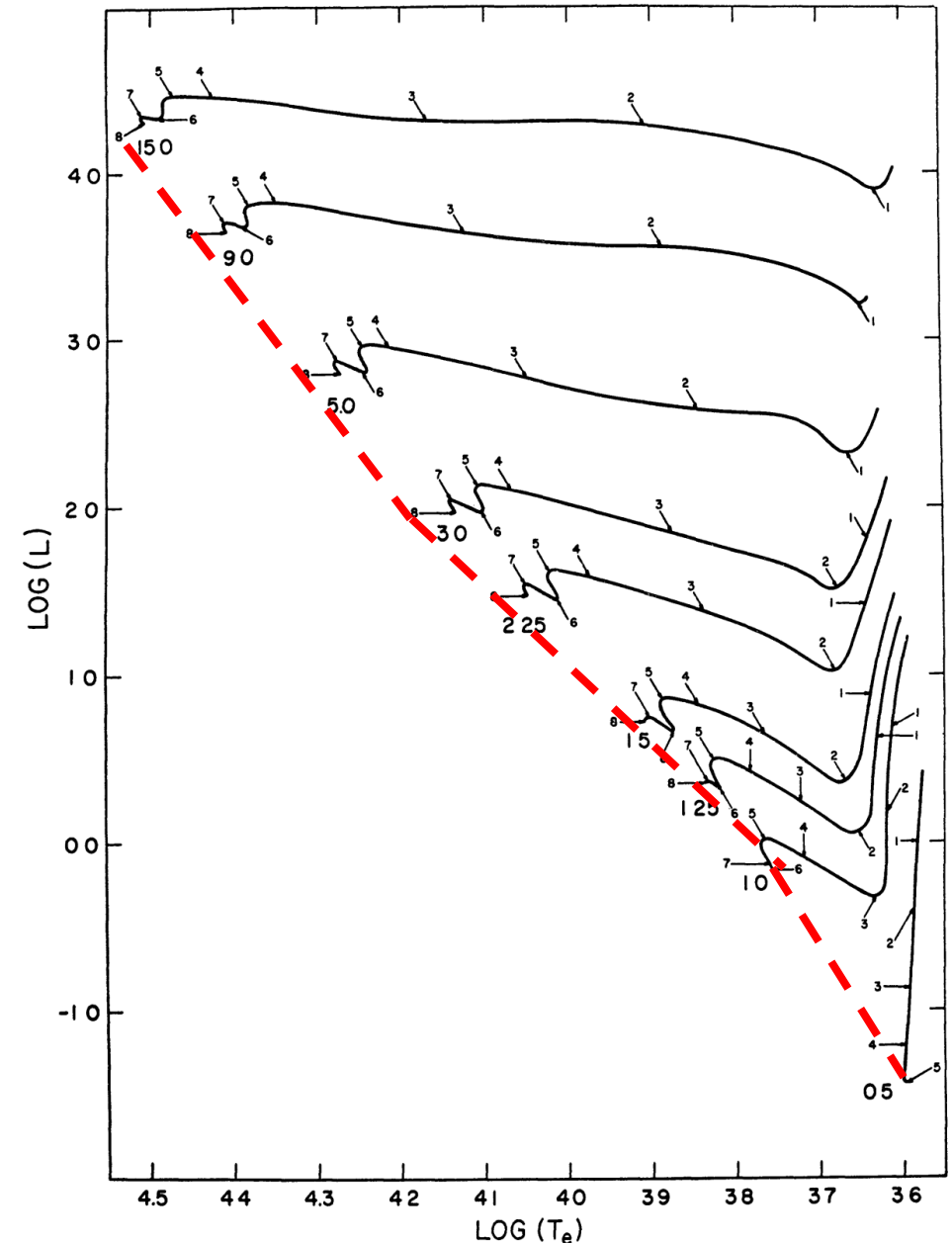


FIG. 17.—Paths in the Hertzsprung-Russell diagram for models of mass $(M/M_\odot)$ = 0.5, 1.0, 1.25, 1.5, 2.25, 3.0, 5.0, 9.0, and 15.0. Units of luminosity and surface temperature are the same as those in Fig. 1.

# Thermonuclear Reactions

- Eddington in 1920s hypothesized that fusion reactions between light elements were the energy source of stars.

- Stellar evolution = (con) sequences of nuclear reactions

- $E_{\text{kinetic}} \approx kT_c \approx 8.62 \times 10^{-8}\, T \sim \text{keV}$,

  but $E_{\text{Coulomb barrier}} = \dfrac{Z_1 Z_2 e^2}{r} = \dfrac{1.44\, Z_1 Z_2}{r[\text{fm}]} \sim \text{MeV}$.
  This is 3 orders higher than the kinetic energy of the particles.

- Tunneling effect in QM proposed by Gamow (1928, Z. Physik, **52**, 510); applied to energy source in stars by Atkinson & Houtermans (1929, Z. Physik, **54**, 656)



George Gamow

# Quantum mechanics tunneling effect
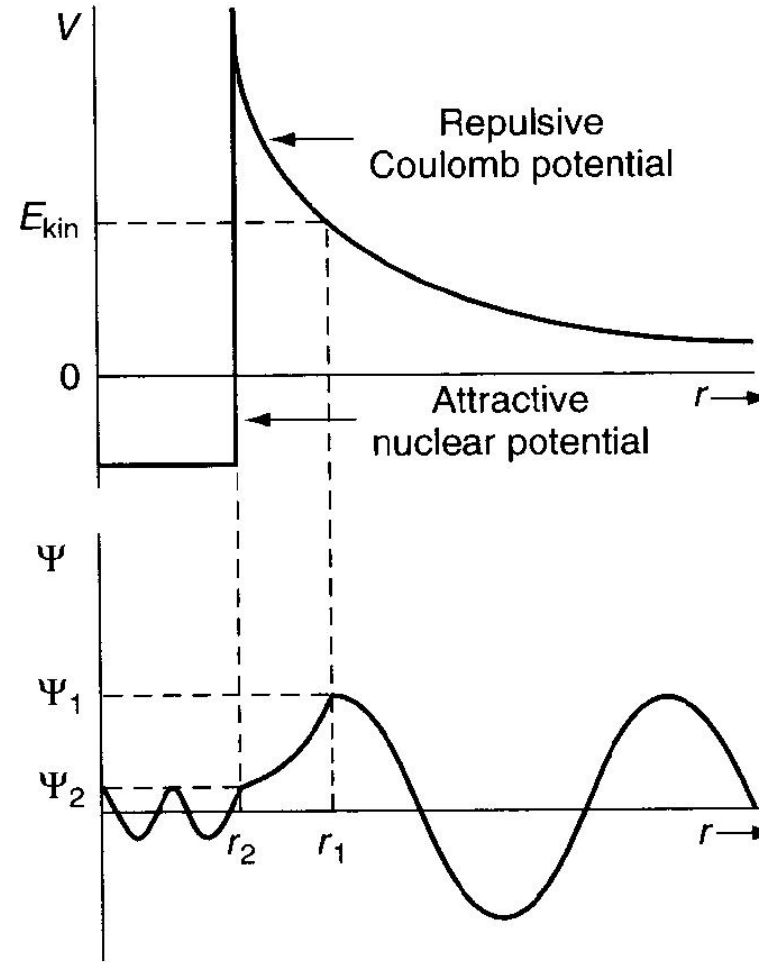


**Figure 3.4** Illustration of the potential seen by particle b when approaching particle A with a kinetic energy $E_{kin}$, and the corresponding wavefunction $\Psi$; classically, particle b would reach only a distance $r_1$ from particle A before being repelled by the Coulomb force

34

**Cross section for nuclear reactions (penetrating probability)**

$$\propto \ e^{-\pi Z_1 Z_2 e^2 / \varepsilon_0 h v}$$

This ↗ as v ↗

**Velocity probability distribution (Maxwellian)**

$$\propto \ e^{-mv^2 / 2kT}$$

This ↘ as v ↗

∴ **Product of these 2 factors** ➜ <span style="color:red">**Gamow peak**</span>

D. Clayton "Principles of Stellar Evolution and Nucleosynthesis"



Maxwellian Velocity Distribution

$e^{-\frac{E}{kT}}$

$e^{-bE^{-\frac{1}{2}}}$ Penetration Probability

Product (magnified)

$\Delta \simeq 4-10$ kev

$E$

$kT \simeq 1-3$ kev

$E_0 \simeq 15-30$ kev
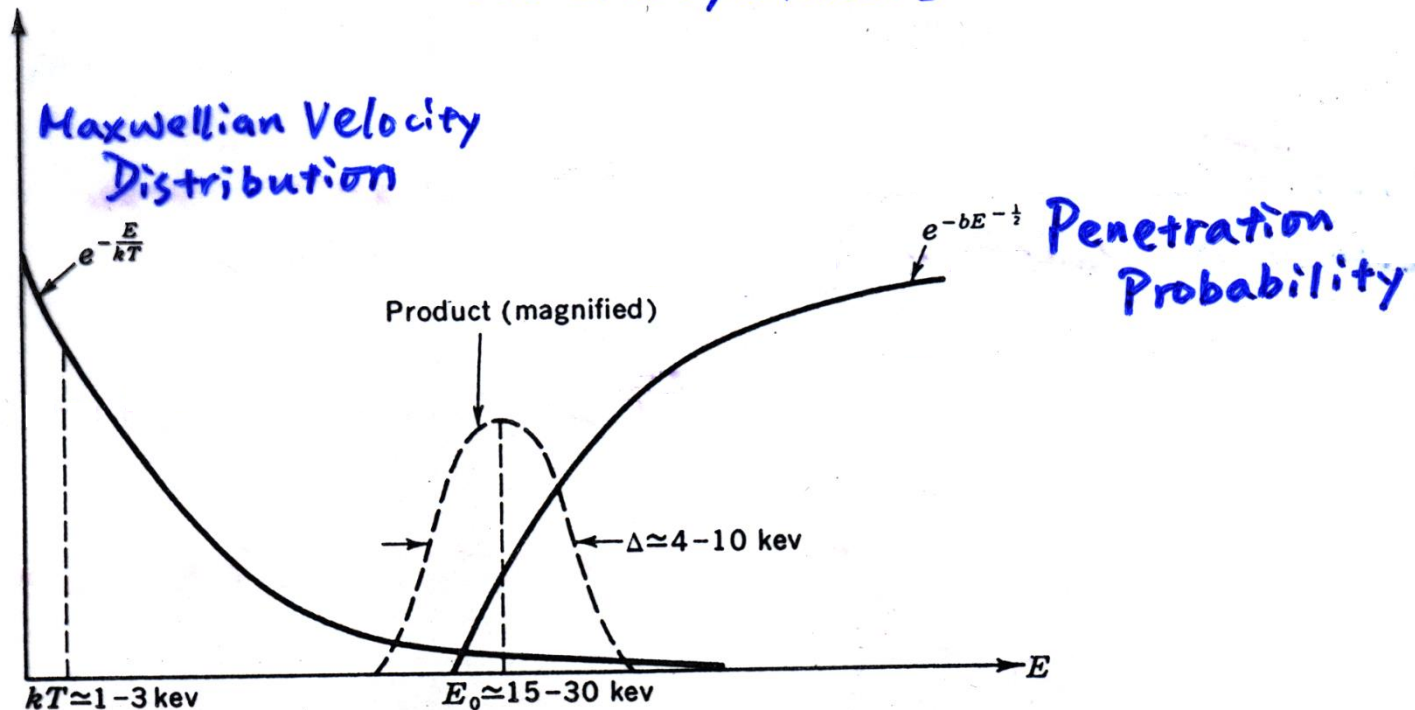
Fig. 4-6   The dominant energy-dependent factors in thermonuclear reactions.   Most of the reactions occur in the high-energy tail of the maxwellian energy distribution, which introduces the rapidly falling factor exp $(-E/kT)$.   Penetration through the coulomb barrier introduces the factor exp $(-bE^{-\frac{1}{2}})$, which vanishes strongly at low energy.   Their product is a fairly sharp peak near an energy designated by $E_0$, which is generally much larger than $kT$.   The peak is pushed out to this energy by the penetration factor, and it is therefore commonly called the *Gamow peak* in honor of the physicist who first studied the penetration through the coulomb barrier.

Clayton

36
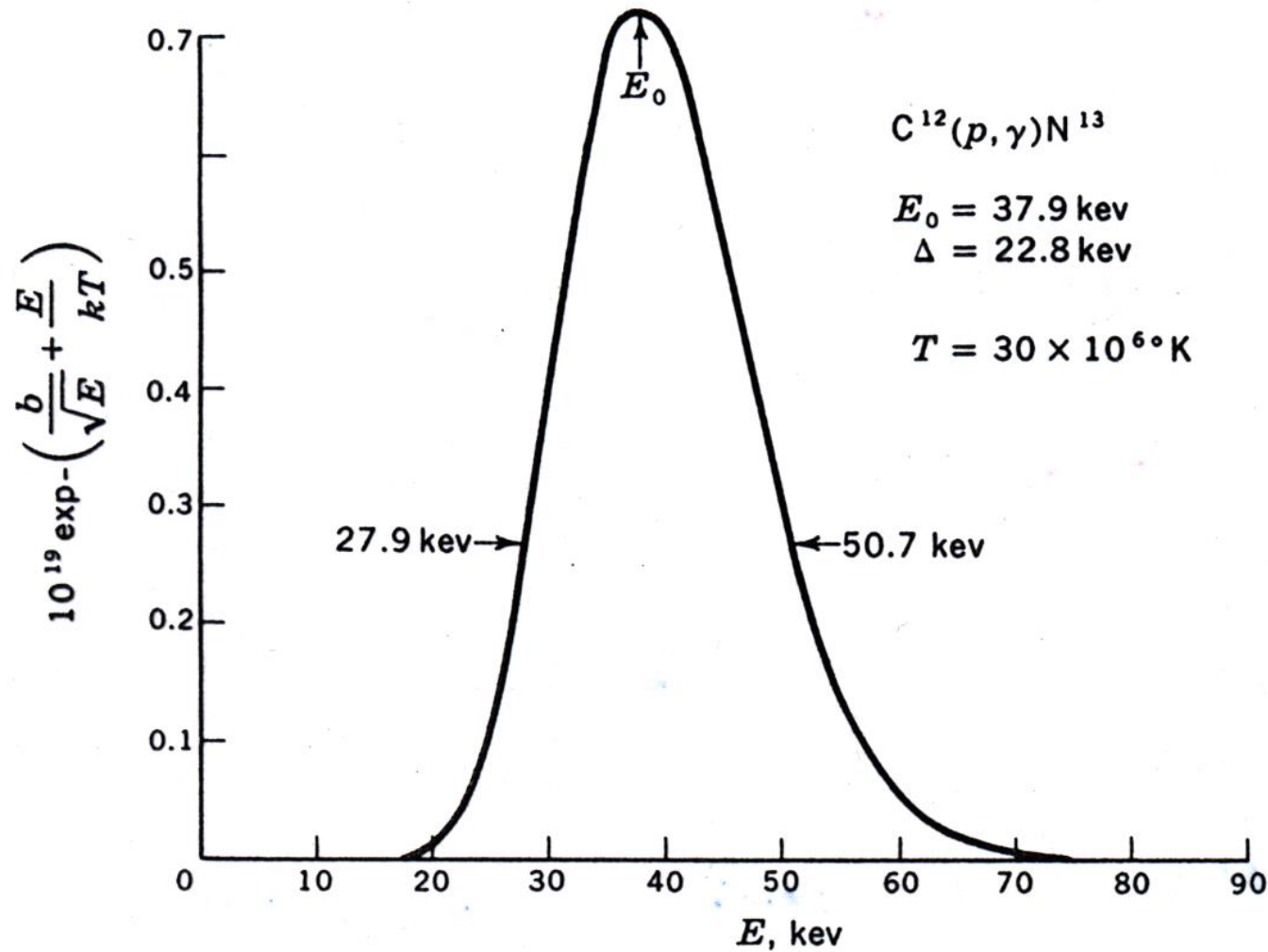
**Fig. 4-7** The Gamow peak for the reaction $C^{12}(p,\gamma)N^{13}$ at $T = 30 \times 10^6$ °K. The curve is actually somewhat asymmetric about $E_0$, but it is nonetheless adequately approximated by a gaussian.

Clayton

37

Resonance → very sharp peak in the reaction rate

So there exists a narrow range of temperature in which the reaction rate ↑↑
→ a power law

→ an "ignition" (threshold) temperature

Resonance reactions
  Energy of interacting particles ≈ Energy level of compound nucleus

For a thermonuclear reaction or a nucleosynthesis (fusion) process, the reaction rate is expressed as

$$q \propto \rho^m T^n$$

38

# Nuclear reaction rate

✓ $r_{12} \propto n_1 n_2 \langle \sigma v \rangle \propto n_1 n_2 \exp\left[-C\left(\frac{z_1^2 z_2^2}{T_6}\right)^{1/3}\right]$ $[\text{cm}^{-3}\text{s}^{-1}]$

✓ As $T \nearrow$, $r_{12} \nearrow\nearrow$

✓ Major reactions are those with smallest $Z_1 Z_2$ , i.e., with the lowest Coulomb barriers.

✓ $n_i$ is the particle volume number density, $n_i m_i = \rho X_i$, where $X_i$ is the mass fraction

✓ $q_{12} \propto Q \rho X_1 X_2 / m_1 m_2$ $[\text{erg g}^{-1}\text{s}^{-1}]$
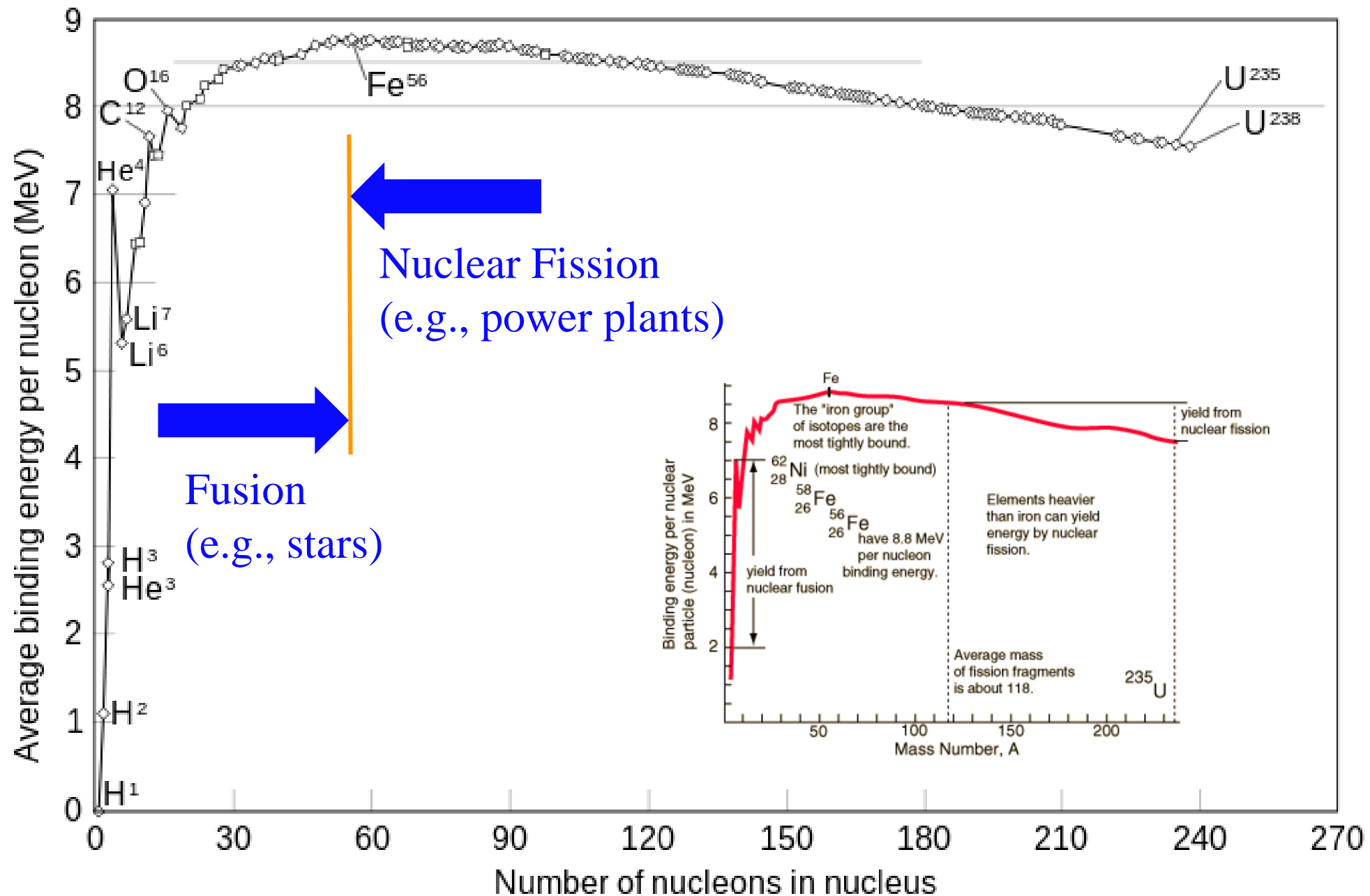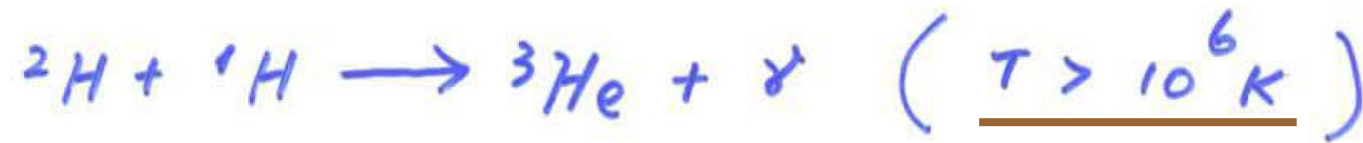
# Binding Energy per Nucleon

| Z | A | Symbol | B (MeV)/A |
|---|---|--------|-----------|
| 0 | 1 | $n$ | 0.0 |
| 1 | 1 | $H$ | 0.0 |
|   | 2 | $D$ | 1.112260 |
|   | 3 | $T$ | 2.827307 |
| 2 | 3 | $He$ | 2.572693 |
|   | 4 |      | 7.074027 |
| 3 | 6 | $Li$ | 5.332148 |
|   | 7 |      | 5.606490 |

Arnett

# Deuterium Burning

$$^2H + {}^1H \longrightarrow {}^3He + \gamma \quad \left( \underline{T > 10^6 K} \right)$$

$$^2H({}^1H, \gamma){}^3He$$
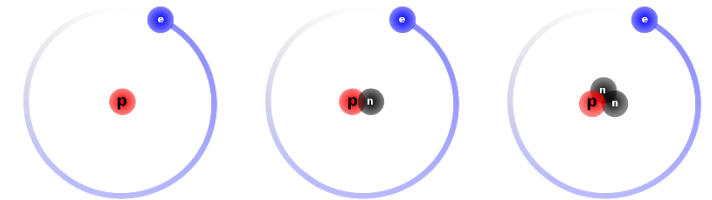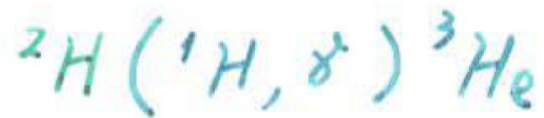


$^1_1H$  Protium   $^2_1H$  Deuterium   $^3_1H$  Tritium

Deuterium: D or ${}^2H$, with the nucleus consisting of 1 $p^+$ and 1 $n^0$

$$Q_{DP} = 5.5 \text{ MeV}$$

$$q_{DP} = 4.19 \times 10^7 \left[ D/H \right] \left( \frac{\rho}{1 \text{ g cm}^{-3}} \right) \left( \frac{T}{10^6 K} \right)^{11.8} \left[ \text{erg g}^{-1} s^{-1} \right]$$

ISM value, $\langle D/H \rangle \sim 2 \times 10^{-5}$

Earth ocean $1.6 \times 10^{-4}$

42

**D/H**

- 156 ppm … Terrestrial seawater $(1.56 \times 10^{-4})$
- 22~26 ppm … Jupiter
- 17 ppm … Saturn
- 55 ppm … Uranus
- 200 ppm … Halley's Comet

**Ionization potential**
- ✓ 12.8 eV for D
- ✓ 13.6 eV for H
- ✓ 24.6, 54.4 eV for He
- ✓ 5.4, 75.6, 122.4 eV for Li
- ✓ 7.9, 16.2, …, 1136.2 eV for Fe

**Hydrostatic equilibrium**

$$\frac{dP}{dr} = -\frac{Gm(r)}{r^2}\rho, \text{ so } \frac{P}{R} = \frac{GM}{R^2}\frac{M}{R^3} \rightarrow \boxed{P = \frac{GM^2}{R^4}} \quad \text{Force/Area}$$

**Ideal gas law**

$$P = \frac{\rho}{\mu m_H}kT; \ \rho = \frac{M}{R^3} \rightarrow \boxed{P = \frac{MT}{R^3\mu}\frac{k}{m_H}}$$

Equating the two pressure terms $\rightarrow$ $T \sim \dfrac{\mu\,GM}{R}$

This should be valid at the star's center, thus

$$\boxed{T_* \sim \frac{\mu\,GM_*}{R_*}}$$

Changes in the slope

$\gtrsim 0.3\ M_{\odot}$
Convective envelope ↓
→ energy transport insufficient
→ $T_c$ ↑

$\gtrsim 1.3\ M_{\odot}$
CNO → energy production ↑
→ convective core ↑
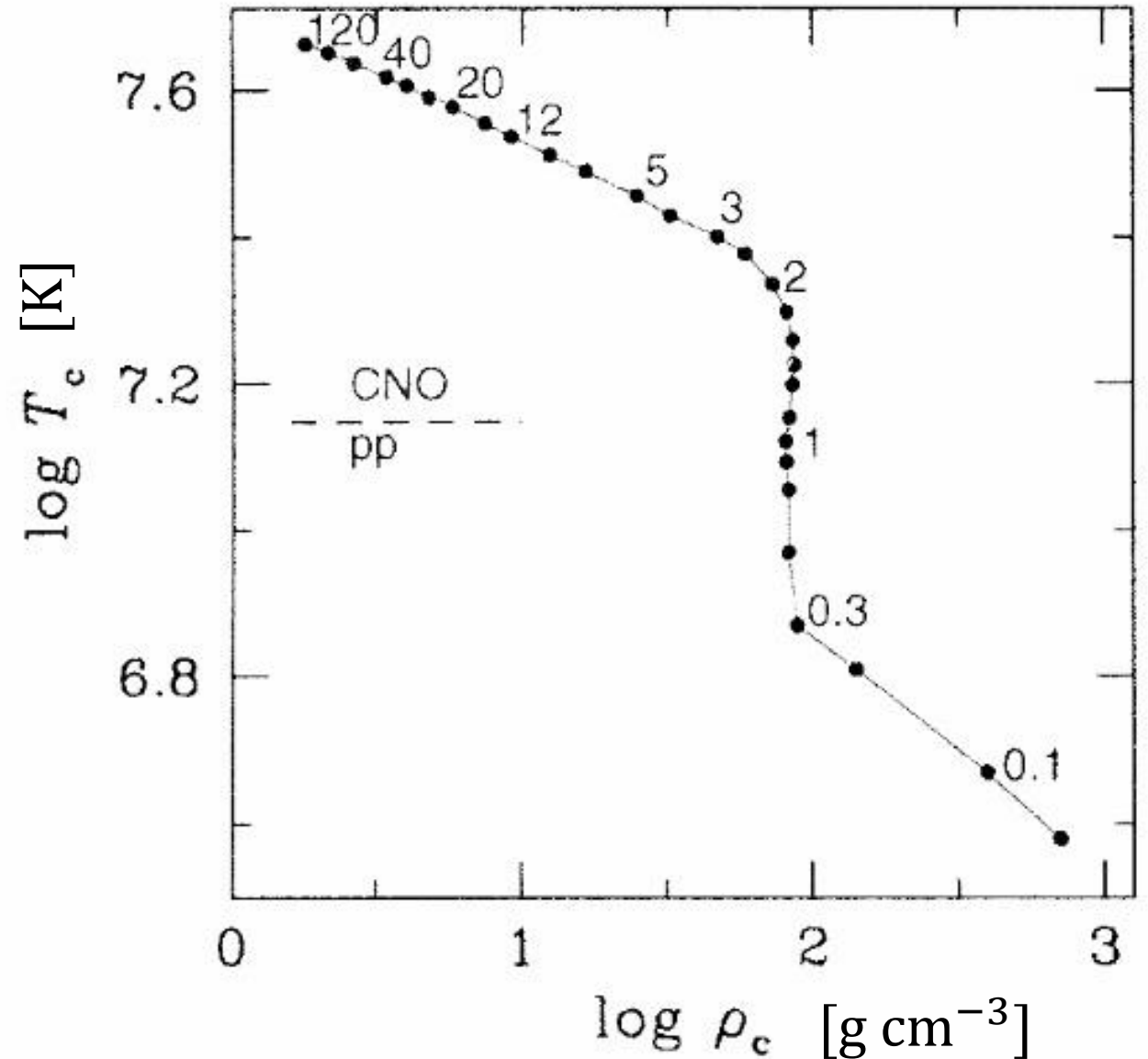


De Boer & Seggewiss, Fig 6.5

46

Recall a star's central temperature

$$T_c \sim \sqrt{\frac{\mu G M}{R}} \cdot \alpha \overset{\text{mass distr.}}{}$$

Numerically

$$T_c = 7.5 \times 10^6 \, K \left( \frac{M_*}{M_\odot} \right) \left( \frac{R_*}{R_\odot} \right)^{-1}$$

$$\therefore \quad M_* = 0.4 \, M_\odot \longrightarrow T_c \sim 10^6 \, K$$
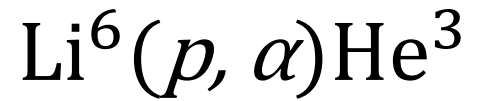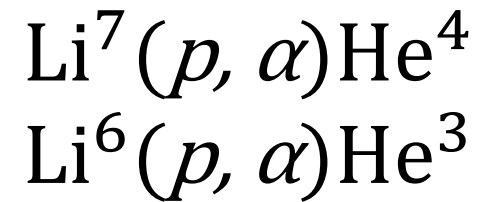
# Lithium Burning

$$^7Li + {}^1H \longrightarrow {}^4He + {}^4He \quad (T > 3 \times 10^6 K)$$

$$ISM \quad [Li/H] \sim 2 \times 10^{-9}$$

Primordial abundance 10 x lower,
produced by cosmic rays $\alpha$ hitting ${}^4He$
( inverse reaction )
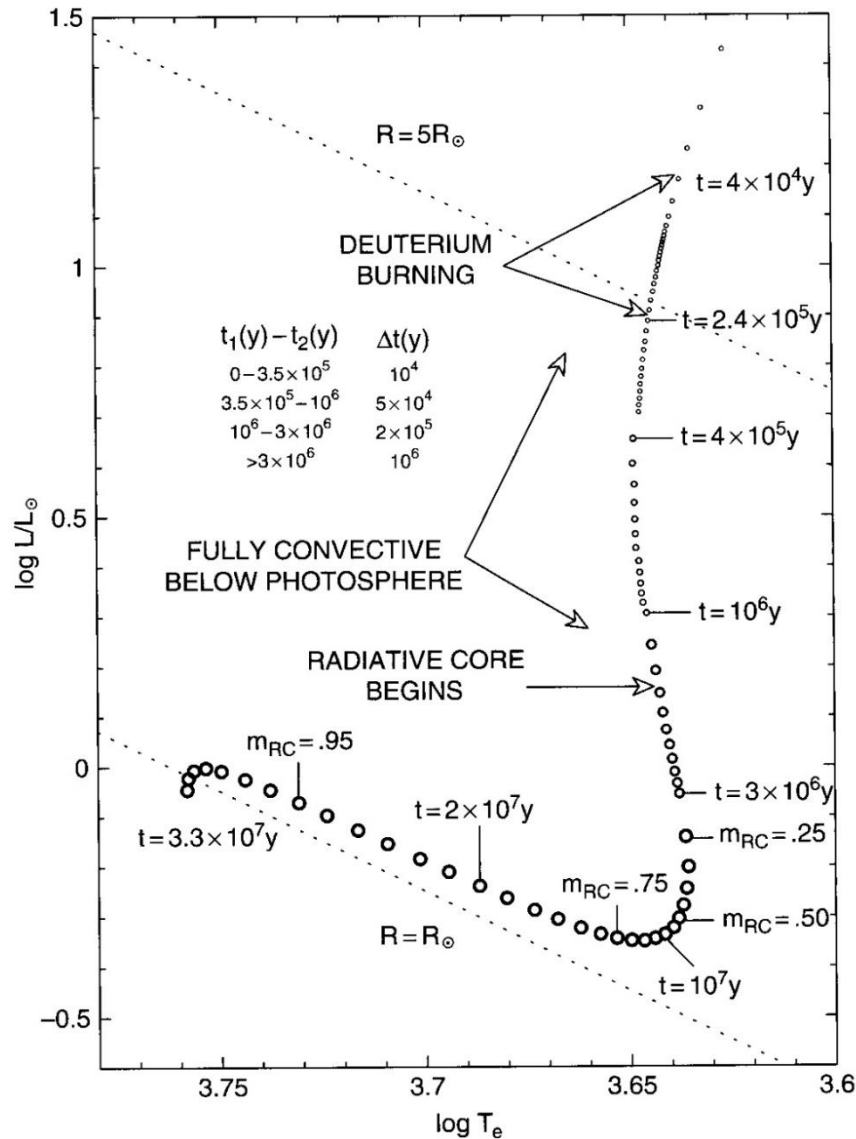
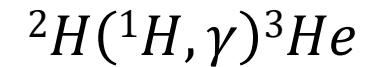Li measurable in Stellar spectra

Li I 6708Å absorption

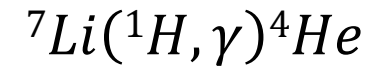actually doublet 6707.78 and 6707.93
but difficult to resolve

$$Li^7(p, \alpha)He^4$$
$$Li^6(p, \alpha)He^3$$

# Pre-main sequence evolution of the Sun



Pre main sequence evolution in the HR diagram of a low mass model ($M = 1M_\odot, Z = 0.01, Y = 0.25$)

$^2$D burns at $T \approx 10^6$ K

$$^2H(^1H,\gamma)^3He$$

$^7$Li burns at $T \approx 3 \times 10^6$ K

$$^7Li(^1H,\gamma)^4He$$

$^1$H burns at $T \approx 5 \times 10^6$ K

Iben 2013

Development of the radiative core

Hayashi track (convective)

Onset of core H fusion

Birthline

Zero-age main sequence (ZAMS)

Henyey track (radiative)

Luminosity $\log(L_*/L_\odot)$

$1.0\ M_\odot$

$0.6\ M_\odot$

$0.2\ M_\odot$

Temperature $\log(T_{eff})$ (K)
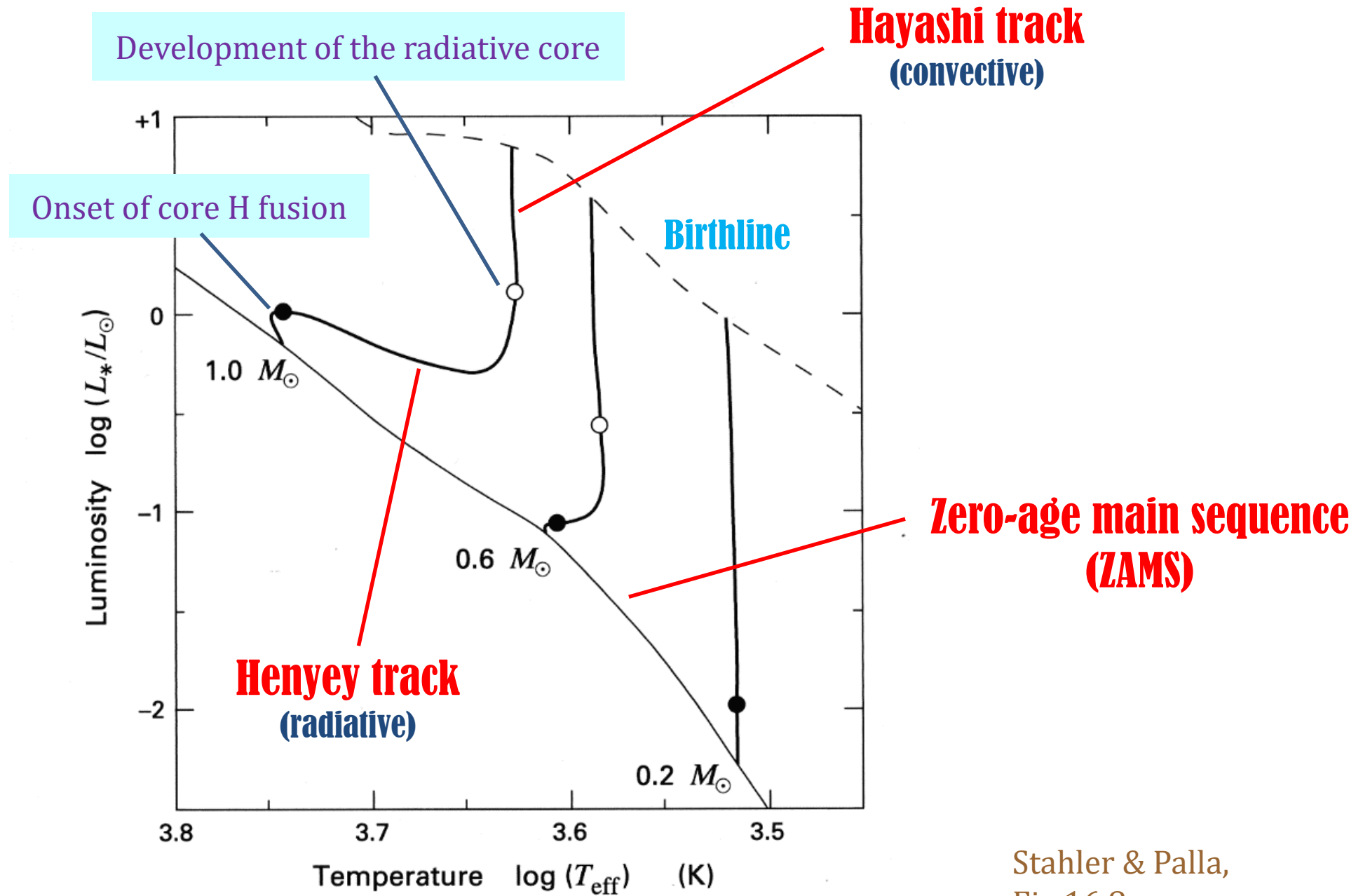
Stahler & Palla, Fig 16.8

Low-mass protostars, $T_c$ too low to ignite Li fusion, so inherit the full ISM Li supply.

Higher-mass protostars can burn and destroy Li promptly, but the base of the convection zone is below $3 \times 10^6$ K, so the surface lithium abundance = ISM value.

Presence of Li I λ6707 absorption → stellar youth
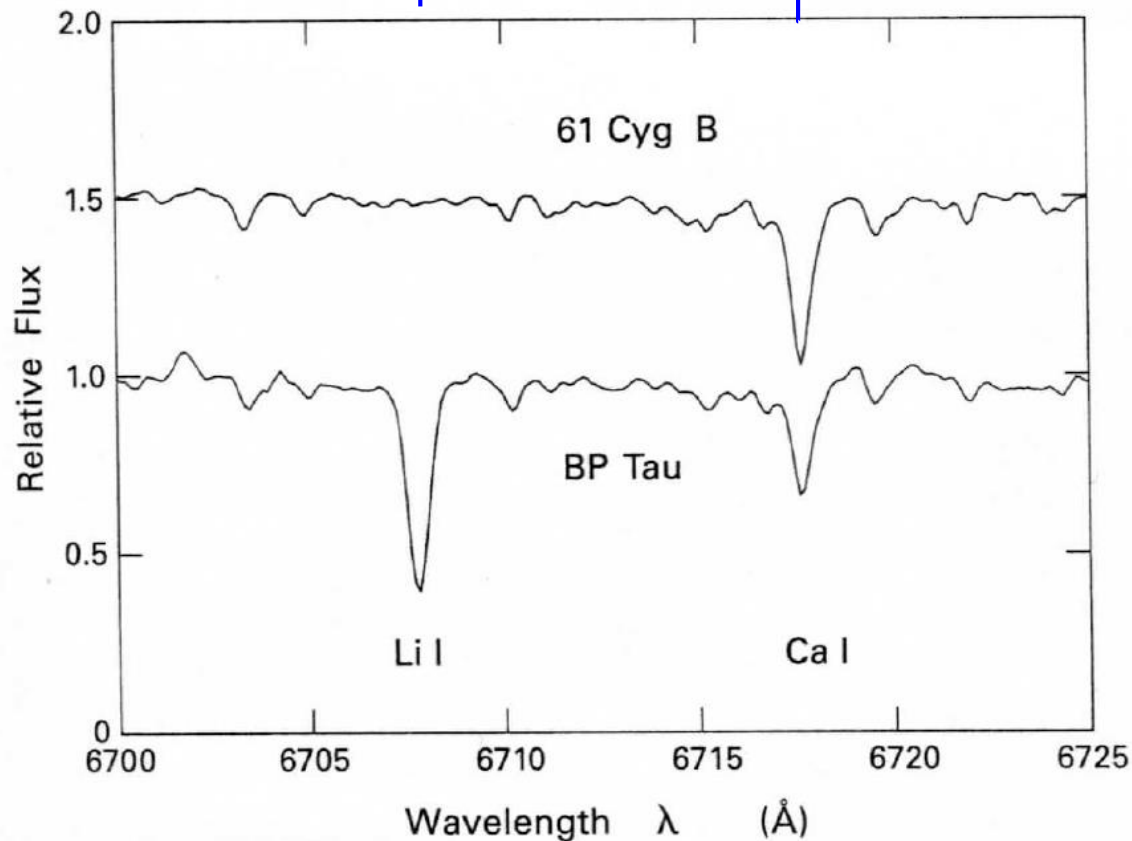Ca I λ6718 prominent in late-type stars

**Figure 16.9** Lithium absorption in a pre-main-sequence star. Shown is a portion of the optical spectrum of BP Tau, a T Tauri star of spectral type K7, corresponding to an effective temperature of 4000 K. Also shown, for comparison, is a main-sequence star of the same spectral type, 61 Cyg B. Only in the first star do we see the Li I absorption line at 6708 Å. Both objects also have a strong line due to neutral calcium.

Stahler & Palla

52

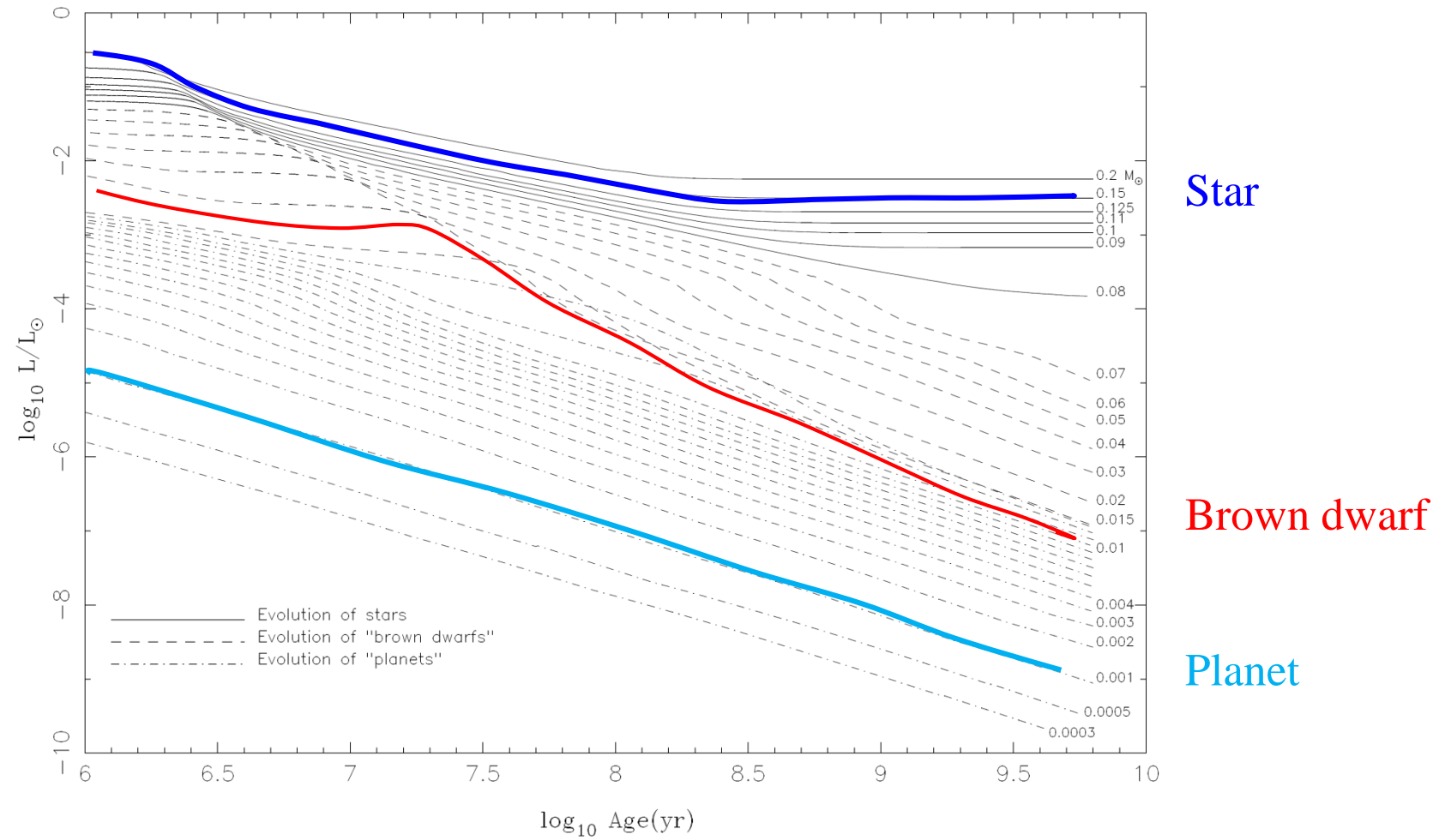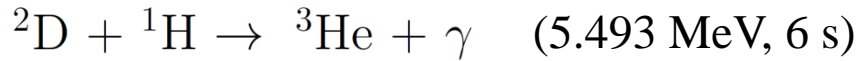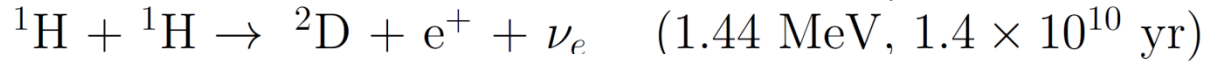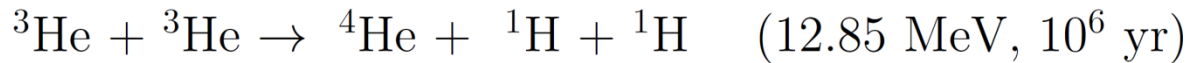| Stars | $\mathcal{M}/\mathrm{M}_\odot > 0.08$, core H fusion |
|---|---|
| | Spectral types O, B, A, F, G, K, M |
| Brown Dwarfs | $0.065 > \mathcal{M}/\mathrm{M}_\odot > 0.013$, core D fusion |
| | $0.080 > \mathcal{M}/\mathrm{M}_\odot > 0.065$, core Li fusion |
| | Spectral types M6.5–9, L, T, Y |
| | Electron degenerate cores |
| | ✓ $10 \text{ g cm}^{-3} < \rho_c < 10^3 \text{ g cm}^{-3}$ |
| | ✓ $T_c < 3 \times 10^6 \text{ K}$ |
| Planets | $\mathcal{M}/\mathrm{M}_\odot < 0.013$, no fusion ever |

$$1 \, M_\odot \approx 1000 \, M_J$$

FIG. 7.—Evolution of the luminosity (in $L_\odot$) of solar-metallicity M dwarfs and substellar objects vs. time (in yr) after formation. The stars, "brown dwarfs" and "planets" are shown as solid, dashed, and dot-dashed curves, respectively. In this figure, we arbitrarily designate as "brown dwarfs" those objects that burn deuterium, while we designate those that do not as "planets." The masses (in $M_\odot$) label most of the curves, with the lowest three corresponding to the mass of Saturn, half the mass of Jupiter, and the mass of Jupiter.

# The proton-proton chain
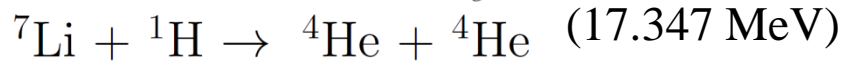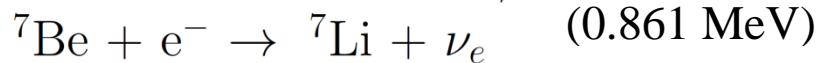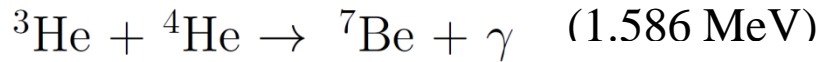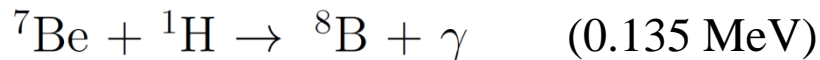
*This neutrino carries away 0.26 MeV*

$$^1H + {}^1H \rightarrow {}^2D + e^+ + \nu_e \quad (1.44 \text{ MeV}, 1.4 \times 10^{10} \text{ yr})$$
$$^2D + {}^1H \rightarrow {}^3He + \gamma \quad (5.493 \text{ MeV}, 6 \text{ s})$$

## pp I chain

$$^3He + {}^3He \rightarrow {}^4He + {}^1H + {}^1H \quad (12.85 \text{ MeV}, 10^6 \text{ yr})$$

$$\underline{\text{Note}}: \text{ net } 6 \ {}^1H \rightarrow {}^4He + 2 \ {}^1H$$

## pp II chain

$$^3He + {}^4He \rightarrow {}^7Be + \gamma \quad (1.586 \text{ MeV})$$
$$^7Be + e^- \rightarrow {}^7Li + \nu_e \quad (0.861 \text{ MeV})$$
$$^7Li + {}^1H \rightarrow {}^4He + {}^4He \quad (17.347 \text{ MeV})$$

## pp III chain

$$^3He + {}^4He \rightarrow {}^7Be + \gamma$$
$$^7Be + {}^1H \rightarrow {}^8B + \gamma \quad (0.135 \text{ MeV})$$
$$^8B + \cdot, \ {}^8Be + e^+ + \nu_e \quad \textit{This neutrino carries away 7.2 MeV}$$
$$^8Be \rightarrow {}^4He + {}^4He \quad (18.074 \text{ MeV})$$
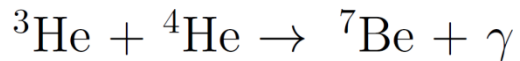
0.420 MeV to the positron and neutrino (0.26 MeV); position and electron (each 0.511 MeV rest energy) annihilate ➜ 1.442 MeV released

## pp I important when
$$T_c > 5 \times 10^6 \text{K}$$

$$Q_{total} = 1.44 \times 2 + 5.49 \times 2$$
$$+12.85 = 26.7 \text{ MeV}$$
$$Q_{net} = 26.7 - 0.26 \times 2 = 26.2 \text{ MeV}$$
$$\rightarrow 6 \times 10^{18} \text{ erg g}^{-1}$$

✓ The baryon number, lepton number, and charges should all be conserved.
✓ All 3 branches operate simultaneously.
✓ pp I is responsible for > 90% of stellar luminosity

Hydrogen burning

p

$^4$He

I

II

III

$^2$D

$^3$He

$^2$D

$^3$He

$^2$D

$^3$He

$^7$Be

$^8$B

$^8$Be

$^7$Li

$e^+, \nu$

$e^+, \nu$

$e^+, \nu$

$e^-$

$\nu$

$e^+, \nu$

$\nu$

**Figure 4.3** The nuclear reactions of the p – p I, II and III chains.

Among all fusion processes, the p-p chain has the lower temperature threshold, and the weakest temperature dependence.

$$Q_{pp} = \left(M_{4H} - M_{He}\right) c^2$$

$$= 26.731 \text{ MeV}$$

$\left(M_{4H} - M_{He}\right)$ : **mass deficit**

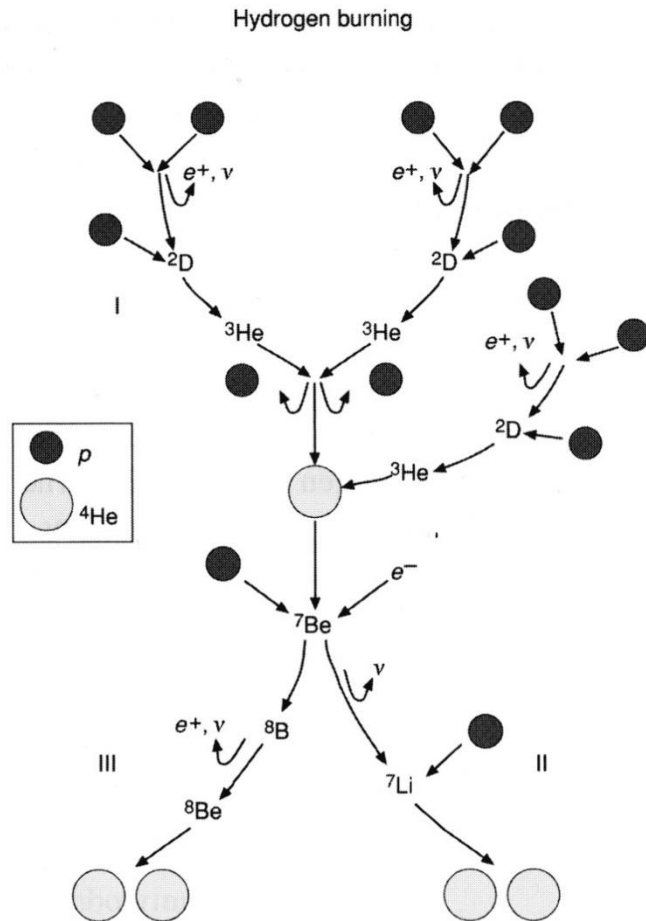But some energy (up to a few MeV, depending on the reactions) is carried away by neutrinos.

… but the nucleus of deuterium, a deuteron, consists of a proton and a neutron!

✓ $p + p \rightarrow {}^{2}He$ (unstable)$\rightarrow p + p$

✓ Hans Bethe (1939) realized that the weak interaction was capable of converting a proton to a neutron (!) first

✓ Weak interaction ➔ a very small cross section

✓ The neutron is more massive, so this requires energy, i.e., it is an <u>endothermic</u> process, but neutron + proton ➔ deuteron (releasing binding energy, i.e., is <u>exothermic</u>)

The thermonuclear reaction rate is

$$r_{pp} = 3.09 \times 10^{-37} \; n_p^2 \; T_6^{-2/3} \exp\left(-33.81 \; T_6^{-1/3}\right)$$

$$(1 + 0.0123 \; T_6^{1/3} + 0.0109 \; T_6^{2/3} + 0.0009 \; T_6) \;\; [\mathrm{cm}^{-3}\mathrm{s}^{-1}],$$

where the factor $3.09 \times 10^{-37} n_p^2 = 11.05 \times 10^{10} \; \rho^2 X_H^2$

And the energy generation rate is

$$q_{pp} = 2.38 \times 10^6 \; \rho \; X_H^2 \; T_6^{-2/3} \exp\left(-33.81 \; T_6^{-1/3}\right)$$

$$(1 + 0.0123 \; T_6^{1/3} + 0.0109 \; T_6^{2/3} + 0.0009 \; T_6) \; [\mathrm{erg\,g}^{-1}\mathrm{s}^{-1}]$$

- PP I vs PP II
  That is, $^3$He to react with $^3$He at a lower temperature,

  or to react with $^4$He at $\boldsymbol{T > 1.4 \times 10^7 \text{ K}}$

- Relative importance of each chain
  $\longrightarrow$ Branching ratio $\longleftrightarrow$ $T, \rho, \mu$

- Above $T > 3 \times 10^7$ K, PP III should dominate, but in reality, at this temperature, other reactions (CNO) take over.

- The overall rate of energy generation is determined by the <u>slowest</u> reaction, i.e., the first one, with reaction time $10^{10}$ yrs
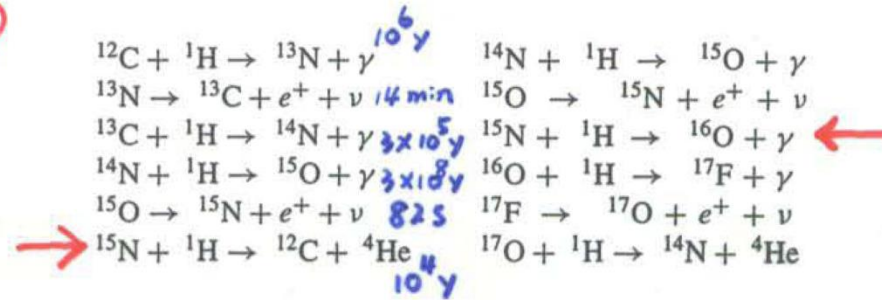
  $Q_{pp} \sim 26.73$ MeV ($\approx 6.54$ MeV per proton)

  $q_{pp} \sim \rho^1 T^n, n \sim 4 - 6$

$n \sim 6$ for T $\approx 5 \times 10^6$ K
$n \sim 3.8$ for T $\approx 15 \times 10^6$ K (Sun)
$n \sim 3.5$ for T $\approx 20 \times 10^6$ K

# CNO cycle
## (bi-cycle)

**C,N,O as catalysts**

$$^{12}C + {}^1H \to {}^{13}N + \gamma \quad 10^6 y$$
$$^{13}N \to {}^{13}C + e^+ + \nu \quad 14\,min$$
$$^{13}C + {}^1H \to {}^{14}N + \gamma \quad 3\times10^5 y$$
$$^{14}N + {}^1H \to {}^{15}O + \gamma \quad 3\times10^8 y$$
$$^{15}O \to {}^{15}N + e^+ + \nu \quad 82s$$
$$\to {}^{15}N + {}^1H \to {}^{12}C + {}^4He \quad 10^4 y$$

$$^{14}N + {}^1H \to {}^{15}O + \gamma$$
$$^{15}O \to {}^{15}N + e^+ + \nu$$
$$^{15}N + {}^1H \to {}^{16}O + \gamma \leftarrow$$
$$^{16}O + {}^1H \to {}^{17}F + \gamma$$
$$^{17}F \to {}^{17}O + e^+ + \nu$$
$$^{17}O + {}^1H \to {}^{14}N + {}^4He$$

Recognized by Bethe and independently by von Weizsäcker

CN cycle + NO cycle

Cycle can start from any reaction as long as the involved isotope is present.

CN cycle more significant
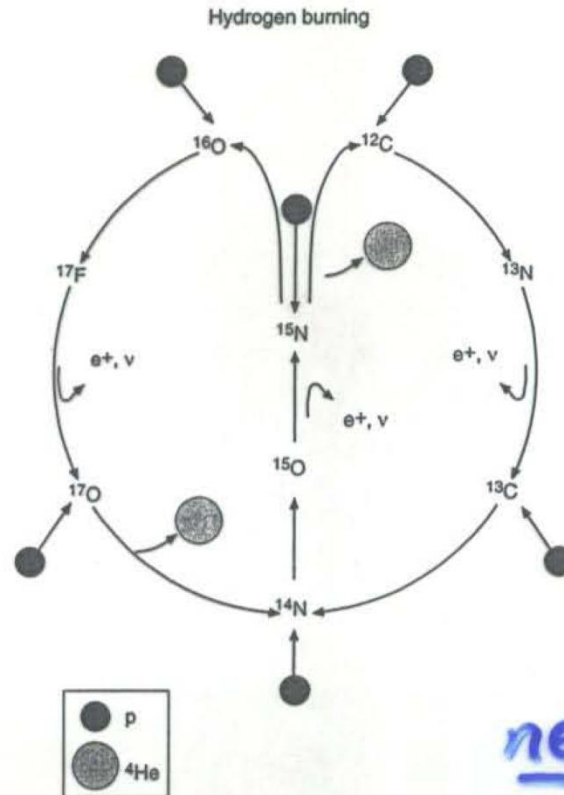
NO cycle efficient only when
$T > 20 \times 10^6$ K

Hydrogen burning



**Figure 4.4** The nuclear reactions of the CNO bi-cycle.

net

$$4H \to {}^4He$$

$$Q_{CNO} \sim 25\ MeV$$

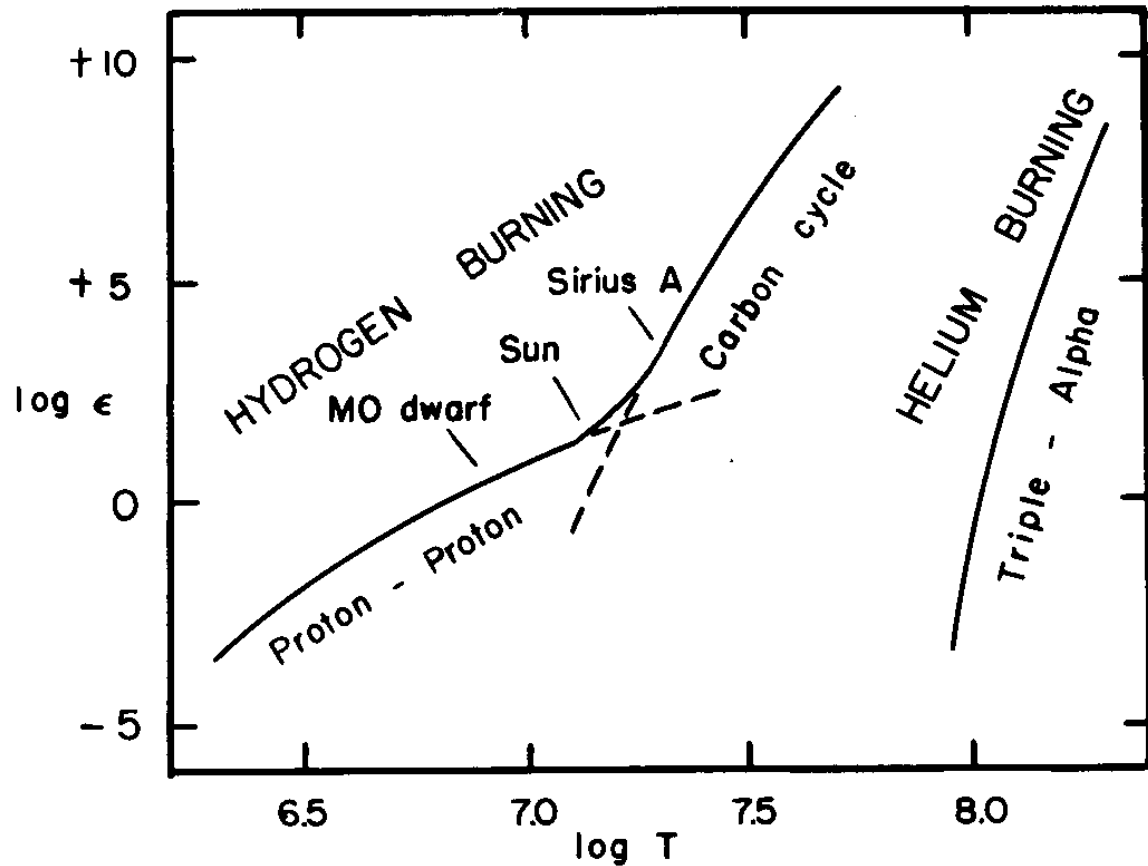after that carried away by the neutrinos

$$\varepsilon_{CNO} \sim \rho T^{16}$$

60

Fig. 10.1. Nuclear energy generation as a function of temperature (with $\rho X^2 = 100$ and $X_{CN} = 0.005X$ for the proton-proton reaction and the carbon cycle, but $\rho^2 Y^3 = 10^8$ for the triple-alpha process).

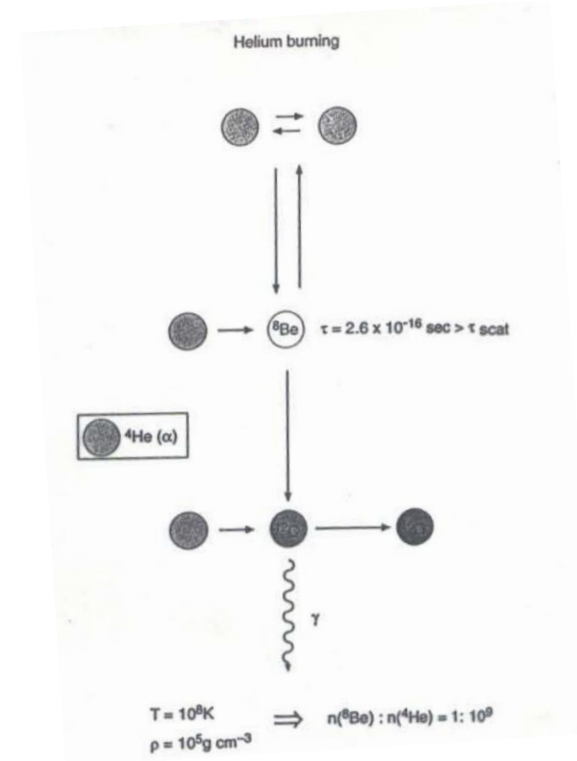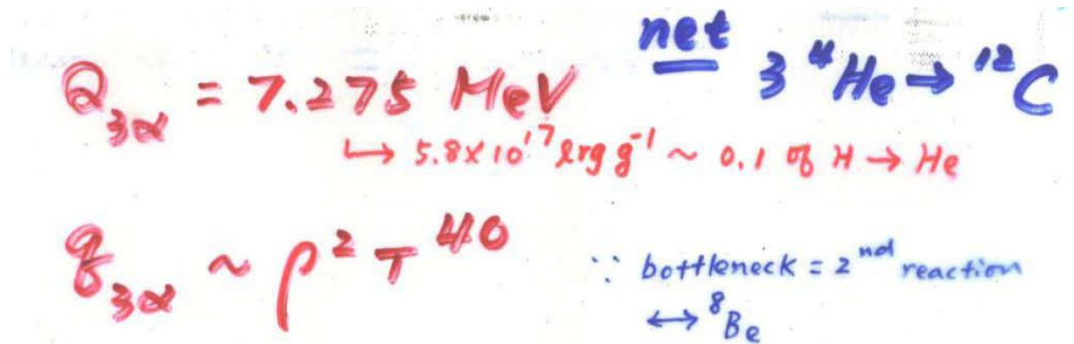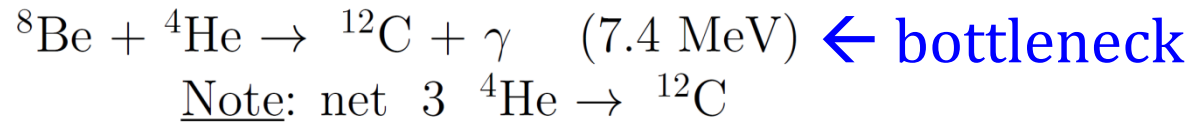Schwarzschild

☐ At the center of the Sun, $q_{CNO}/q_{pp} \approx 0.1$

☐ CNO dominates in stars $> 1.2$ M$_\odot$, i.e., of a spectral type F7 or earlier
→ large energy outflux
➔ a convective core

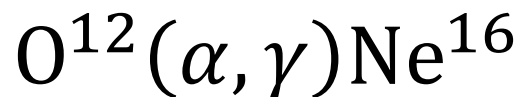☐ This separates the lower and upper MS.

✓ CN cycle takes over the PP chains near T$_6$ =18
✓ Helium burning starts $\sim 10^8$ K.

61

# A He Gas — the triple-alpha process  <span style="color:blue">He-burning ignites at $T_c \sim 10^8$ K</span>

$^4\text{He} + {}^4\text{He} \rightarrow {}^8\text{Be}$  $(-95$ keV, i.e., endothermic$)$

The lifetime of $^8\text{Be}$ is $2.6 \times 10^{-16}$ s but is still longer than the mean-free time between $\alpha$ particles at $T_8$ (Edwin Salpeter, 1952)

$^8\text{Be} + {}^4\text{He} \rightarrow {}^{12}\text{C} + \gamma$  $(7.4$ MeV$)$ <span style="color:blue">$\leftarrow$ bottleneck</span>

Note: net $3\ {}^4\text{He} \rightarrow {}^{12}\text{C}$

$$Q_{3\alpha} = 7.275 \text{ MeV} \quad \underline{\text{net}} \quad 3\ {}^4\!He \rightarrow {}^{12}C$$

$$\hookrightarrow 5.8 \times 10^{17} \text{ erg g}^{-1} \sim 0.1\ \% \ H \rightarrow He$$

$$g_{3\alpha} \sim \rho^2 T^{40}$$

$$\therefore \text{bottleneck} = 2^{nd} \text{ reaction}$$
$$\hookleftarrow {}^8Be$$



Helium burning

$\tau = 2.6 \times 10^{-16}$ sec $> \tau$ scat

$^4$He ($\alpha$)

$T = 10^8$K  $\Rightarrow$  $n(^8\text{Be}) : n(^4\text{He}) = 1 : 10^9$
$\rho = 10^5$g cm$^{-3}$

## Nucleosynthesis during helium burning
$$C^{12}(\alpha, \gamma)O^{16}, \quad Q = 7.162 \text{ MeV}$$
$$O^{12}(\alpha, \gamma)Ne^{16}$$

<span style="color:purple">A succession of $(\alpha, \gamma)$ processes
$\rightarrow {}^{16}O, {}^{20}Ne, {}^{24}Mg$ ... (the $\alpha$-process)</span>

# A carbon/oxygen Gas

$$^{12}C + {}^{12}C$$

$$T \gtrsim 5 \times 10^8 \, K$$

$$Q_{CC} \sim 13 \, MeV$$

$$^{12}C + {}^{12}C \rightarrow {}^{24}Mg + \gamma$$
$$\rightarrow {}^{23}Mg + n$$
$$\rightarrow {}^{23}Na + p$$
$$\rightarrow {}^{20}Ne + \alpha$$
$$\rightarrow {}^{16}O + 2\alpha$$

$$^{16}O + {}^{16}O \rightarrow {}^{32}S + \gamma$$
$$\rightarrow {}^{31}S + n$$
$$\rightarrow {}^{31}P + p$$
$$\rightarrow \boxed{{}^{28}Si} + \alpha$$
$$\rightarrow {}^{24}Mg + 2\alpha$$

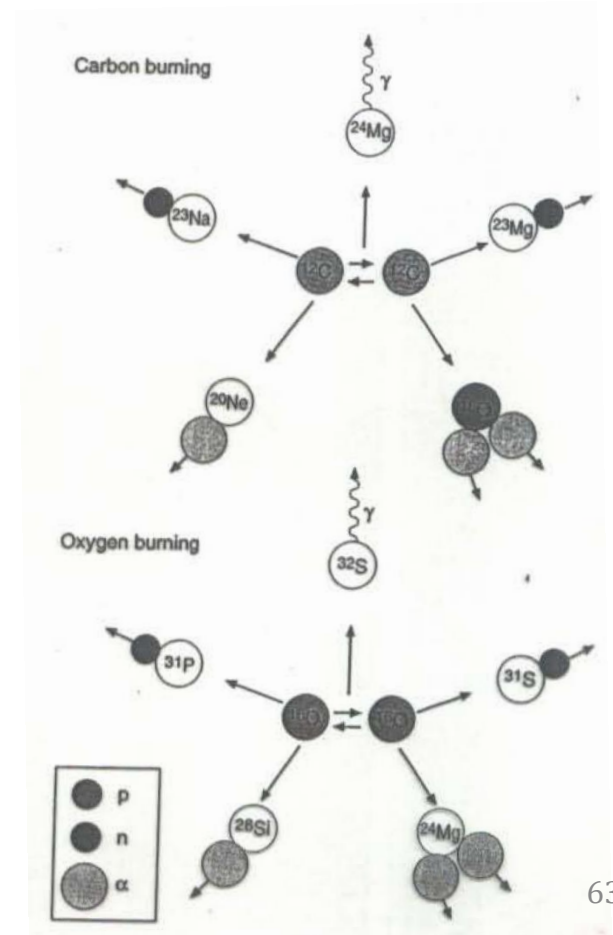$$^{16}O + {}^{16}O$$

$$T \gtrsim 10^9 \, K$$
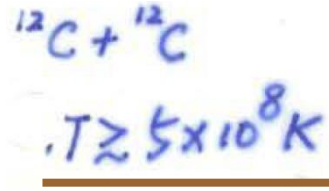
$$Q_{OO} \sim 16 \, MeV$$
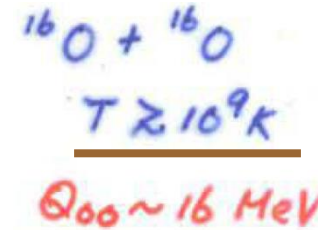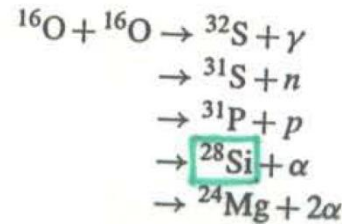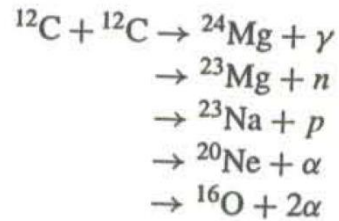
C-burning ignites when $T_c \sim (0.3\text{-}1.2) \times 10^9$ K, i.e., for stars 15-30 $M_\odot$

O-burning ignites when $T_c \sim (1.5\text{-}2.6) \times 10^9$ K, i.e., for stars > 15-30 $M_\odot$

The $p$ and $\alpha$ particles produced are captured immediately (because of the low Coulomb barriers) by heavy elements
➜ isotopes

O burning ➜ Si


Carbon burning / Oxygen burning

63

$$q_{PP} = 2.4 \times 10^6 \, \rho \, X^2 \, {T_6}^{-2/3} \exp\left[-33.8 \, {T_6}^{-1/3}\right] \quad [\text{erg g}^{-1} \text{s}^{-1}]$$

$$q \propto \rho \, X_H^2 \, T^4$$

$$q_{CN} = 8 \times 10^{27} \, \rho \, X \, X_{CN} \, {T_6}^{-2/3} \exp\left[-152.3 \, {T_6}^{-1/3}\right] \quad [\text{erg g}^{-1} \text{s}^{-1}]$$

$$q \propto \rho \, X_H X_{CN} \, T^{16} \qquad \frac{X_{CN}}{X_H} = 0.02 \text{ ok for Pop I}$$

$$q_{3\alpha} = 3.9 \times 10^{11} \, \rho^2 {X_\alpha}^3 \, {T_8}^{-3} \exp\left[-42.9 \, T_8\right] \quad [\text{erg g}^{-1} \text{s}^{-1}]$$

$$\approx 4.4 \times 10^{-8} \, \rho^2 {X_\alpha}^3 \, {T_8}^{40} \quad [\text{erg g}^{-1} \text{s}^{-1}] \quad (\text{if } T_8 \approx 1)$$

Does $^{28}Si$ follow the same scenario?

$^{28}Si + ^{28}Si \rightarrow ^{56}Fe$ ?

$C+C$   $6 \times 10^8 K$

$O+O$   $10^9 K$

?
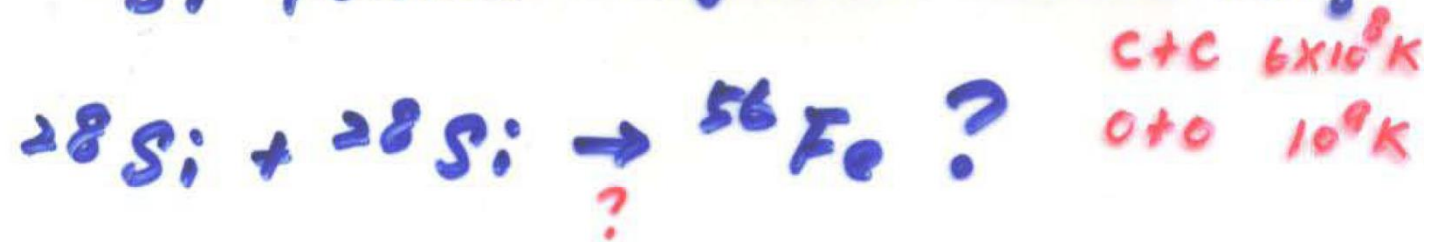
Coulomb barrier becomes extremly high; another nuclear reaction takes place

No!

eg.   $h\nu \rightsquigarrow O$ atom $< \begin{array}{l} ion \\ e^- \end{array}$

EM binding force

**Photoionization**
to break up an atom

Likewise

$h\nu \rightsquigarrow$ nucleus $< \begin{array}{l} \cdot \\ \cdot \end{array}$

nuclear binding force

**Photodisintegration**
to break up a nucleus

**Photodissociation**
to break up a molecule

For example, $^{16}O + \alpha \leftrightarrow {}^{20}Ne + \gamma$
If $T < 10^9$ K $\rightarrow$
but if $T \geq 1.5 \times 10^9$ K (in radiation field) $\leftarrow$

So $^{28}Si$ disintegrates at $\approx 3 \times 10^9$ K to lighter elements
   (then recaptured …)
until a nuclear statistical equilibrium is reached

But the equilibrium is not exact
   $\rightarrow$ a pileup of the iron group nuclei (Fe, Co, Ni)
      which can resist photodisintegration until $7 \times 10^9$ K

| Nuclear Fuel | Process | $T_{threshold}$ $(10^6 \text{ K})$ | Products | Energy per nucleon (MeV) |
|---|---|---|---|---|
| H | p-p | ~4 | He | 6.55 |
| H | CNO | 15 | He | 6.25 |
| He | $3\alpha$ | 100 | C, O | 0.61 |
| C | C + C | 600 | O, Ne, Na, Mg | 0.54 |
| O | O + O | 1,000 | Mg, S, P, Si | ~0.3 |
| Si | Nuc. Equil. | 3,000 | Co, Fe, Ni | <0.18 |

From Prialnik Table 4.1

- ❑ Interactions among charged particles ⟶ Coulomb barrier

- ❑ If there are enough neutrons around ⟶ neutron capture, not limited by Coulomb barrier, so proceed at relatively low $T$s
  ⟶ ever heavier isotopes or
  ⟶ radioactive decay
  ➔ a new element $+e^-$ (beta decay) $+ \bar{\nu}$ (antineutrino)

- ❑ Stable nuclei: neutron captures

- ❑ Unstable nuclei: neutron capture <u>or</u> $\beta^-$ decay

- ❑ $\beta^-$ decay has a constant time scales

- ❑ $n^0$ capture time scales $\longleftrightarrow (T, \rho)$
  ⟶ May proceed slower (***s*-process**) or more rapidly (***r*-process**) than the competing $\beta^-$ decays
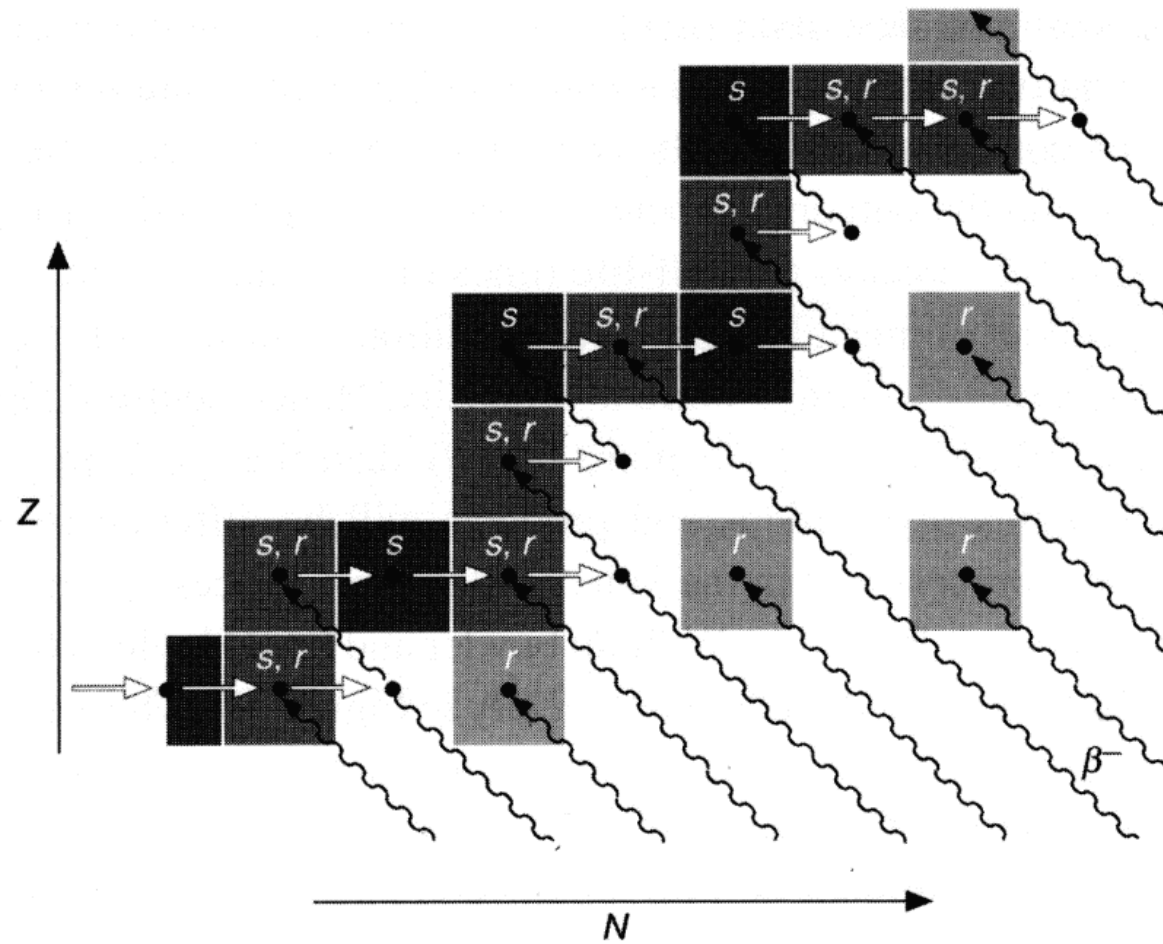
s-process
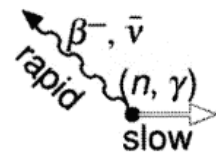
r-process
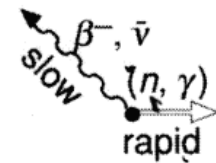
Prialnik Fig. 4.7

- ☐ Nuclear reactions: mass to energy (light)
- ☐ The reverse, energy into mass, is also possible; e.g., a photo → an electron + a position, if $h\nu > 2m_e c^2$, with the presence of a nucleus
- ☐ $kT \approx h\nu \approx 2m_e c^2, T \approx 1.2 \times 10^{10}$ K
- ☐ In reality, at $T \gtrsim 10^9$ K, sufficient photons (tail of the Planck function) for <span style="color:red">pair production. Annihilation</span> immediately destroys the positrons.

$$^{56}Fe + 124 \text{ MeV} \rightarrow 13 \, ^{4}He + 4 \, n$$

If $T \uparrow\uparrow\uparrow$, even $^{4}He \rightarrow p^{+} + n^{0}$

So stellar interior has to be between a few $T_6$ and a few $T_9$.

Lesson: Nuclear reactions that absorb (rather than emit) energy from ambient radiation field (in stellar interior) can lead to catastrophic consequences.

6/ $\qquad \rho = \rho_0 \left(1 - r/R_0\right)$

(a) $m(r) = \int_0^r 4\pi r^2 \rho(r)\, dr = \int_0^r 4\pi r^2 \cdot \rho_0 \left(1 - r/R_0\right) dr$

$\qquad = 4\pi \rho_0 \left(\dfrac{r^3}{3} - \dfrac{r^4}{4R_0}\right) = \dfrac{4}{3}\pi r^3 \rho_0 \left(1 - \dfrac{3r}{4R_0}\right)$

$\qquad \qquad \qquad \qquad \qquad \qquad \qquad \qquad \qquad \qquad \qquad \pi r^3 \rho_0 \left(\dfrac{4}{3} - \dfrac{r}{R_0}\right)$

(b) $M = \cancel{m} m(R) = \dfrac{6}{3}\pi R_0^3 \rho_0 = \cancel{\dfrac{4}{3}\left(\dfrac{4\rho_0}{\pi R_0}\right)^2}$

(c) $\dfrac{dP(r)}{dr} = -\rho_{(r)} \dfrac{G\, m(r)}{r^2}$

$\qquad dP = -\rho_0 \left(1 - \dfrac{r}{R_0}\right) G \cdot \dfrac{4}{3}\pi r^3 \rho_0 \left(1 - \dfrac{3r}{4R_0}\right) dr \Big/ r^2 \quad \text{\textcircled{1}}$

$\int_0^{R_0} \rightarrow$

$P(R_0) - P_c = \int \left\{ -\dfrac{4}{3}\pi G \rho_0^2 \left[ r - \dfrac{7}{4}\dfrac{r^2}{R_0} + \dfrac{3}{4}\dfrac{r^3}{R_0^2} \right]_0^{R_0} \right\} dr$

$\qquad P_c = \dfrac{4}{3}\pi G \rho_0^2 R_0^2 \left( \dfrac{1}{2} - \dfrac{7}{12} + \dfrac{3}{16} \right) \qquad \dfrac{-1}{12} + \dfrac{3}{16} = \dfrac{-16 + 36}{12 \cdot 16} = \dfrac{2}{12 \cdot}$

$\qquad = \dfrac{5}{36}\pi G \rho_0^2 R_0^2 \quad \text{\textcircled{2}} \quad = \dfrac{5}{4}\dfrac{GM^2}{\pi R_0^4} \quad \text{\textcircled{3}}$

If now integrating from 0 to r of $\text{\textcircled{1}}$ $\qquad\qquad \dfrac{P(r)}{P_c} = \left(1 - \dfrac{24}{5}\dfrac{r^2}{R_0^2} + \dfrac{28}{5} \cdots \right)$

$\qquad \int_0^r dP =$

$\qquad P(r) - P_c = -\dfrac{4}{3}\pi G \rho_0^2 \left[ \dfrac{r^2}{2} - \dfrac{7}{12}\dfrac{r^3}{R_0} + \dfrac{3}{16}\dfrac{r^4}{R_0^2} \right]$

$\qquad \qquad \text{\textcircled{2}}\nearrow \qquad\qquad \pi G \rho_0^2 R_0^2 \left[ \dfrac{5}{36} - \dfrac{2}{3}\dfrac{r^2}{R_0^2} + \dfrac{7}{9}\dfrac{r^3}{R_0^3} - \dfrac{1}{4}\dfrac{r^4}{R_0^4} \right]$

$\therefore P(r) = \dfrac{5}{36}\pi G \rho_0^2 R_0^2 \cdot$

$\qquad\qquad \left(1 - \dfrac{24}{5}\dfrac{r^2}{R_0^2} + \dfrac{28}{5}\dfrac{r^3}{R_0^3} - \dfrac{9}{5}\dfrac{r^4}{R_0^4}\right)$

(d) $\qquad \qquad \qquad \qquad \qquad \qquad \qquad \qquad \qquad \qquad \left(\dfrac{5}{36}\pi \dfrac{G\mu m_H}{k_B} R_0^2 \rho_0\right)$

$T_c = \dfrac{P_c}{k_B} \cdot \dfrac{\mu m_H}{\rho_0} = \dfrac{1}{k_B} \cdot \dfrac{5}{4}\dfrac{GM^2}{\pi R_0^4} \mu m_H \cdot \dfrac{\frac{1}{3}\pi R_0^3}{M} = \dfrac{5}{12}\dfrac{G\mu m_H}{k_B}\left(\dfrac{M}{R_0}\right) \propto \dfrac{M}{R_0}$

73

2. (a) From hydrostatic equilibrium and mass continuity:

$$\frac{dP(r)}{dr} = -\frac{Gm(r)}{r^2}\rho(r), \quad \frac{dm(r)}{dr} = 4\pi r^2 \rho(r)$$

where $\rho(r) = \rho_0\left(1 - \frac{r}{R_0}\right)$

$$\frac{dm(r)}{dr} = 4\pi r^2 \rho_0\left(1 - \frac{r}{R_0}\right) = 4\pi\rho_0\left(r^2 - \frac{r^3}{R_0}\right) \Rightarrow dm(r) = 4\pi\rho_0\left(r^2 - \frac{r^3}{R_0}\right)dr$$

$$m(r) = \int dm(r) = \int 4\pi\rho_0\left(r^2 - \frac{r^3}{R_0}\right)dr = \boxed{4\pi\rho_0\left(\frac{r^3}{3} - \frac{r^4}{4R_0}\right)} \quad \checkmark$$

(b) The stellar mass $M = m(R_0)$, substitute the answer (a)

$$M = 4\pi\rho_0\left(\frac{R_0^3}{3} - \frac{R_0^4}{4R_0}\right) = 4\pi\rho_0\left(\frac{1}{12}R_0^3\right) = \boxed{\frac{1}{3}\pi\rho_0 R_0^3} \quad \checkmark$$

(c) Rewrite hydrostatic equilibrium by $m(r)$, $\rho(r)$:

$$\frac{dP(r)}{dr} = -\frac{Gm(r)}{r^2}\rho(r) = -\frac{G 4\pi\rho_0^2\left(\frac{r^3}{3} - \frac{r^4}{4R_0}\right)}{r^2}\rho_0\left(1 - \frac{r}{R_0}\right) = -4\pi G\rho_0^2\left(\frac{1}{3}r - \frac{1}{3R_0}r^2 - \frac{1}{4R_0}r^2 + \frac{1}{4R_0^2}r^3\right)$$

$$P(r) = \int dP(r) = \int_{R_0}^{r} -4\pi G\rho_0^2\left(\frac{1}{3}r - \frac{1}{3R_0}r^2 - \frac{1}{4R_0}r^2 + \frac{1}{4R_0^2}r^3\right) = -4\pi G\rho_0^2\left(\frac{r^2}{6} - \frac{r^3}{9R_0} - \frac{r^3}{12R_0} + \frac{r^4}{16R_0^2}\right)\Big|_{R_0}^{r}$$

$$= -4\pi G\rho_0^2\left(\frac{r'^2}{6} - \frac{r'^3}{9R_0} - \frac{r'^3}{12R_0} + \frac{r'^4}{16R_0^2} - \frac{5}{144}R_0^2\right)$$

The central pressure $P_c$, where $r' = 0$: $P_c = 4\pi G\rho_0^2\frac{5}{144}R_0^2$

The relative pressure:

$$\frac{P}{P_c} = \frac{-4\pi G\rho_0^2\left(\frac{r'^2}{6} - \frac{r'^3}{9R_0} - \frac{r'^3}{12R_0} + \frac{r'^4}{16R_0^2} - \frac{5}{144}R_0^2\right)}{4\pi G\rho_0^2\frac{5}{144}R_0^2} = \boxed{-\frac{24}{5}\left(\frac{r'}{R_0}\right)^2 + \frac{28}{5}\left(\frac{r'}{R_0}\right)^3 - \frac{9}{5}\left(\frac{r'}{R_0}\right)^4 + 1} \quad \checkmark$$

Plot the relation between $\left(\frac{P}{P_c}\right)$ and $\left(\frac{r}{R_0}\right)$ by Python.



Pressure—Radius diagram

$\checkmark$
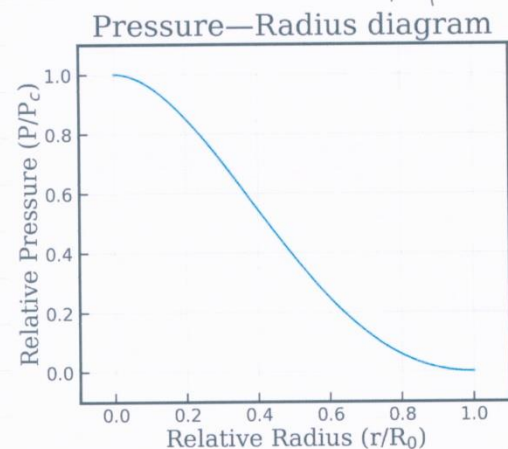
(d) From ideal gas law:

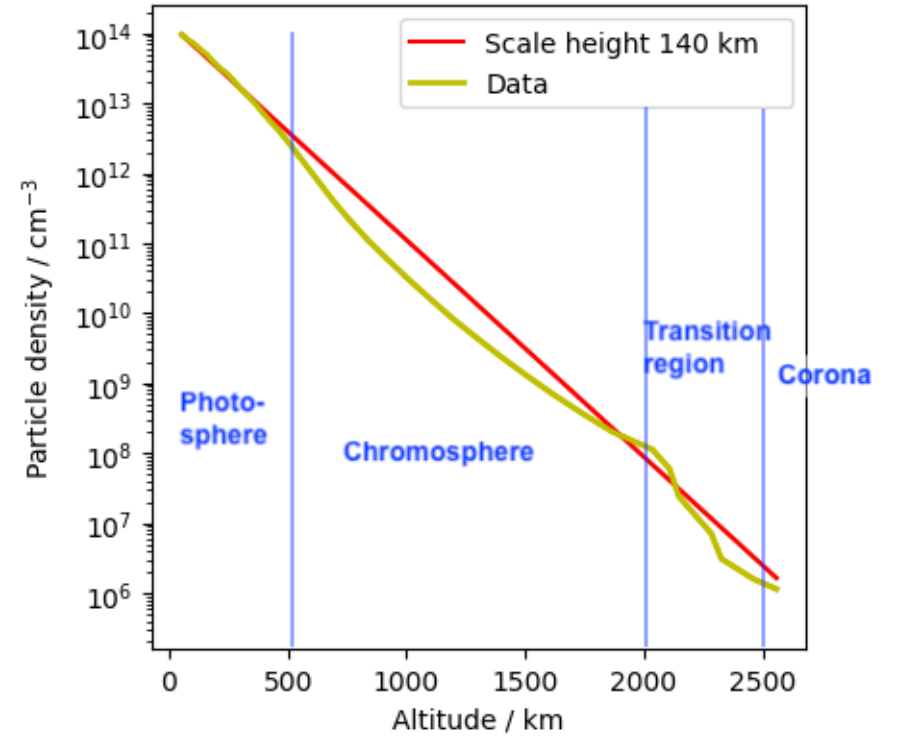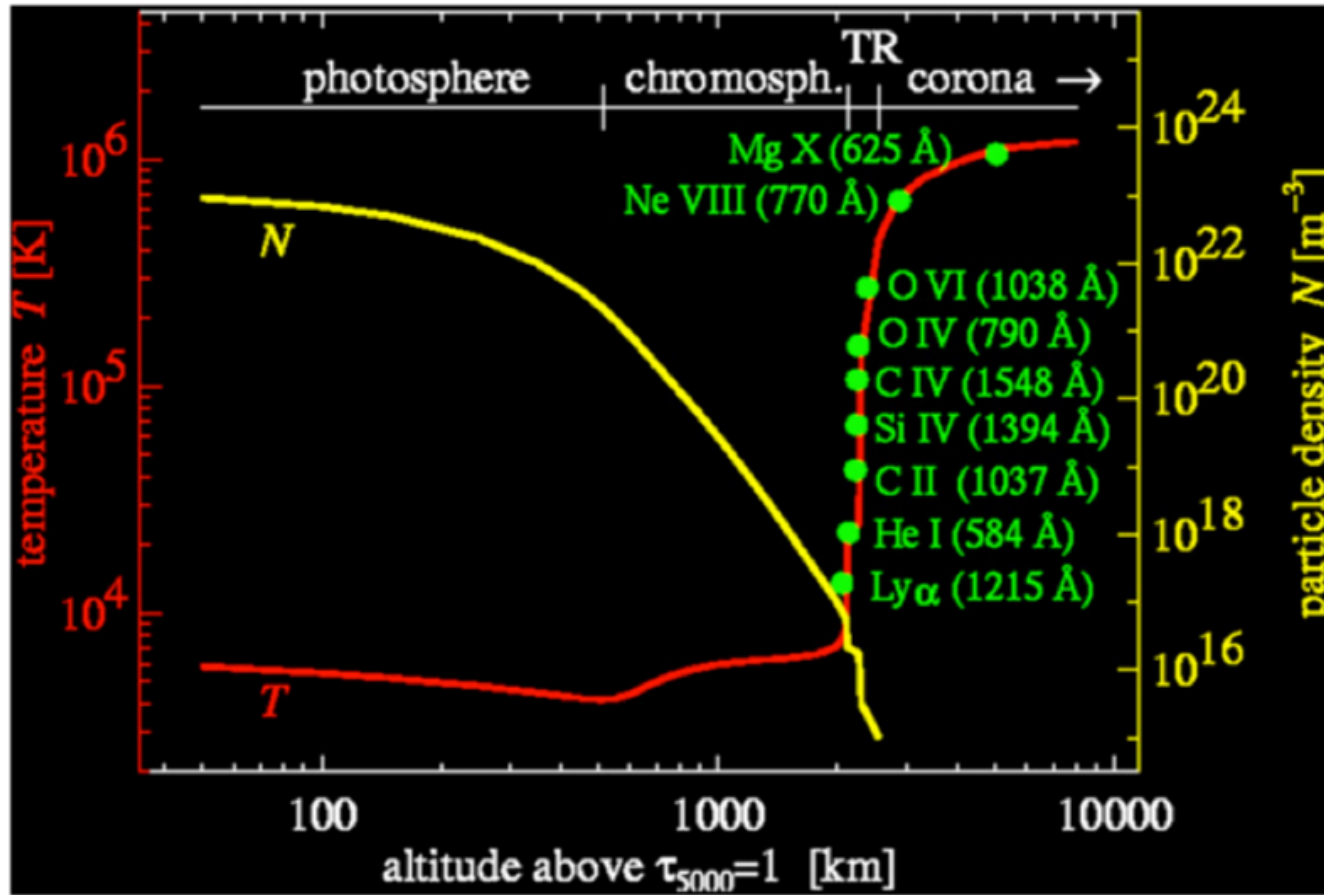$$P = \frac{\rho}{\mu m_H}kT \Rightarrow T = \frac{\mu m_H}{\rho k}P$$

The central temperature:

$$T_c = \frac{\mu m_H}{\rho_0 k}P_c = \frac{\mu m_H}{\rho_0 k}\left(\frac{5}{36}\pi G\rho_0^2 R_0^2\right) = \boxed{\frac{5}{36}\frac{\mu m_H}{k}\pi G\rho_0 R_0^2} \quad \checkmark$$

Scale height $H = K_B T/mg$ ; $g = \dfrac{GM}{r^2}$

assuming all H (neutral) $\begin{array}{l}\text{fully ion. } \mu = 0.6 \\ \text{fully neu, } \mu = 1.25\end{array}$ $g_\odot \sim 2.7 \times 10^4 \text{ cm s}^{-2}$

$$H_\odot \doteq \frac{K_B T R_\odot^2}{G M_\odot m_p} \sim 170 \text{ km} \quad \left(\begin{array}{l}\sim 290 \text{ km if } \mu = 0.6 \\ \sim 140 \text{ km if } \mu = 1.25\end{array}\right.$$

https://astronomy.stackexchange.com/questions/30232/does-the-suns-atmosphere-have-a-scale-height

$$p \sim \hbar/a \qquad E \sim \frac{p^2}{2m} \sim \frac{\hbar^2}{2ma^2}$$

4.

(1) Electronic transitions

$$E_e \sim \frac{Ze^2}{a} \qquad \text{where } a \sim 1\,\text{Å}$$

$$\Rightarrow \text{typically a few eV} \quad \nu_e \sim 10^{15}\,s^{-1} \quad \lambda \sim 0.3\,\mu m$$

$$\therefore \text{ in UV and visible}$$
$$\uparrow$$
$$\text{higher level} \quad \text{transitions}$$

(2) Rotational transitions

$$E_{rot} \sim \frac{L^2}{2I} \qquad \text{where } L = n\hbar \text{ and } I = \mu R^2$$

$$\text{taking typical } R \sim 1\,\text{Å} \quad \mu \sim 10^{-24}\,g$$

$$\Rightarrow \text{typically a few} \times 10^{-3}\,eV$$

$$\nu_{rot} \sim 10^{12}\,s^{-1} \quad \lambda \sim 300\,\mu m$$

$$\therefore \text{ in far-IR and sub-mm}$$

(3) Vibrational transitions

$$E_{vib} \sim (n + \tfrac{1}{2})\,\hbar\omega \qquad \text{where } \omega \sim \sqrt{\frac{e^2}{\mu R^3}}$$

$$R \sim 1\,\text{Å}$$

$$\Rightarrow \text{typically } E_{vib} \sim \text{a few} \times 10^{-1}\,eV$$

SHO $\qquad T = \frac{2\pi}{\omega} \qquad \nu_{vib} \sim 10^{14}\,s^{-1} \quad \lambda \sim 3\,\mu m$

$$\frac{e^2}{r^2} = \frac{4\pi^2 r}{T^2}\mu = \mu r \omega^2$$

$$\therefore \text{ in IR}$$

$$\therefore \omega = \sqrt{\frac{e^2}{\mu r^3}}$$

巨門文具再生紙系列・沒有一棵樹因它而倒

## Synthesis of the Elements in Stars[*]

E. MARGARET BURBIDGE, G. R. BURBIDGE, WILLIAM A. FOWLER, AND F. HOYLE

*Kellogg Radiation Laboratory, California Institute of Technology, and
Mount Wilson and Palomar Observatories, Carnegie Institution of Washington,
California Institute of Technology, Pasadena, California*

"It is the stars, The stars above us, govern our conditions";
(*King Lear*, Act IV, Scene 3)

but perhaps

"The fault, dear Brutus, is not in our stars, But in ourselves,"
(*Julius Caesar*, Act I, Scene 2)
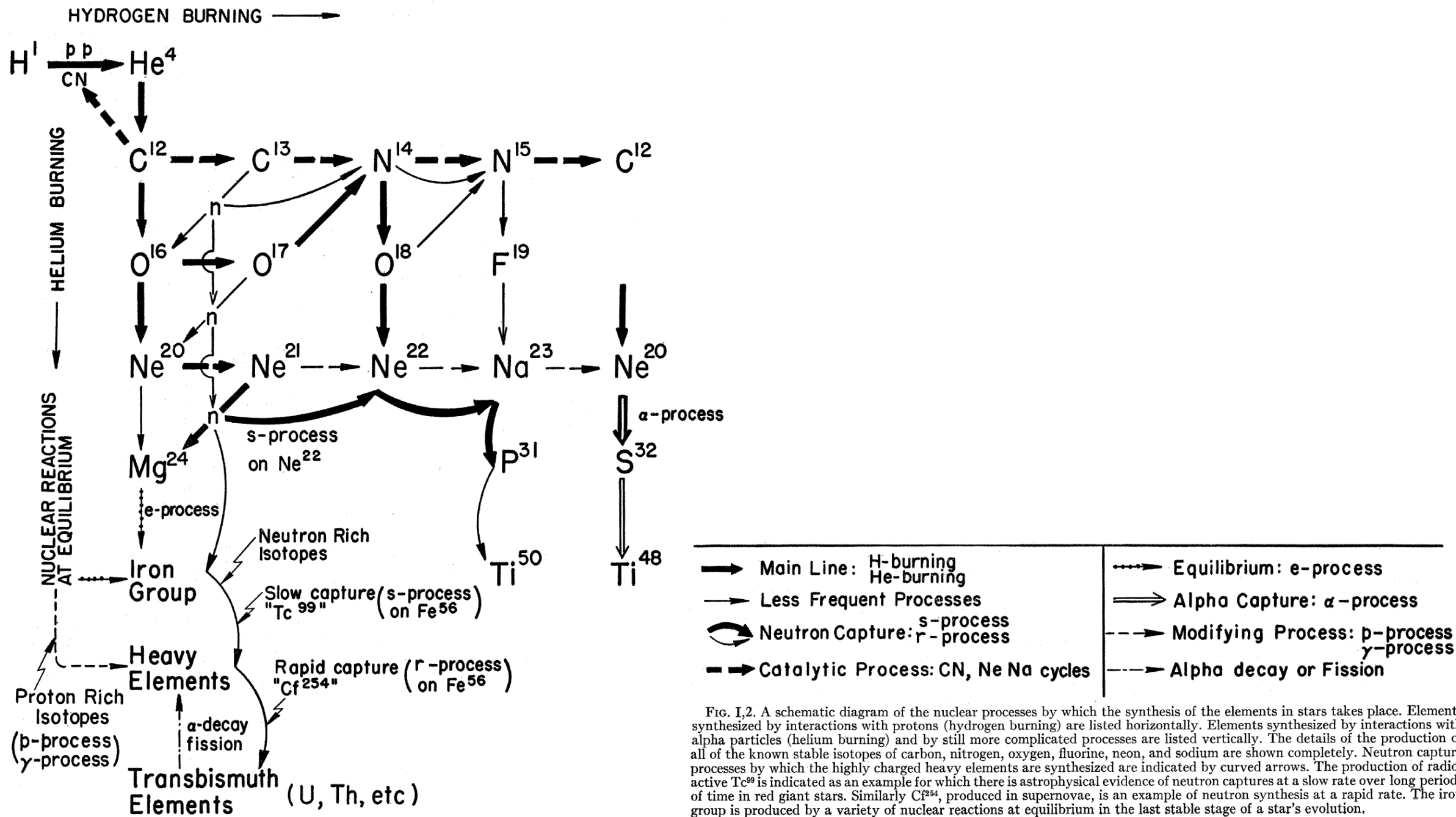
FIG. I,2. A schematic diagram of the nuclear processes by which the synthesis of the elements in stars takes place. Elements synthesized by interactions with protons (hydrogen burning) are listed horizontally. Elements synthesized by interactions with alpha particles (helium burning) and by still more complicated processes are listed vertically. The details of the production of all of the known stable isotopes of carbon, nitrogen, oxygen, fluorine, neon, and sodium are shown completely. Neutron capture processes by which the highly charged heavy elements are synthesized are indicated by curved arrows. The production of radioactive Tc[99] is indicated as an example for which there is astrophysical evidence of neutron captures at a slow rate over long periods of time in red giant stars. Similarly Cf[254], produced in supernovae, is an example of neutron synthesis at a rapid rate. The iron group is produced by a variety of nuclear reactions at equilibrium in the last stable stage of a star's evolution.

### (iii) $\alpha$ Process

These processes include the reactions in which $\alpha$ particles are successively added to $Ne^{20}$ to synthesize the four-structure nuclei $Mg^{24}$, $Si^{28}$, $S^{32}$, $A^{36}$, $Ca^{40}$, and probably $Ca^{44}$ and $Ti^{48}$. This is also discussed in Sec. III. The source of the $\alpha$ particles is different in the $\alpha$ process than in helium burning.

### (iv) e Process

This is the so-called equilibrium process previously discussed by Hoyle (Ho46, Ho54) in which under conditions of very high temperature and density the elements comprising the iron peak in the abundance curve (vanadium, chromium, manganese, iron, cobalt, and nickel) are synthesized. This is considered in detail in Sec. IV.

### (v) s Process

This is the process of neutron capture with the emission of gamma radiation $(n,\gamma)$ which takes place on a long time-scale, ranging from $\sim$100 years to $\sim 10^5$ years for each neutron capture. The neutron captures occur at a *slow* (s) rate compared to the intervening beta decays. This mode of synthesis is responsible for the production of the majority of the isotopes in the range $23 \leq A \leq 46$ (excluding those synthesized predominantly by the $\alpha$ process), and for a considerable proportion of the isotopes in the range $63 \leq A \leq 209$. Estimates of the time-scales in different regions of the neutron-capture

### (vi) r Process

This is the process of neutron capture on a very short time-scale, $\sim$0.01–10 sec for the beta-decay processes interspersed between the neutron captures. The neutron captures occur at a *rapid* (r) rate compared to the beta decays. This mode of synthesis is responsible for production of a large number of isotopes in the range $70 \leq A \leq 209$, and also for synthesis of uranium and thorium. This process may also be responsible for some light element synthesis, e.g., $S^{36}$, $Ca^{46}$, $Ca^{48}$, and perhaps $Ti^{47}$, $Ti^{49}$, and $Ti^{50}$. Details of this process and the results of the calculations are discussed in Secs. VII and VIII. The r process produces the abundance peaks at $A=80$, 130, and 194.

### (vii) p Process

This is the process of proton capture with the emission of gamma radiation $(p,\gamma)$, or the emission of a neutron following gamma-ray absorption $(\gamma,n)$, which is responsible for the synthesis of a number of proton-rich isotopes having low abundances as compared with the nearby normal and neutron-rich isotopes. It is discussed in Sec. IX.

### (viii) x Process

This process is responsible for the synthesis of deuterium, lithium, beryllium, and boron. More than one type of process may be demanded here (described collectively as the x process), but the characteristic of all

80

# Luminosity

Ohm's law in a circuit, $I = V / R$,

in electromagnetics, $\vec{J}$ [current density] $= \sigma$ [conductivity] $\vec{E}$ [electric field]
In hydraulics, [flow] $\propto$ [pressure gradient] / [resistance]

$$L \sim 4\pi R^2 \frac{d\left(\frac{1}{3}aT^4\right)/dr}{\kappa\rho}$$

(unit) Pressure = [energy] / [volume]

$$\sim 4\pi R^2 \frac{4}{3}\frac{aT^3}{\kappa\rho}\frac{dT}{dr}$$

$$\sim \frac{R^2 T^3}{\kappa\rho}\frac{dT}{dr}$$

Blackbody radiation
Energy density $u = aT^4$
Radiation pressure $P_{\text{rad}} = (1/3)\,u$

For a given structure,

$$\frac{dT(r)}{dr} = -\frac{3\kappa\rho L(r)}{4ac\ 4\pi r^2 T^3}$$

$$T \sim T_c, \frac{dT}{dr} \sim \frac{T_c}{R}, T_c \sim \frac{\mu GM}{R}$$

$$L \sim \frac{R^2\ T^4/R}{\kappa(M/R^3)} \sim \frac{R^4 T^4}{\kappa M} \sim \frac{R^4}{\kappa M}\left(\frac{\mu GM}{R}\right)^4$$

$$\boxed{L \sim \frac{\mu^4 G^4 M^3}{\kappa}}$$

The opacity $\kappa = \kappa(\rho, T, \mu)$

$$L \sim \frac{\mu^4 G^4 M^3}{\kappa}$$

☐ For <u>solar composision</u>, <u>Kramers opacity</u>

$$\kappa \sim \rho T^{-3.5} \quad \text{valid for } 10^4\text{--}10^6 \text{ K.}$$

$$T \sim \frac{\mu \, GM}{R}$$

So $\kappa \sim \mu^{-3.5} G^{-3.5} M^{-2.5} R^{0.5}$

and $\boxed{L \sim \mu^{7.5} G^{7.5} M^{5.5} R^{-0.5}}$

☐ For <u>high-mass stars</u>, i.e., high temperature and low density, opacity by <u>electron scattering</u>

$$\kappa = 0.2 \, (1 + X) \text{ cm}^2\text{g}^{-1} = \text{const.}$$

and $\boxed{L \sim \mu^4 G^4 M^3}$

# Mass-luminosity relation for main-sequence stars
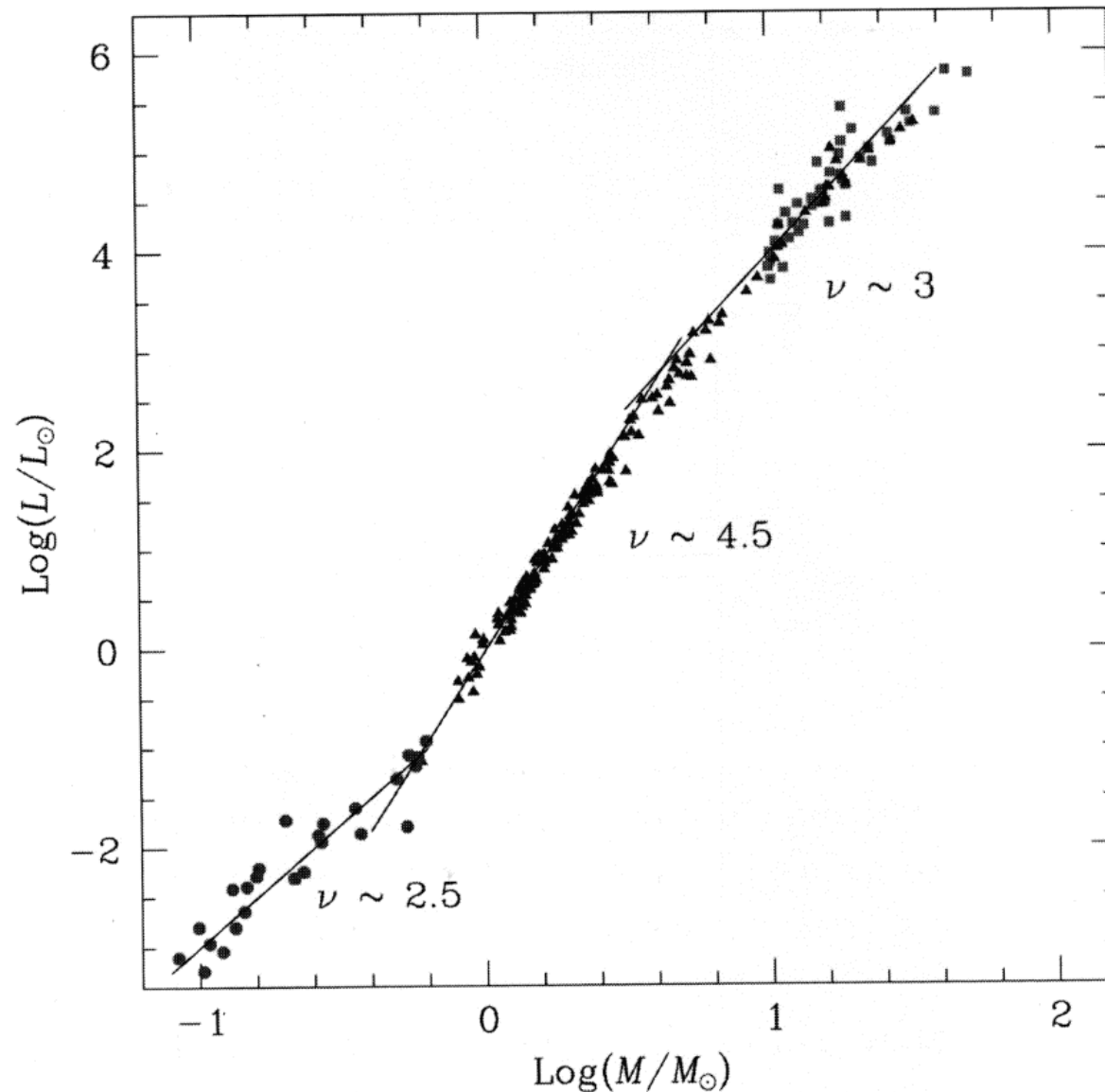


$$\frac{L}{L_\odot} = \left(\frac{M}{M_\odot}\right)^\nu$$

Prianik Fig. 1.6

84

$$T_c \approx \frac{\mu\, GM}{R}$$

So for a given $T_c$, $M \rightarrow R$
$\left. \begin{array}{c} \\ \text{MLR} \rightarrow L \end{array} \right\}$ $L \left(\propto R^2 T_{\text{eff}}^4\right)$ and $T_{\text{eff}}$

Main sequence is a run of $L$ and $T_{\text{eff}}$ as a function of stellar mass, with $T_c$ nearly constant.

Why $T_c \approx$ constant?
Because onset of H burning $\sim 10^7$ K regardless of the stellar mass

# The main sequence

Recall for low-mass stars, $L \propto M^{5.5} R^{-0.5}$, pp chain $q \propto \rho_c T^4$

The energy-generation equation,

$$\frac{dL}{dr} = 4\pi r^2 \rho_c \, q$$

$$\Rightarrow L \propto R^3 \rho_c^2 \, T^4 = R^3 \left(\frac{M}{R^3}\right)^2 \left(\frac{M}{R}\right)^4 = \frac{M^6}{R^7}$$

$R \sim M^{1/13}$ ............... Stellar radius $\leftrightarrow$ very weakly on the mass

$L \sim M^{71/13} \approx M^{5.5}$ ... Stellar Luminosity $\leftrightarrow$ strongly on the mass

# The main sequence in the HRD

Recall for <u>low-mass stars</u>, $L \propto M^{5.5} R^{-0.5}$, pp chain $q \propto \rho_c T^4$

The energy-generation equation,

$$\frac{dL}{dr} = 4\pi r^2 \rho_c \, q$$

$$\implies L \propto R^3 \rho_c^2 \, T^4 = R^3 \left(\frac{M}{R^3}\right)^2 \left(\frac{M}{R}\right)^4 = \frac{M^6}{R^7}$$

$R \sim M^{1/13}$ .............. Stellar radius varies weakly with the mass

$L \sim M^{71/13} \approx M^{5.5}$ ... Stellar Luminosity varies strongly ...

In the HRD, $L \propto R^2 T_e^4 \longrightarrow L^{981/1007} \propto T_e^4$

   or $\log L \approx 4 \log T_e + $ const (i.e., constant radius)

For <u>high-mass stars</u>, $L \propto M^3$,
CNO cycle $q \propto \rho_c \, T^{16}$

Then, $M^{15} \propto R^{19}$, so $L \propto T_e^{76/9}$
   or $\log L \approx 8.4 \log T_e + \text{const}$

That is, a steeper MS slope in the HRD
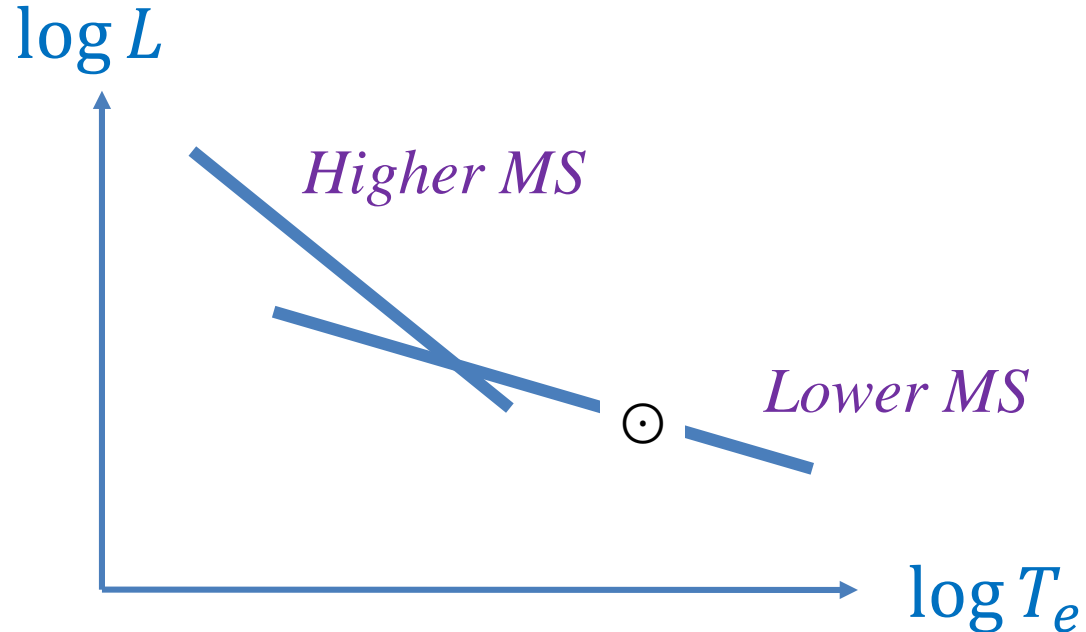




→ GAIA'S HERTZSPRUNG-RUSSELL DIAGRAM
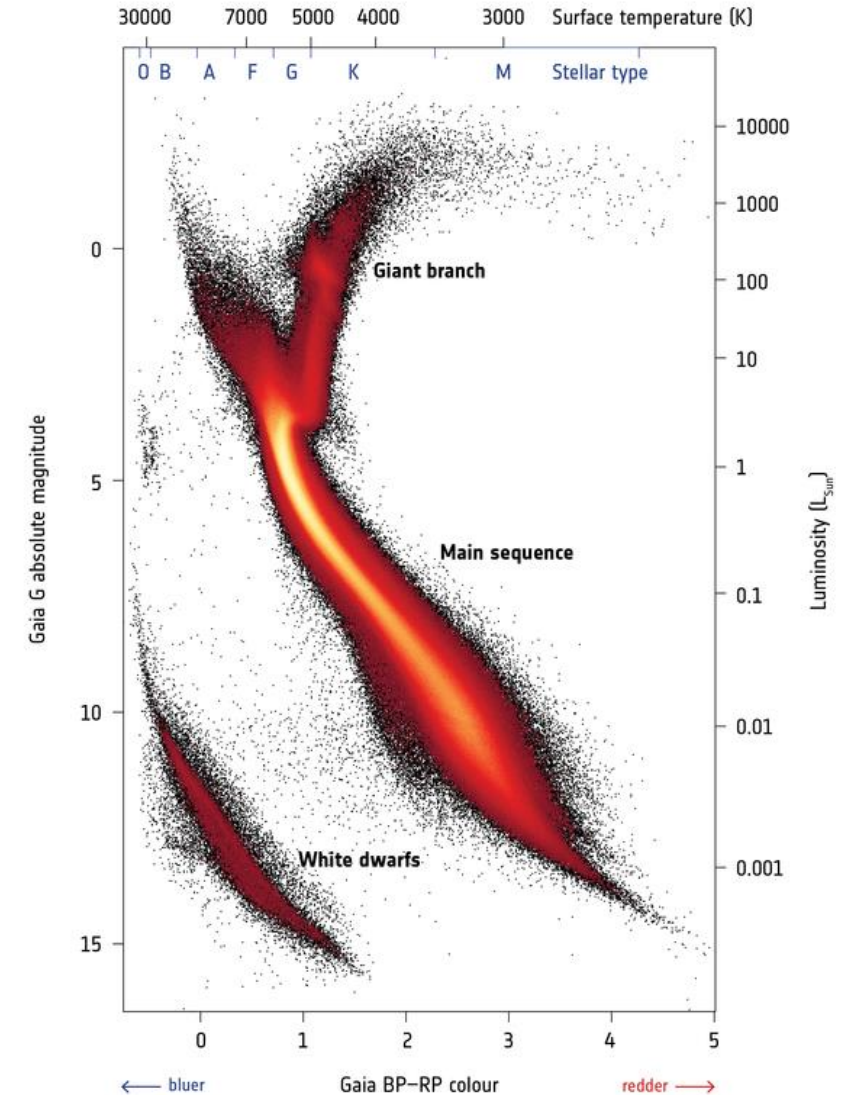
# Main sequence with different composition

Less metals → lower opacity → more compact envelope and denser cores → $T_c \uparrow, L \uparrow$

ZAMS to the left and higher



data from Schaller et al. (1992)

$X = 0.70$

ZAMS for
Z =
0.001
0.004
0.008
0.020

2.0 M$_\odot$

1.5 M$_\odot$

1.0 M$_\odot$
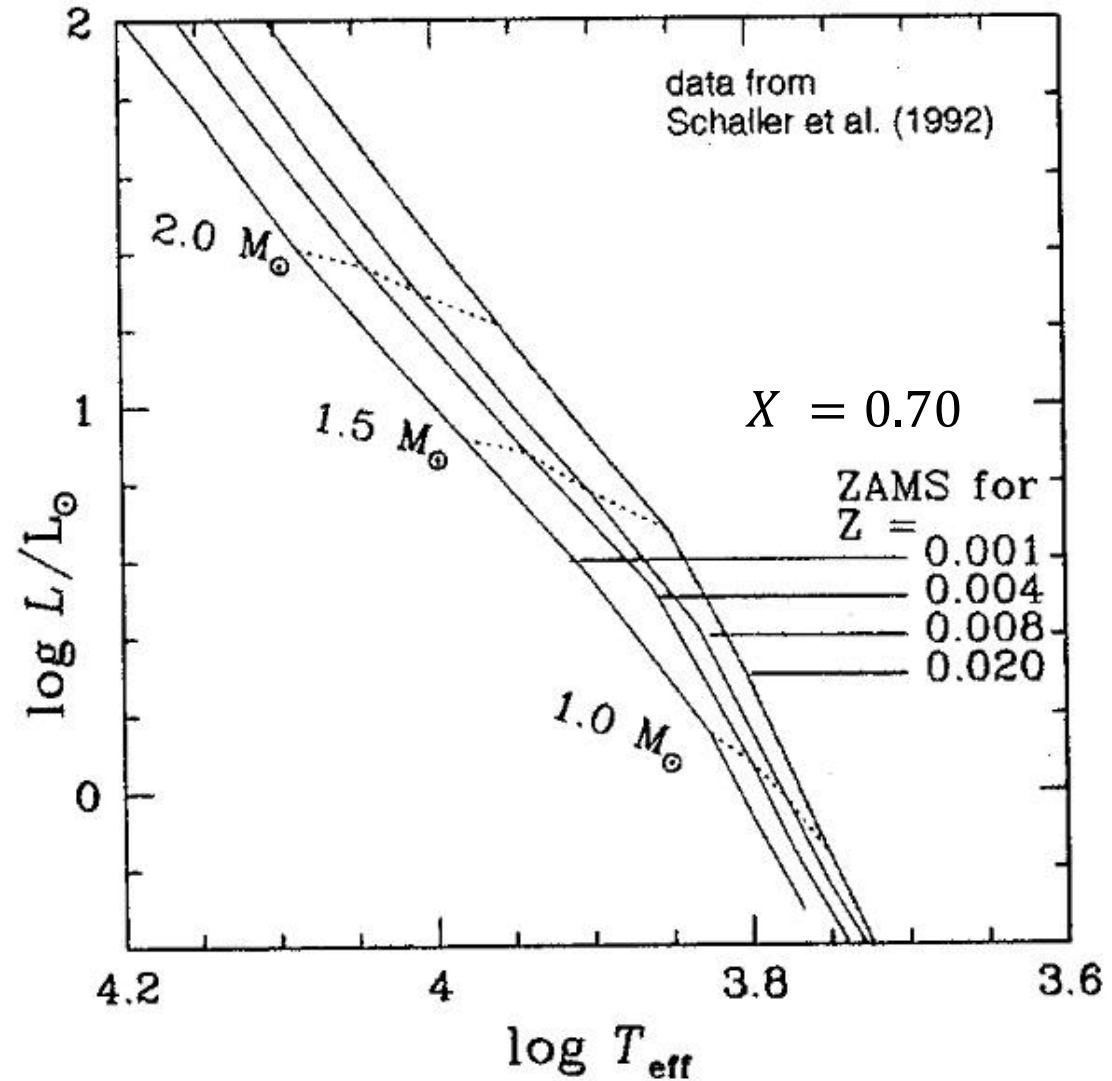
De Boer & Seggewiss, Fig 6.7
data from Schaller+92

# Main Sequence Lifetimes

$$\tau_{\text{Nuclear}} \propto \frac{M}{L}$$

$\propto M^{-4.5}$ (for low-mass stars)

or

$\propto M^{-2}$ (for massive stars)

Calibrated with the Sun.

# Main-Sequence Lifetime of the Sun

## Energy Gained in a PP Chain

- 4H → 1 He + neutrinos + energy
- Mass of 4 H = 6.693 x $10^{-27}$ kg
- − Mass of 1 He = 6.645 x $10^{-27}$ kg
- **Mass deficit ➜ 0.048 × $10^{-27}$ kg = 0.7%**

$$M_\odot \approx 2 \times 10^{33} \ [\text{g}]$$
$$L_\odot \approx 4 \times 10^{33} \ [\text{ergs/s}]$$

**Fusion efficiency**

| Nuclear physics | | Stellar physics |

$$\tau_\odot^{\text{MS}} \approx M_\odot \frac{(0.007)(0.1) \, c^2}{L_\odot} = 3.15 \times 10^{17} [\text{s}] = 10^{10} \ [\text{yr}]$$

$$\text{Given } L_{\text{MS}}/L_\odot \approx \left(M/M_\odot\right)^{3.5} \rightarrow \tau^{\text{MS}} \approx 10^{10} \left(M_\odot/M\right)^{2.5} [\text{yr}]$$

Energy can be transported by conduction or convection, or radiation.

Conduction: by microscopic collision of particles and movement of electrons.
Flux density [erg/s/cm$^2$] $= -\kappa \nabla \mathrm{T}$


NASA

Convection: by bulk motion of particles in a fluid (gas or liquid): *advection*（平流）(directional flow of energy) or *diffusion*（擴散）(non-directional along a concentration gradient).

Convection does not happen in solids.

Stars transport energy by either radiation or convection. Conduction is effective only in compact objects, e.g., in isothermal cores in WDs.
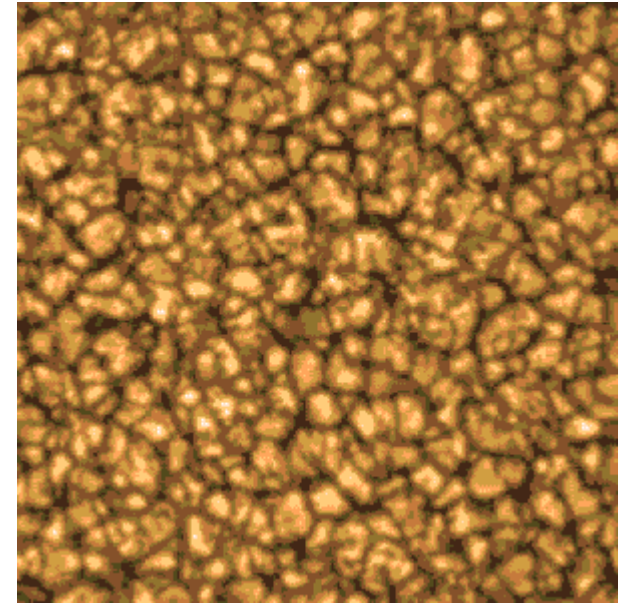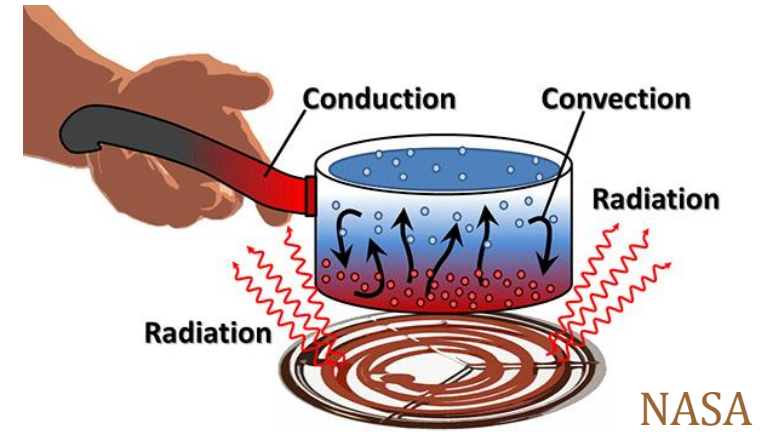
# Convective equilibrium (stability vs instability)

Convection takes over? When an element moves vertically, does it continue to move? Key: Temperature gradients

Element maintaining pressure equilibrium with surrounding, $P_2' = P_2$, ideal gas law $\rightarrow \rho_2 T_2 = \rho_2' T_2'$,

Consider an element cell floats upwards

$P_2', T_2', \rho_2'$    $P_2, T_2, \rho_2$    If $\rho_2' > \rho_2$ (or $T_2' < T_2$) $\rightarrow$ sink back; no convection

$T_2 < T_1$

To <u>have</u> convection, the element (rising adiabatically) should cool slower than the surrounding (in radiative equilibrium), i.e.,

$P_1', T_1', \rho_1'$    $P_1, T_1, \rho_1$    $\left(\dfrac{dT}{dr}\right)_{\text{element}} < \left(\dfrac{dT}{dr}\right)_{\text{surrounding}}$    or $\left(\dfrac{dT}{dr}\right)_{\text{ad}} < \left(\dfrac{dT}{dr}\right)_{\text{rad}}$
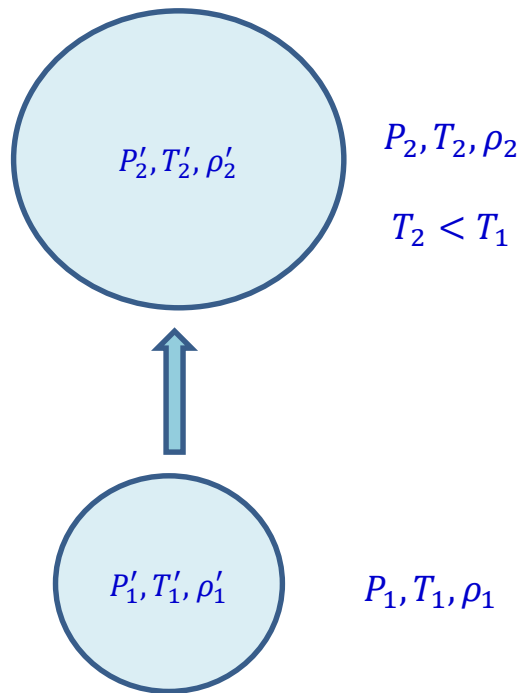
$\Rightarrow$ Convection sets in when the adiabatic temp. gradient is smaller than temp. gradient by radiative equil.

Compared with the surrounding temperature gradient

i.e., $\boxed{\left(\dfrac{dT}{dr}\right)_{ad} < \left(\dfrac{dT}{dr}\right)_{rad}}$

Radiation can no longer transport the energy efficiently enough
→ Convective instability

For an adiabatic process, $PV^{\gamma} = constant$

The rising height is typified by the mixing length $\ell$, or parameterized as the scale height $H$, defined as the pressure (or density) varies by a factor of $e$ times. Usually $0.5 \lesssim \ell/H \lesssim 2.0$

Since $\dfrac{dP}{dr} = -\rho g$ and $P = \rho k T$

$$dT \cdot \dfrac{dP}{dr} \dfrac{1}{P} \propto \dfrac{1}{T} \cdot dT$$

$$\therefore \quad \dfrac{dT}{dr} \propto \dfrac{dT/T}{dP/P} = \dfrac{d\ln T}{d\ln P}$$

$\Rightarrow$ Criterion for convection equilibrium becomes

$$\left( \dfrac{d\ln T}{d\ln P} \right)_{ad} < \left( \dfrac{d\ln T}{d\ln P} \right)_{rad}$$

With the notation $\nabla$ ( nabla )

$$\nabla_{ad} < \nabla_{rad}$$

96

Convection takes place when the temperature gradient is "sufficiently" high (compared with the adiabatic condition) or the pressure gradient is low enough.

Such condition also exists when the gas absorbs a great deal of energy without temperature increase, e.g., with phase change or ionization

➔ when $c_V$ is large or $\gamma$ is small

$$\left(\frac{dT}{dr}\right)_{ad} < \left(\frac{dT}{dr}\right)_{rad}$$

$$\left(\frac{d\ln T}{d\ln P}\right)_{ad} < \left(\frac{d\ln T}{d\ln P}\right)_{rad}$$

$$\gamma = \frac{Nk}{c_V} + 1$$

In meteorology, dry and cool air tends to be stable, whereas wet and warm air (smaller gamma values) is vulnerable to convection ➔ thunderstorm

Note that for an adiabatic process for an ideal gas

☐ $P = nkT \propto \rho T$

So $\dfrac{dP}{P} = \dfrac{d\rho}{\rho} + \dfrac{dT}{T}$

And recall again

✓ $nk = c_p - c_v$

✓ $\gamma = \dfrac{c_p}{c_v} = \dfrac{1+n/2}{n/2} = 1 + \dfrac{2}{n}$, here $n$ is d.o.f.

✓ Note $n \nearrow, \gamma \searrow$

Note.     $\nabla_{rad} \propto P$

At surface   $\nabla_{rad} \to 0$

$\therefore \quad \overset{always}{\nabla_{ad} >} \nabla_{rad} \Rightarrow$ no convection!

The outermost layers of a star are always
in radiative equilibrium.


$\therefore$  Convection occurs  either

① large temperature gradient for
                        radiative equilibrium
② small adiabatic temperature gradient

Convection occurs when $\nabla_{\text{rad}} > \nabla_{\text{ad}}$

That is, when $\nabla_{\text{rad}}$ is large, or when $\nabla_{\text{ad}}$ is small.

To recap

$$\nabla_{\text{rad}} = \frac{dT}{dr} = \frac{L_r}{r^2}\frac{\kappa\rho}{\sigma T^3}$$

$$\nabla_{\text{ad}} = 1 - \frac{1}{\gamma}, \text{ where } \gamma = \left. c_p \middle/ c_v \right.$$

→ $\nabla_{\text{ad}}$ small → $c_v$ large ➜ $H_2$ dissociation (PMS Hayashi tracks)

H ionization, T~6,000 K

He ionization, T~20,000 K

He II ionization, T~50,000 K

**<span style="color:red">Ionization</span>** satisfies <u>both</u> conditions because

1. Opacity $\uparrow$

2. $e^-$ receive energy $\longrightarrow$ d.o.f. $\nearrow$, so $\gamma \searrow \longrightarrow \nabla_{ad} \searrow$
   $\Rightarrow$ susceptable to convection

➔ Development of hydrogen convective zones inside stars.

Similarly, there are $1^{st}$ and $2^{nd}$ helium convective zones.

Pulsating stars: Cepheids, RR Lyrae stars, Delta Scuti stars

Changes in the stellar radius → varying temperature and luminosity; radial/nonradial … regular/irregular

**<span style="color:red">Kappa (opacity) mechanism</span>** (Eddington/ionization valve)

Normally, $\kappa \searrow$ as $T \nearrow$ (recall $\kappa_{\text{Kramers}} \propto \rho/T^{3.5}$)

    squeezing a star $\Rightarrow T \nearrow \Rightarrow \kappa \searrow \Rightarrow$ energy escapes $\Rightarrow T \searrow \Rightarrow$ expansion
    Self-regulated value

But when $\kappa \nearrow$ as $T \nearrow$   contraction $\Rightarrow T \nearrow \Rightarrow \kappa \nearrow \Rightarrow$ keep contracing

                      $\Rightarrow$ until $P \uparrow\uparrow \Rightarrow$ expansion (cyclic → pulsation)

Ionization of He (or heavier elements)
        or H: Mira, rapidly oscillating Ap stars (roAp), ZZ Ceti

For a **very low-mass star** $\left(M \lesssim 0.4\ M_\odot\right)$, ionization of H and He leads to a <u>fully convective</u> star
➡ H completely burns off → a red dwarf to become a black dwarf
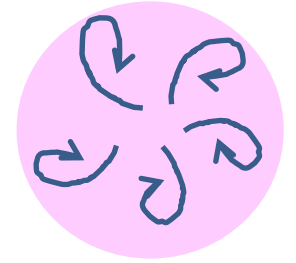


For a **sun-like star**, ionization of H and He, and also the large opacity of $H^-$ ions ➡ a <u>convective envelope</u> (outer 30% radius)
➡ H core burns out → expelled envelop (PN) and a white dwarf
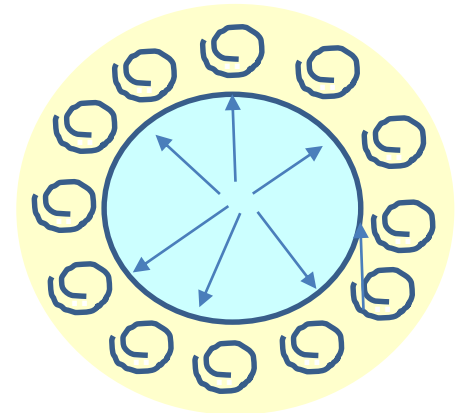


For a **massive star** $\left(M \gtrsim 1.2\ M_\odot\right)$, the core produces fierce amount of energy (via CNO) → a <u>convective core</u>
➡ a large fraction of material to take part in the thermonuclear reactions
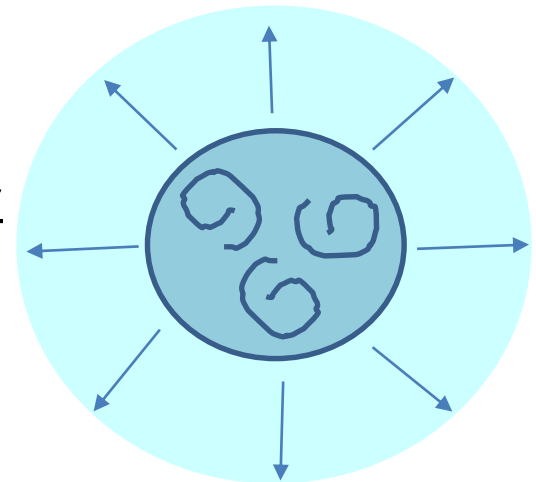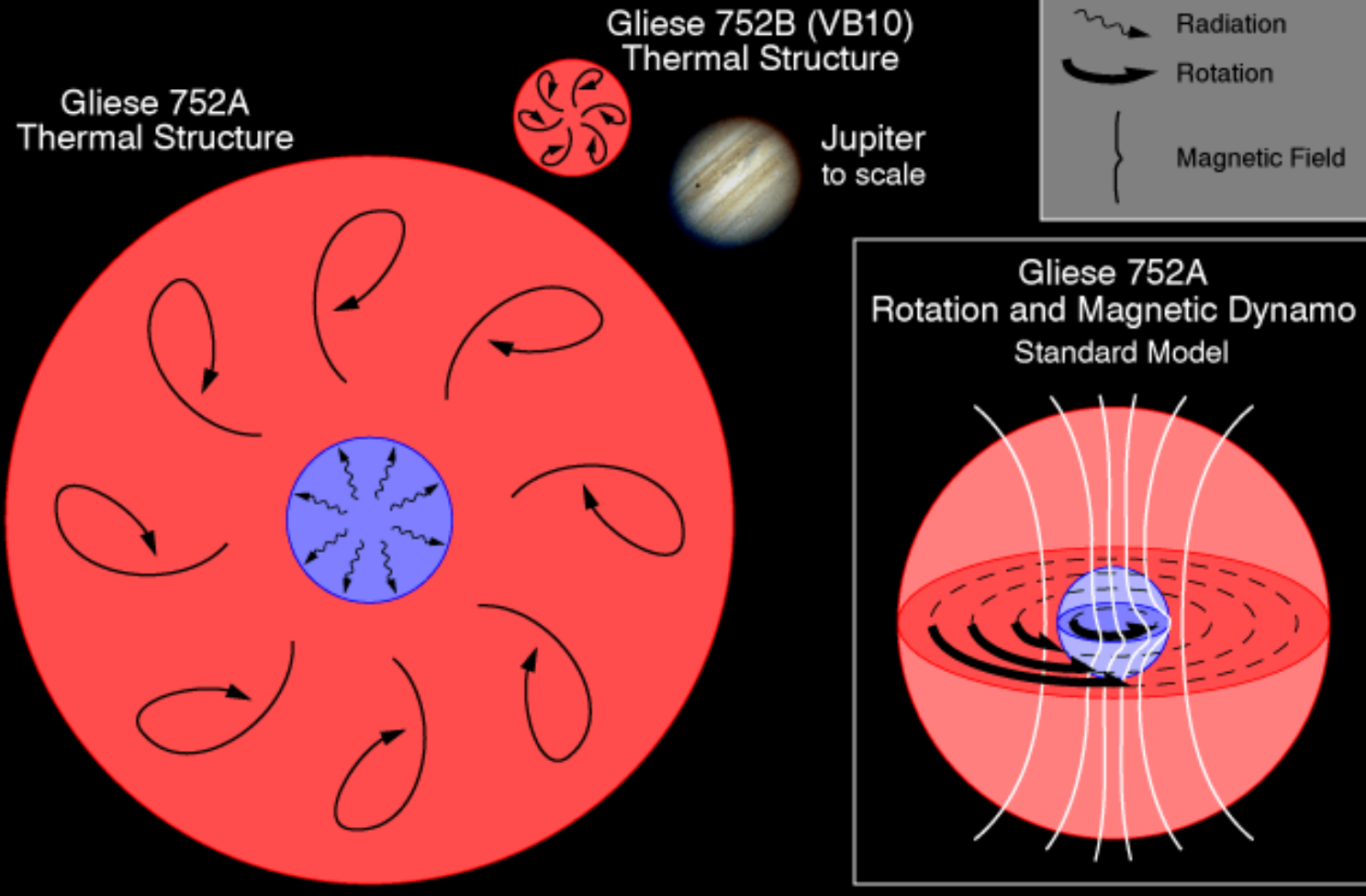
A binary system at 5.74 pc.  Gliese 752A (=Wolf 1055) is an M2.5 red dwarf (mass ~0.46 solar, $m_V$~9.13), whereas Gliese 752B (VB 10) is an M8V (mass ~0.075 solar, $m_V$~17.30).

Low-mass (T Tauri stars) are convective during the early pre-main sequence phase (Hayashi tracks; contracting, elevated chromosphere).

Ultra-cool dwarfs are fully convection; they are magnetically active.



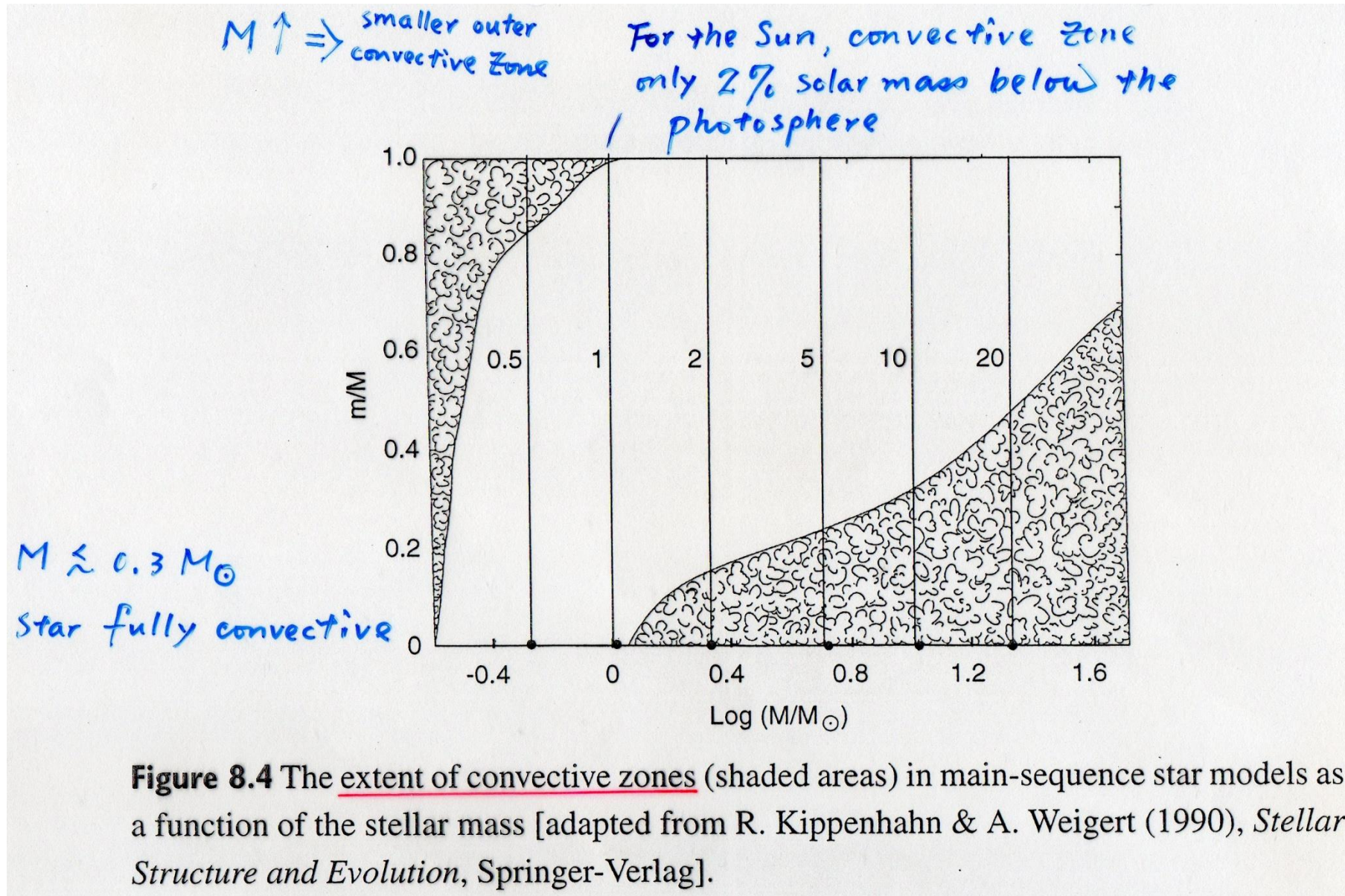Lin CL+21
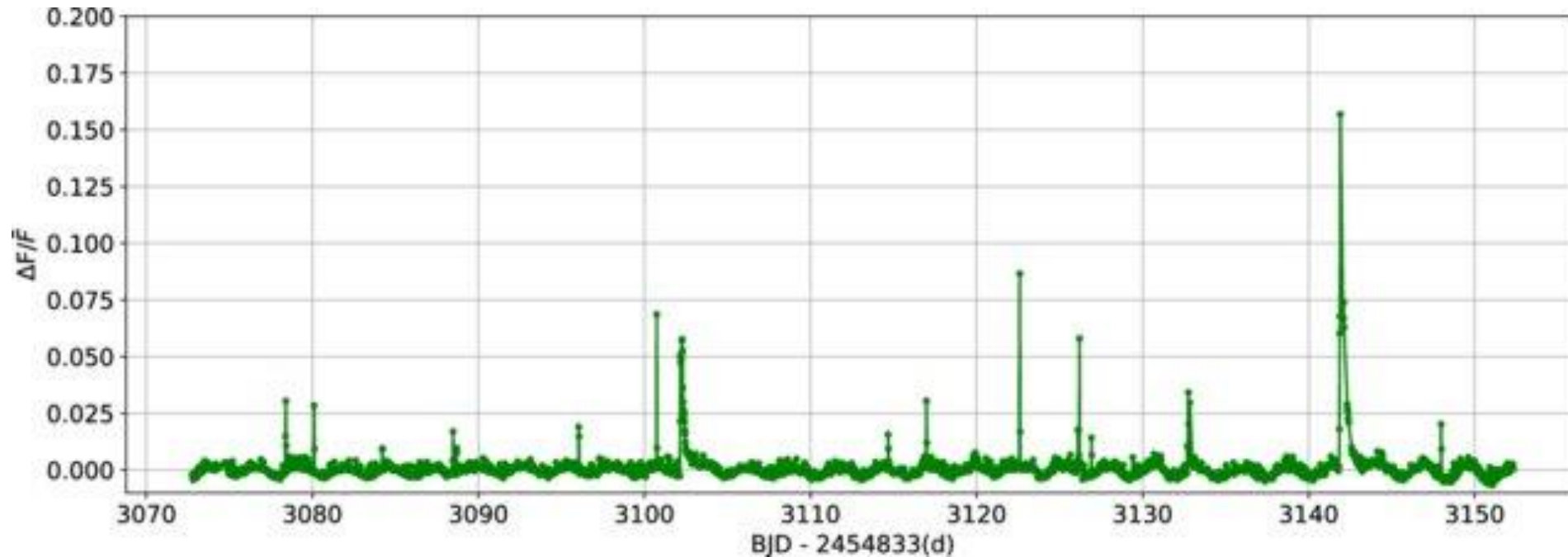
# Dynamical collapse → quasi-static contraction
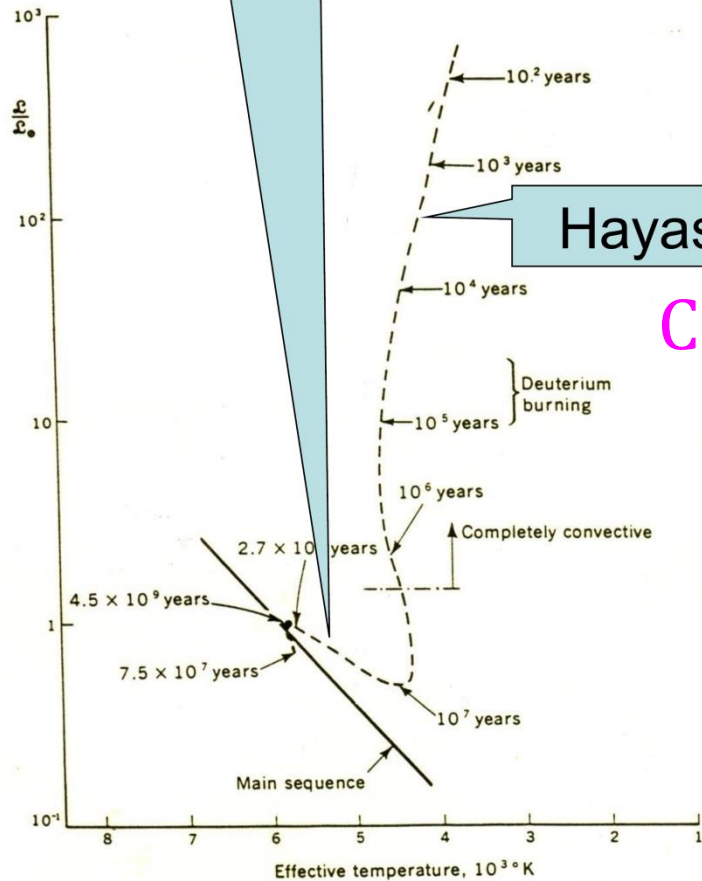


Fig. 5-1 The path on the H-R diagram of the contraction of the sun to the main sequence. The interior has become sufficiently hot to burn deuterium after about $10^5$ years. The contraction ceases near the main sequence when the core has become hot enough to replenish the solar luminosity with the thermonuclear power generated by the fusion of hydrogen into helium. [After D. Ezer and A. G. W. Cameron, The Contraction Phase of Stellar Evolution, in R. F. Stein and A. G. W. Cameron (eds.), "Stellar Evolution," Plenum Press, New York, 1966.]

- Henyey track — Radiative
- Hayashi track — Convective

□ half $E_{\mathrm{grav}}$ becomes particle $E_{\mathrm{kin}}$ (internal energy); half radiated away

□ Matter from optically thin to thick
→ thermodynamical equilibrium,
$$T_{\mathrm{rad}} = T_{\mathrm{kin}}$$

□ Energy used for ionization (for H, $T < 10^4$ K), so the surface temperature remains almost constant.
The protosun ~60 $R_\odot$

□ D burning; fully convective
→ Hayashi track (nearly vertical in HRD)

□ Eventually a radiative core develops

Check out http://www.peripatus.gen.nz/Astronomy/HerRusDia.html for a good summary

109

**Figure 8.4** The <u>extent of convective zones</u> (shaded areas) in main-sequence star models as a function of the stellar mass [adapted from R. Kippenhahn & A. Weigert (1990), *Stellar Structure and Evolution*, Springer-Verlag].
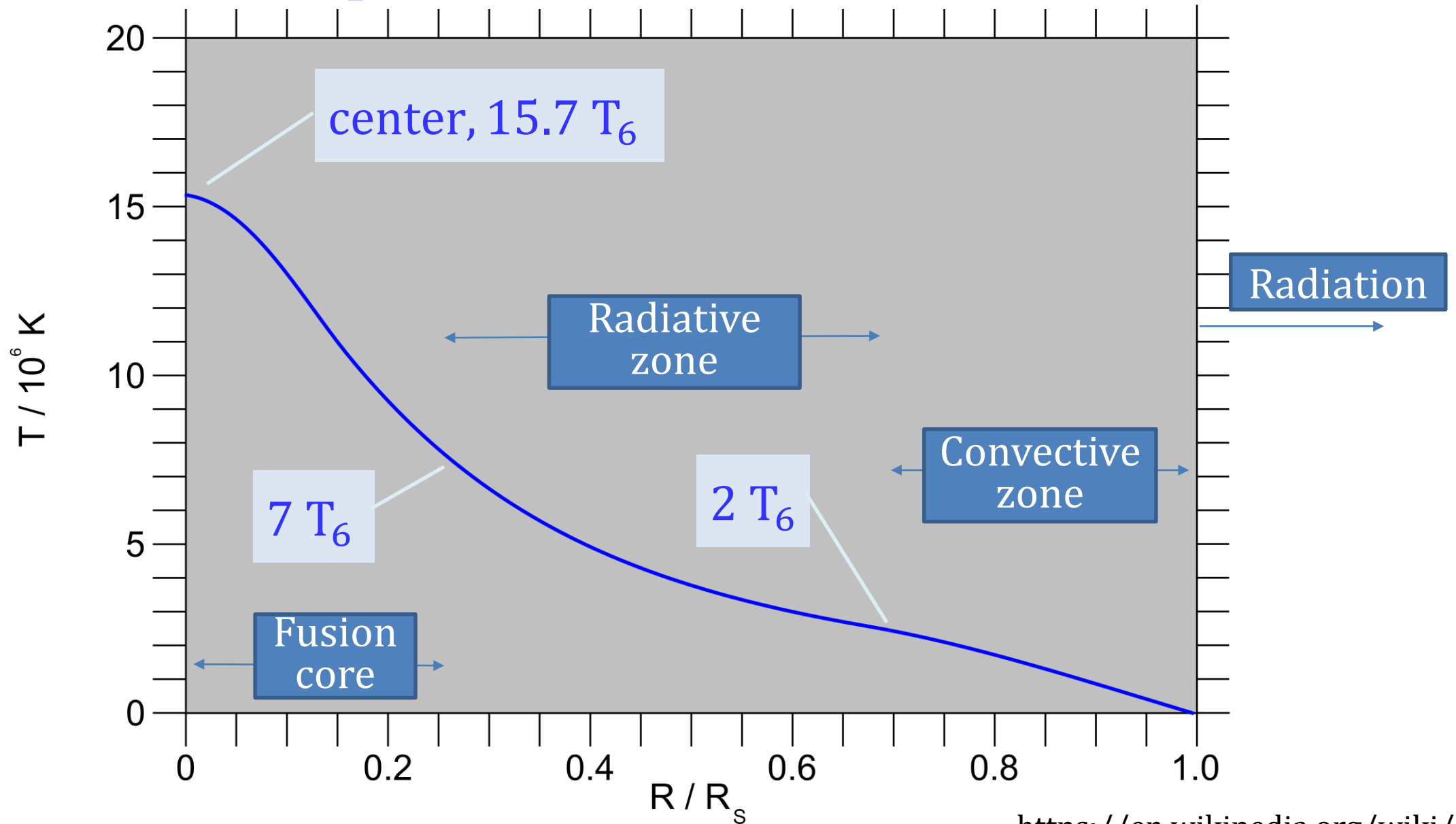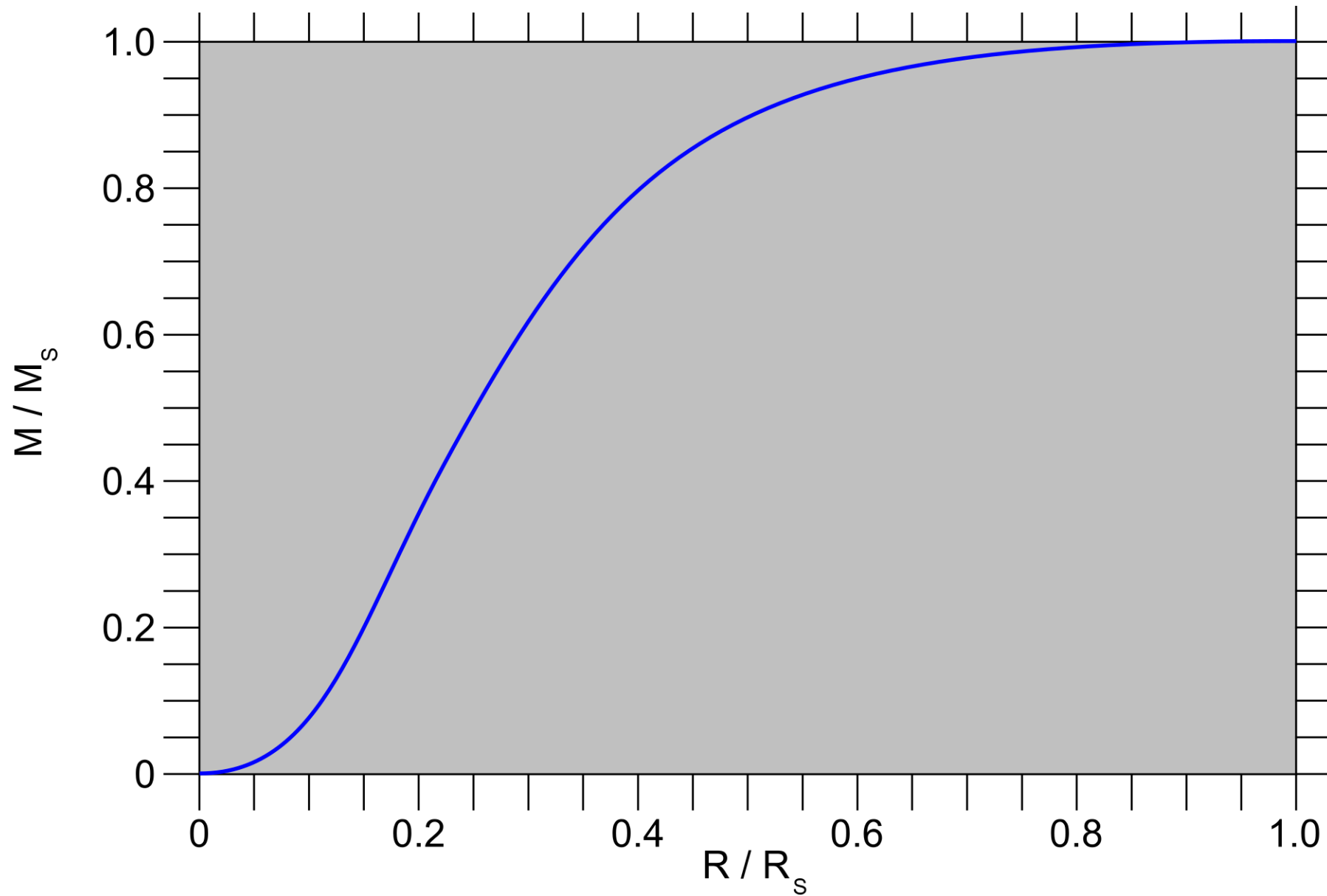
# Subdwarfs: The Pop II Main Sequence

◆ Luminosity class VI

◆ 1.5 to 2 mag fainter than a Pop I MS star of the same spectral type

◆ Low metallicity → low opacity → (UV excess) → low radiation pressure, so smaller, hotter for the same stellar mass
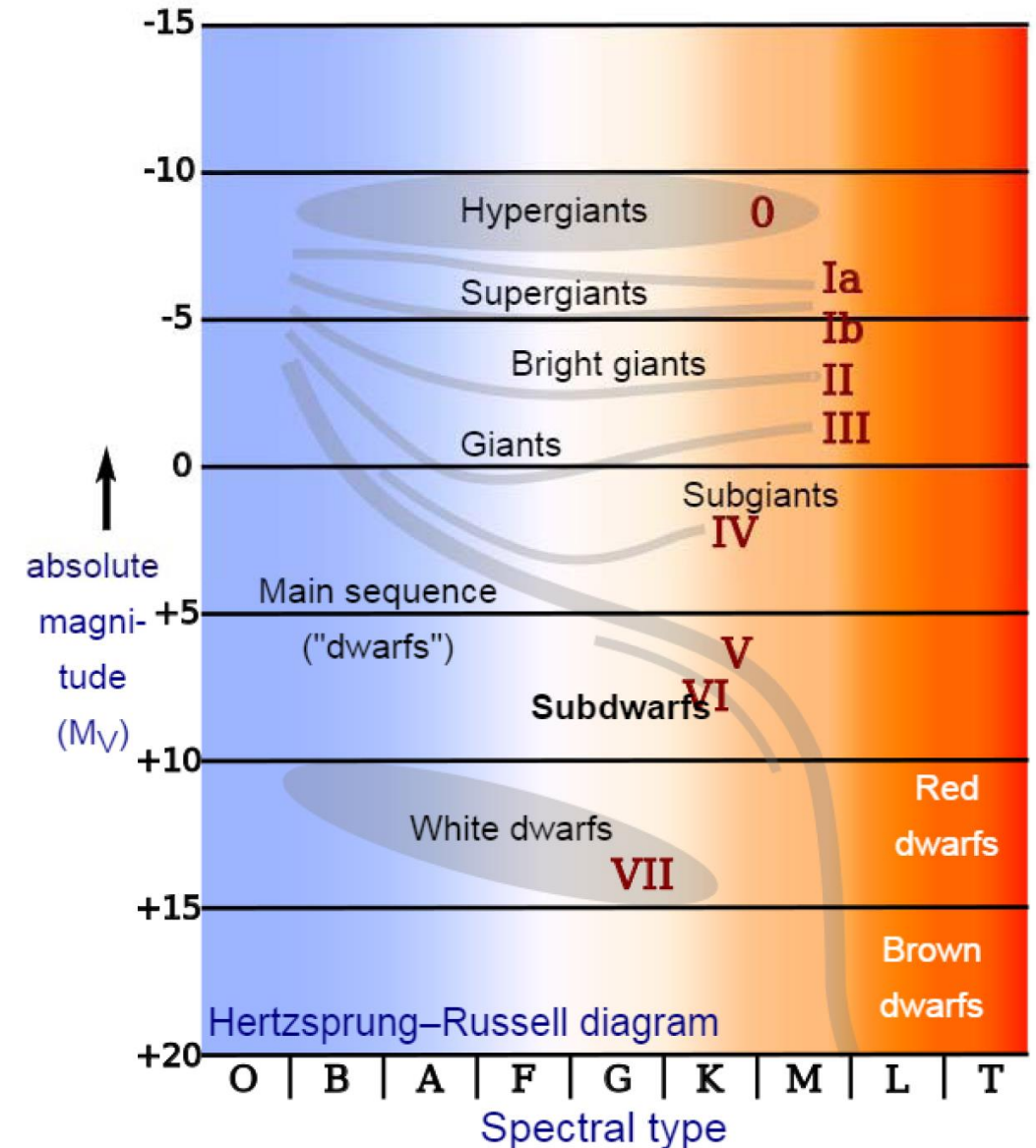
# Temperature Distribution of the Sun



center, 15.7 $T_6$

Radiative zone

Radiation

7 $T_6$

2 $T_6$

Convective zone

Fusion core

T / $10^6$ K

R / $R_s$

https://en.wikipedia.org/wiki/Sun

# Mass Distribution of the Sun

Pressure Distribution of the Sun
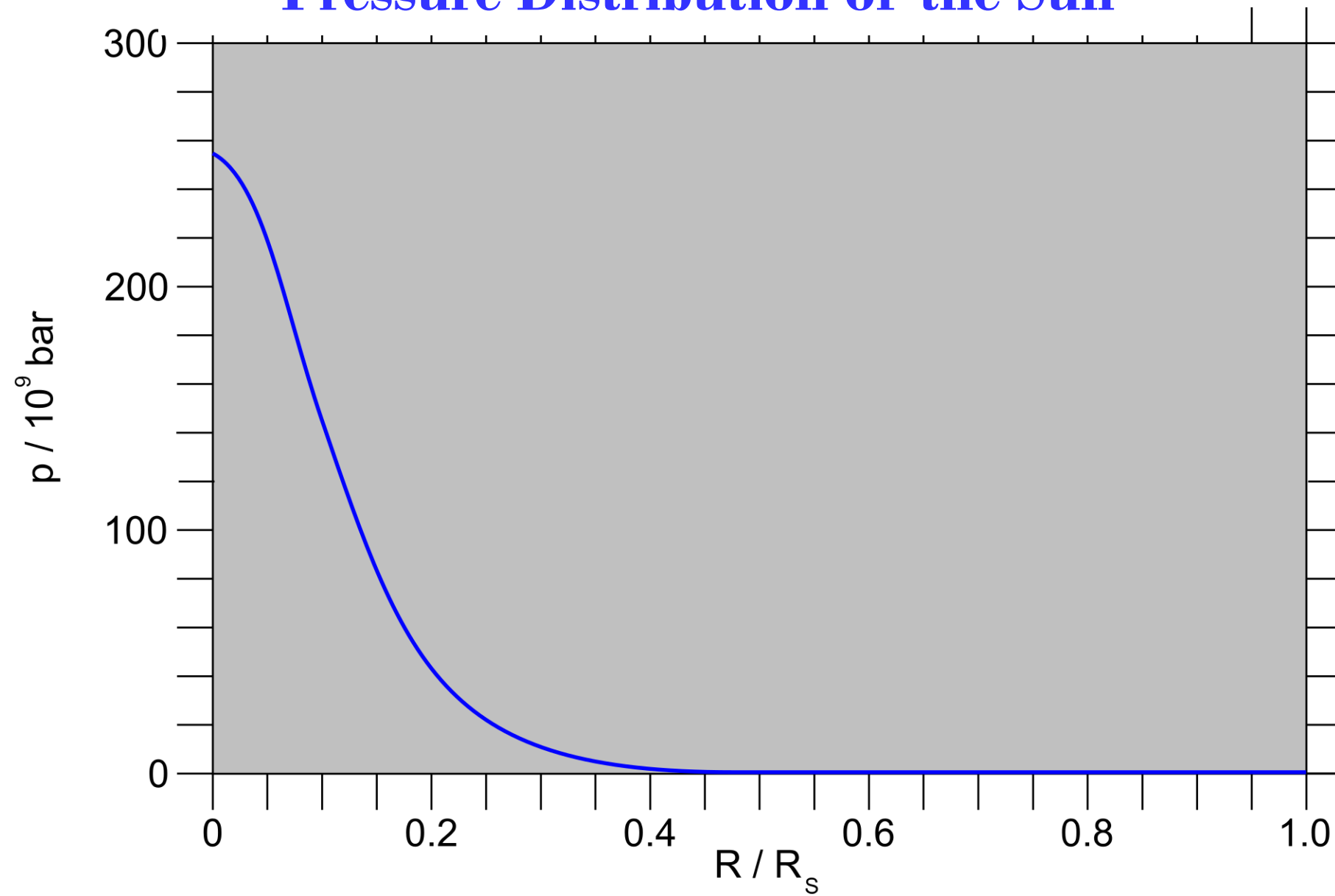
**Density Distribution of the Sun**
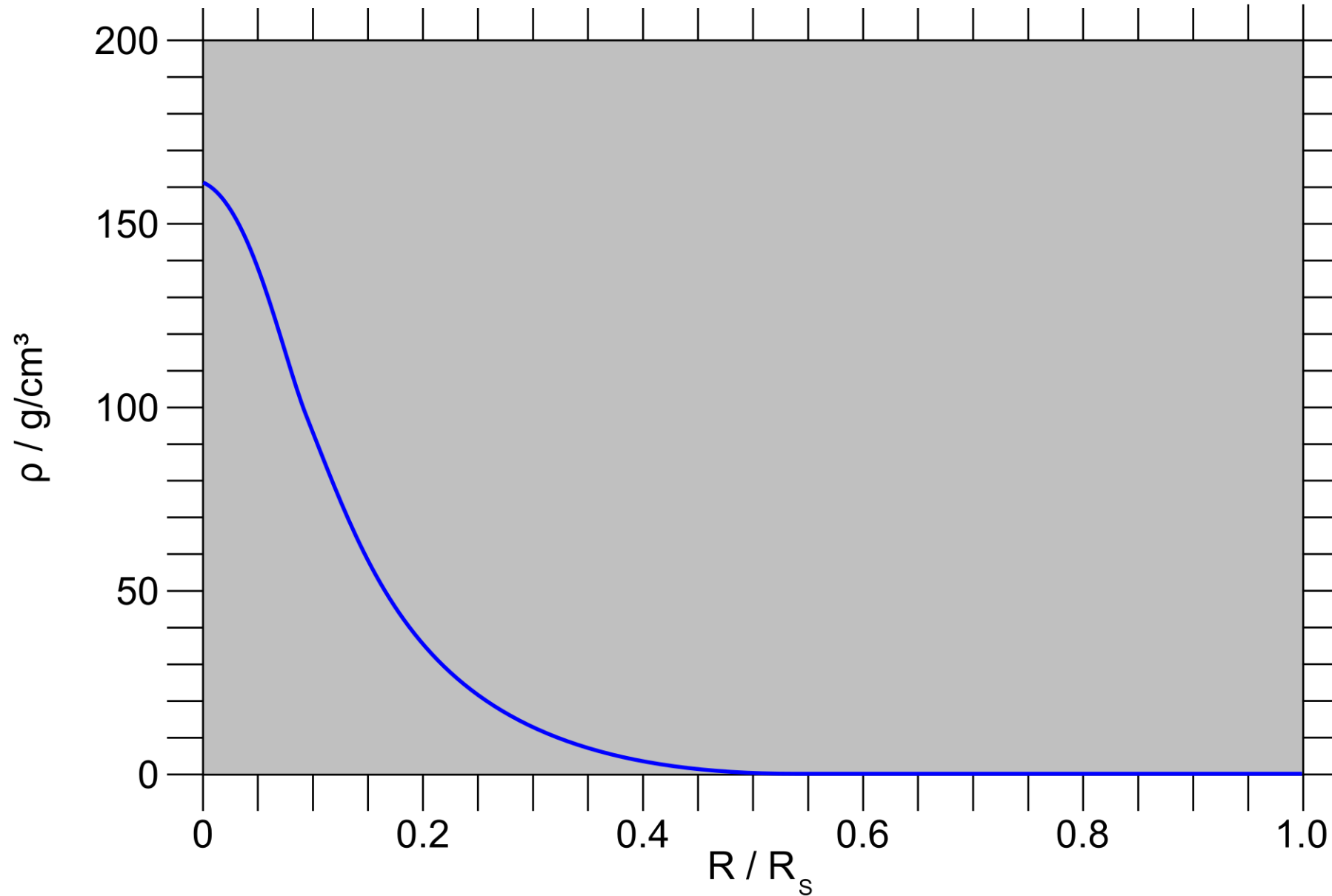
Along the ZAMS, $M_* \propto R_*$, so the central density

$$\rho_c \propto M_*/R_*^3 \propto M_*^{-2}$$
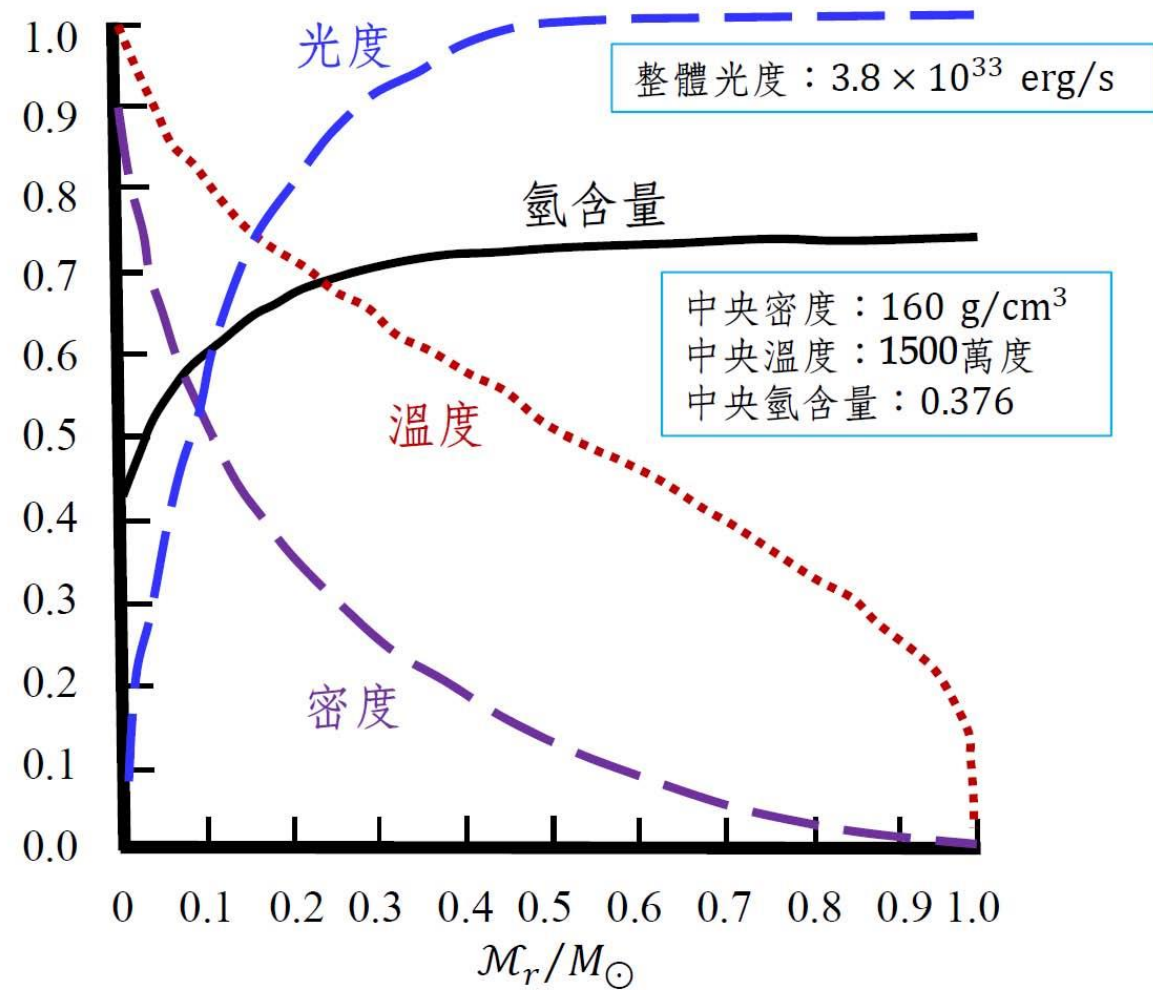
That is, lower-mass MS stars are denser at the cores
→ to provide sufficient pressure

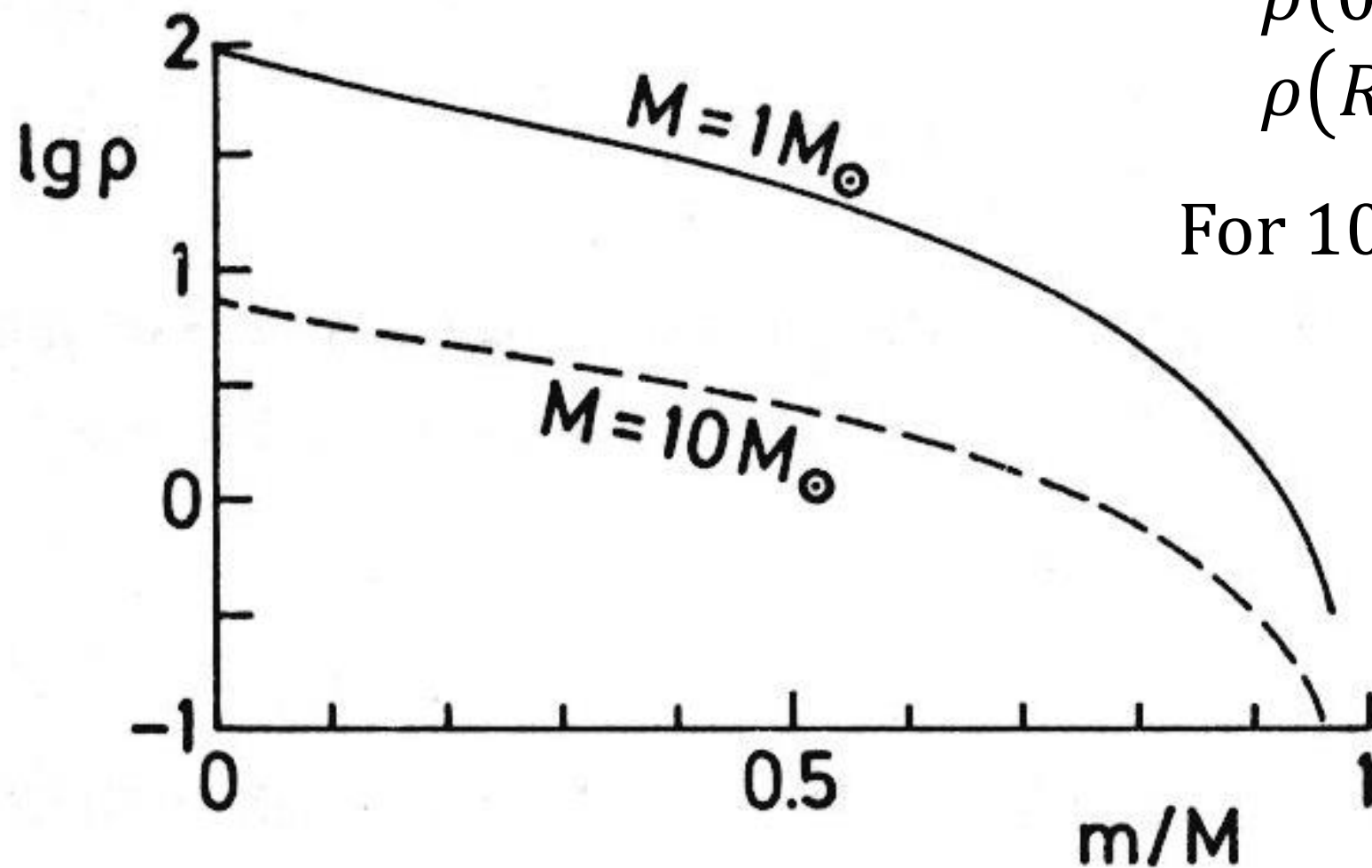So temperature may never get high enough for H fusion

→ Degeneracy important



Stahler & Palla, Fig 16.12

# 年齡46億年（當今）的太陽數值模型



整體光度：$3.8 \times 10^{33}$ erg/s

中央密度：160 g/cm$^3$
中央溫度：1500萬度
中央氫含量：0.376

光度

氫含量

溫度

密度

$\mathcal{M}_r / M_\odot$
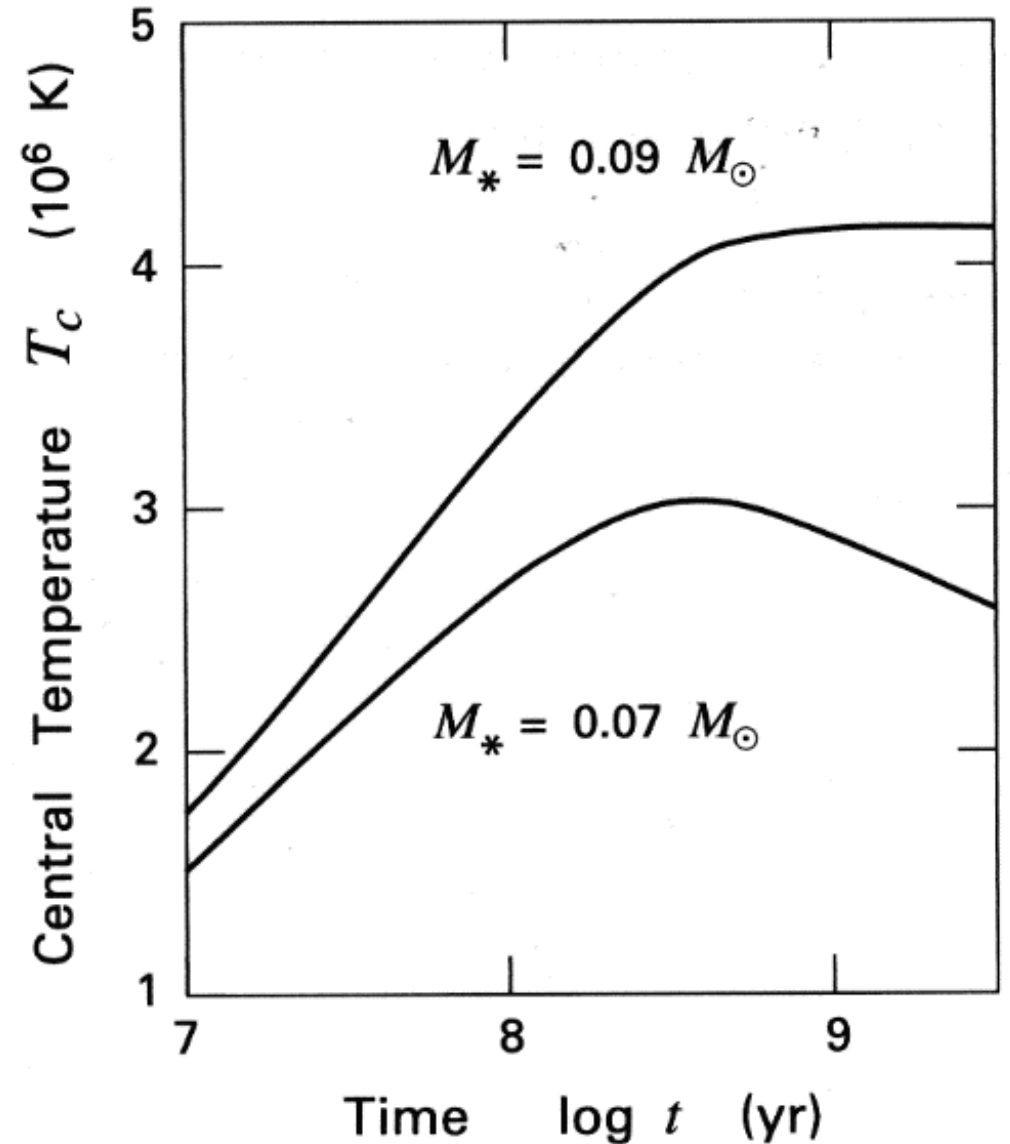
Density profile --- $\rho$ increases toward center.



For 1 $M_\odot$,
$$\rho(0) \approx 10^2 \text{ g cm}^{-3}$$
$$\rho(R_\odot) \approx 10^{-7} \text{ g cm}^{-3}$$

For 10 $M_\odot$, $\rho(0)$ 10× lower

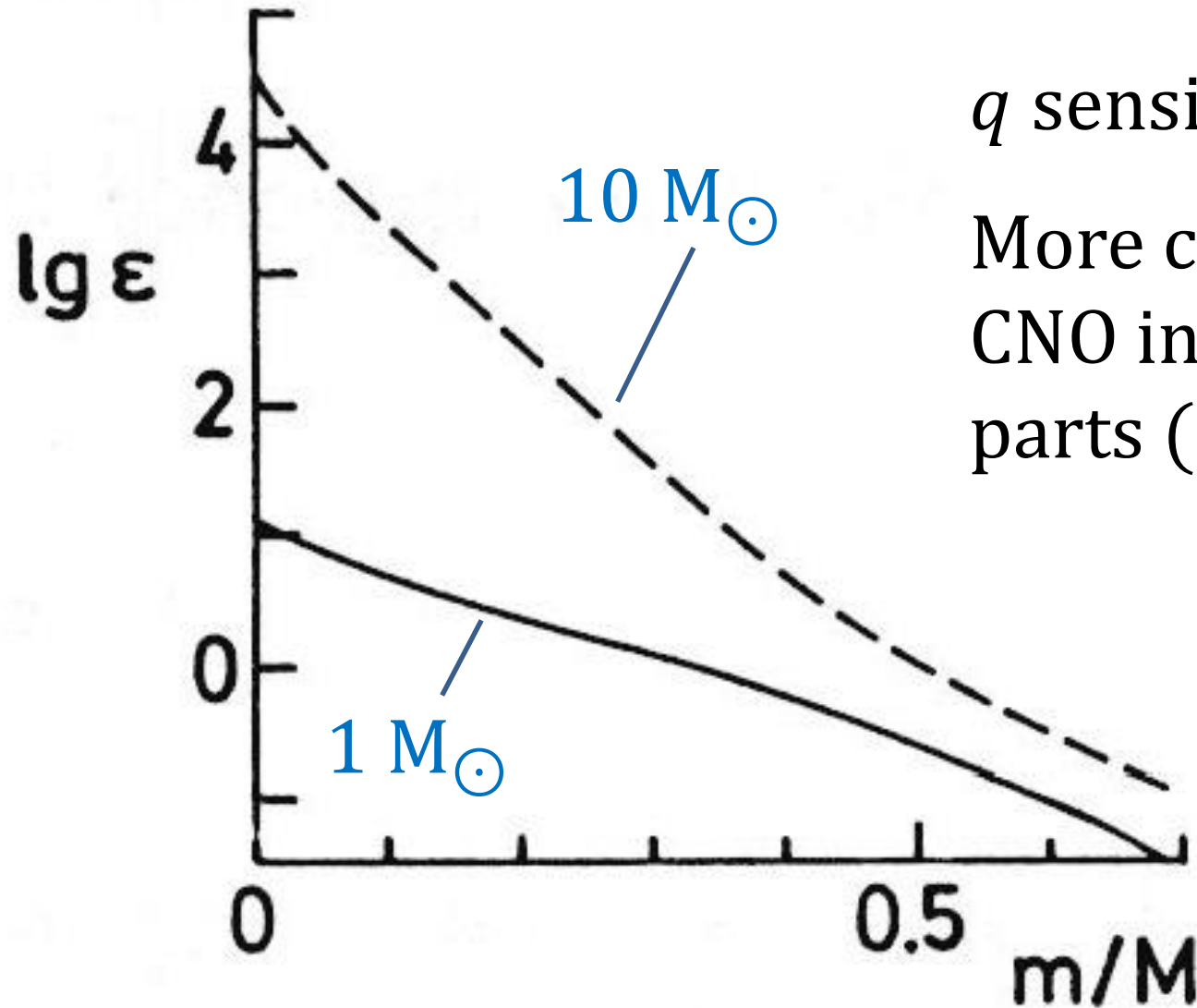Temperature profile --- $T$ increases toward center.
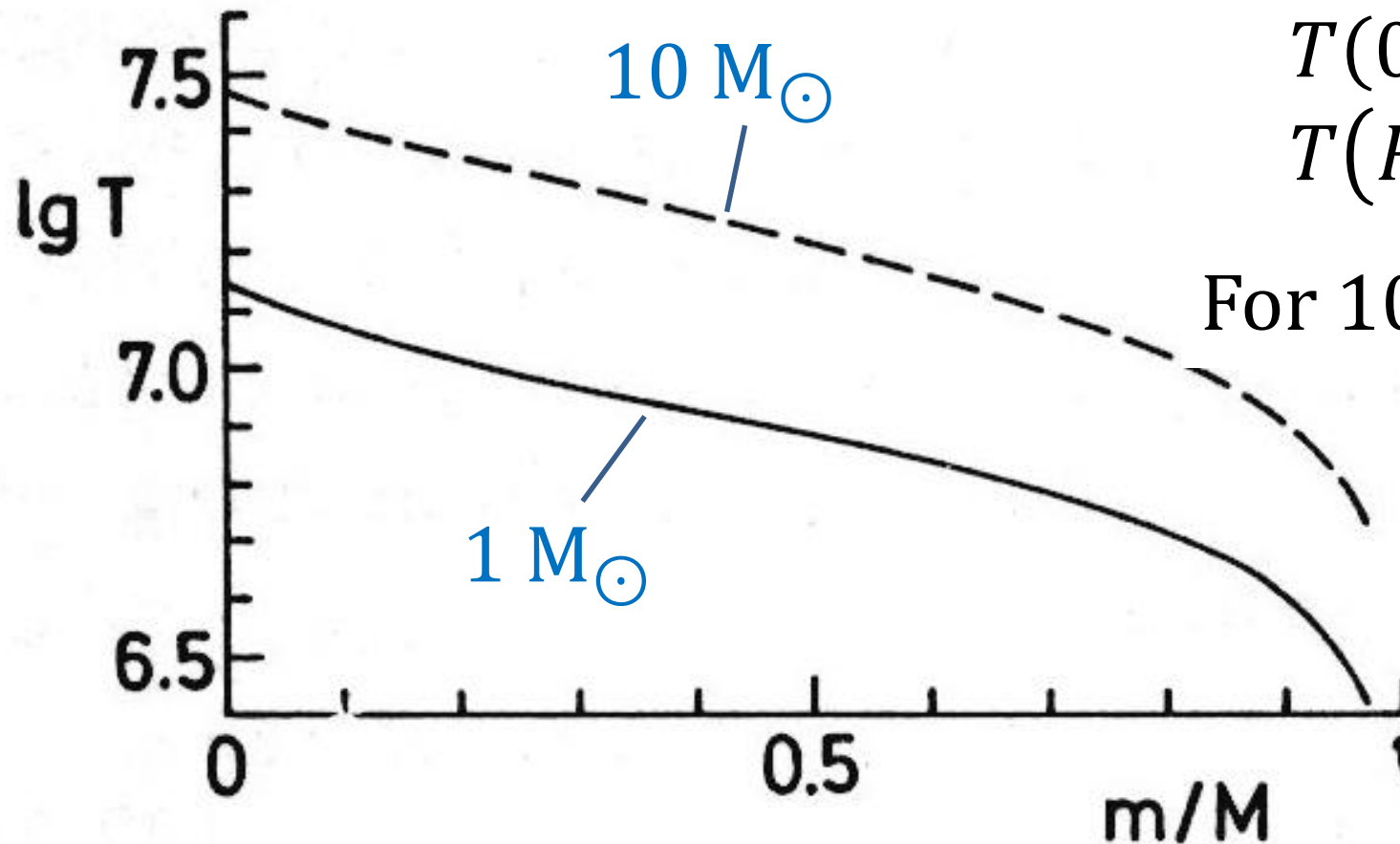


For 1 $M_\odot$,
$$T(0) \approx 1.5 \times 10^7 \text{ K}$$
$$T(R_\odot) \approx 5800 \text{ K}$$

For 10 $M_\odot$, $T(0) \approx 2 \times$ hotter

For more massive stars, the center: (1) hotter, (2) less dense, and (3) higher pressure

Energy generation rate --- $q$ increases toward center.



$q$ sensitive to $T$ + $T$ gradient

More concentrated for higher $M$: CNO in the core, p-p in the outer parts (slope as in low-mass stars)

# Mass-radius relation

In general, $M_* \nearrow \Rightarrow R_* \nearrow$

There is a slope break near $M_* \approx M_\odot$ because of the structural changes.

☐ $M < 1.2\ M_\odot$, pp chain
   ➔ a <u>radiative</u> core

☐ $M > 1.2\ M_\odot$, CNO cycle
   ➔ strong $T$ dependence
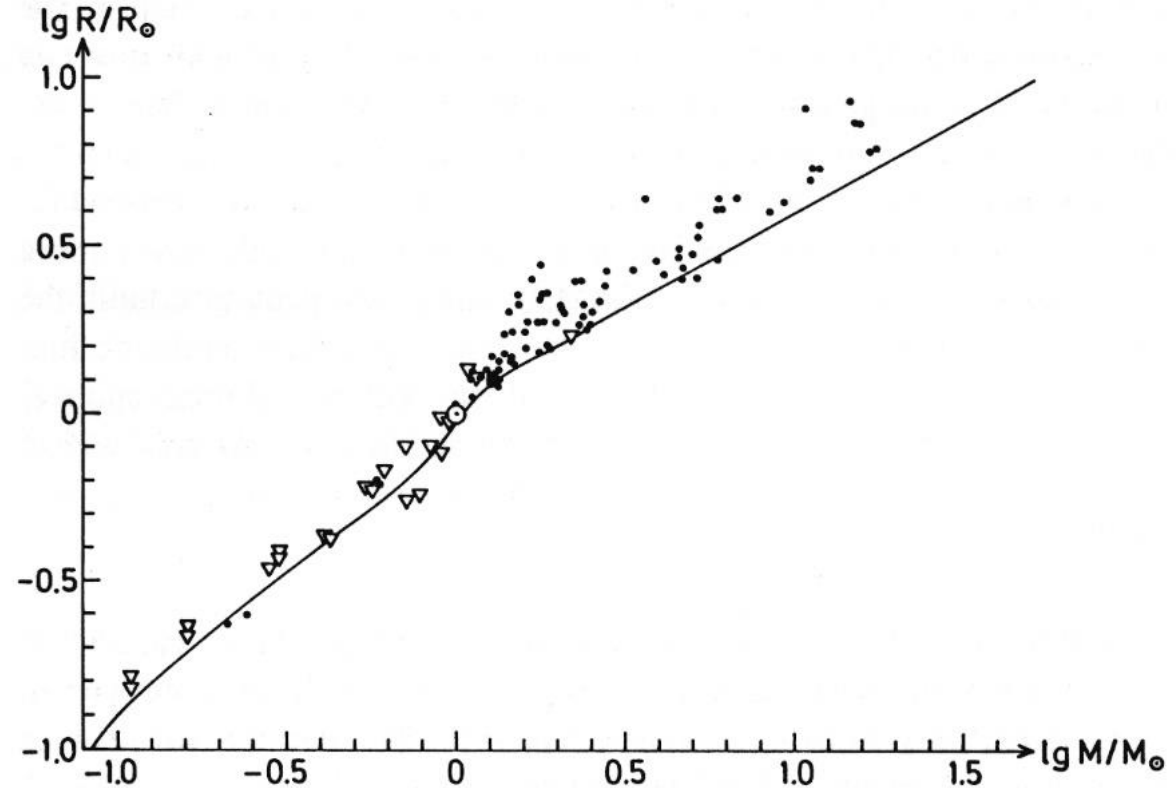      ➔ steeper $T$ gradient
   ➔ a <u>convective</u> core



**Fig. 22.2.** The line shows the mass–radius relation for the models of the zero-age main sequence plotted in Fig. 22.1. For comparison, the best measurements (as selected by POPPER, 1980) of main-sequence components of detached (*dots*) and visual (*triangles*) binary systems are indicated

Kippenhahn & Weigert

125

$$\frac{L}{L_\odot} \approx 0.23 \left(\frac{M}{M_\odot}\right)^{2.3} \quad \left(\frac{M}{M_\odot} < 0.43\right)$$

$$\frac{L}{L_\odot} \approx 0.23 \left(\frac{M}{M_\odot}\right)^{4} \quad \left(0.43 < \frac{M}{M_\odot} < 2\right)$$

$$\frac{L}{L_\odot} \approx 0.23 \left(\frac{M}{M_\odot}\right)^{3.5} \quad \left(2 < \frac{M}{M_\odot} < 55\right)$$

$$\frac{L}{L_\odot} \approx 32000 \left(\frac{M}{M_\odot}\right)^{1} \quad \left(\frac{M}{M_\odot} > 55\right)$$

# Mass-luminosity relation



In general, $M_* \nearrow \Rightarrow L_* \nearrow$

Slope varies with respect to different mass ranges.

Overall,

$$\frac{L}{L_\odot} \approx \left(\frac{M}{M_\odot}\right)^{3.5}$$
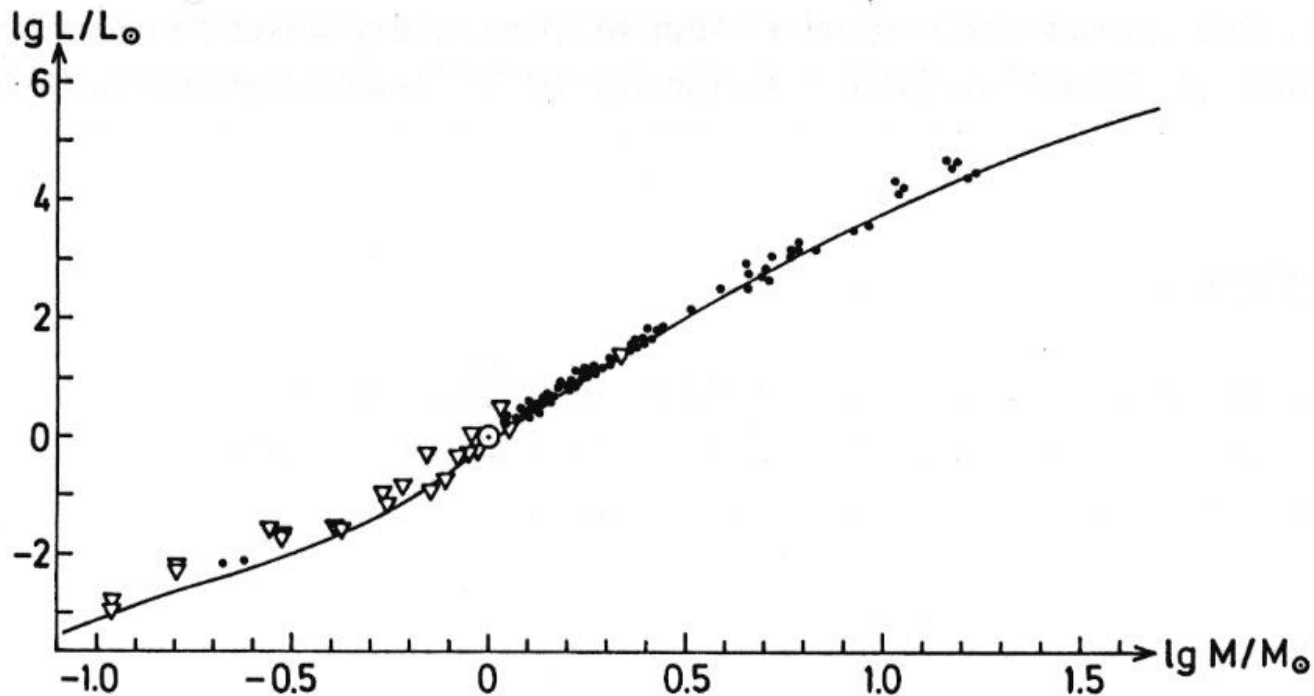
**Fig. 22.3.** The line gives the mass–luminosity relation for the models of the main sequence shown in Fig. 22.1. Measurements of binary systems are plotted for comparison (the symbols have the same meaning as in Fig. 22.2)
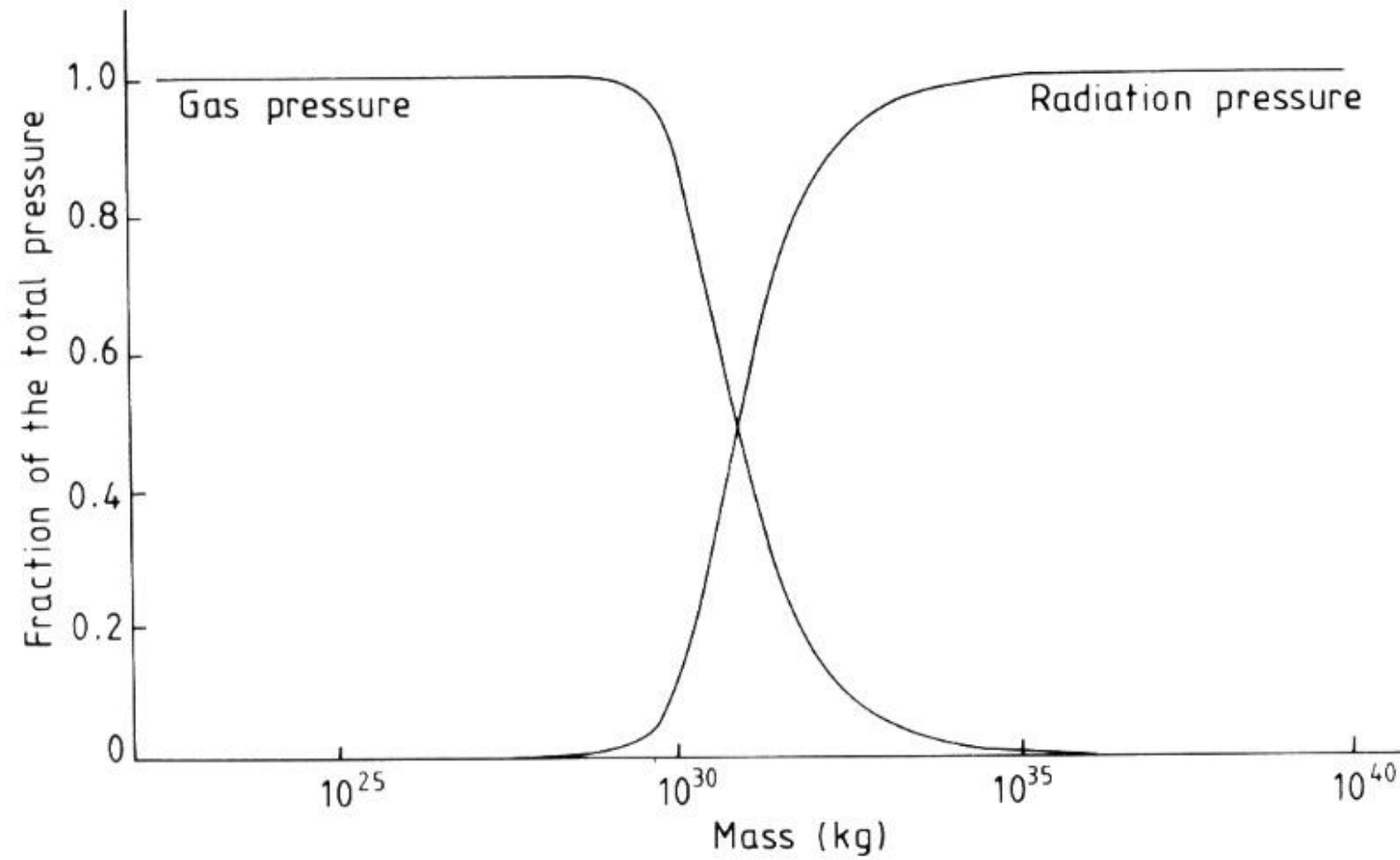
# Radiation Pressure versus Gas Pressure

$P_{\text{gas}} \propto T$ balances self-gravitation OK; but $P_{\text{rad}} \propto T^4$, so as stellar $M \nearrow$, $T_c \nearrow \implies P_{\text{rad}} \nearrow\nearrow$

$P_{\text{rad}}$ plays an ever dominant role in more massive stars.

$P_{\text{rad}} \approx P_{\text{gas}}$ around 5 $M_\odot$

$\implies$ A limit when $P_{\text{rad}}$ predominates

Eddington (1930)

# Maximum Radiation Pressure

$$L < L_{\text{Edd}} = \frac{4\pi cGM}{\kappa} = \frac{4\pi cGMm_p}{\sigma_T} \text{ (assuming ionized H)}$$

$$\approx 3.2 \times 10^4 \left(\frac{M_*}{M_\odot}\right) [L_\odot] = 1.26 \times 10^{38} \left(\frac{M_*}{M_\odot}\right) [\text{erg/s}]$$

This is the **Eddington limit.**

If $L > L_{\text{Edd}}$ → hydrostatic equilibrium is violated

→ super-Eddington luminosity → stellar wind

# Stellar Mass Upper Limits

$$L \sim M^3$$

$$\frac{L_{\mathrm{Edd}}}{L_\odot} = \frac{1.26 \times 10^{38}}{4 \times 10^{33}} \left(\frac{L_*}{L_\odot}\right)^{1/3} \rightarrow L_* \sim 5 \times 10^6 \ \mathrm{L_\odot} \rightarrow M_*^{\mathrm{max}} \approx 170 \ M_\odot$$

Observationally, there seems indeed a limit,
    e.g., Eta Carina, $\sim 150 \pm 50 \ M_\odot$

$$L_{\mathrm{Edd}} \leftrightarrow \kappa, \qquad \text{so } L_{\mathrm{Edd}}^{\mathrm{Pop\ I}} < L_{\mathrm{Edd}}^{\mathrm{Pop\ II}} < L_{\mathrm{Edd}}^{\mathrm{Pop\ III}} (\approx 300 \ \mathrm{M_\odot})$$

# Stellar Mass Lower Limits

$$q_{PP} \propto \exp\left[-33.8 \, T_6^{-1/3}\right]$$

Highly sensitive to temperature.

Below about at $5 \, T_6$, the rate becomes too low to supply energy (recall the Gamow peak).

This corresponds to about $0.1 \; M_\odot$;
    more precise modeling leads to $\approx 0.08 \; M_\odot$.

There could be stars in which only the first two stages of the p-p chain occur, so the stars will accumulate $^3_2\text{He}$ in the interior.

**Stars have masses ranging from ~0.1 to ~100 solar masses.**

# Time Scales

Different physical processes inside a star,
e.g., nuclear reactions (changing chemical composition) are
slow (longer time scales); structural adjustments ($dP/dt$)
take places on relatively shorter time scales.

- ✓ Dynamical timescale
- ✓ Thermal timescale
- ✓ Nuclear timescale
- ✓ Diffusion timescale

# Dynamical Timescale

hydrostatic equilibrium $\xrightarrow{\text{perturbation}}$ motion $\xrightarrow{\text{adjustment}}$ hydrostatic equilibrium

## Free-fall collapse

Equation of motion $\ddot{r} = -\dfrac{GM_r}{r^2} - \dfrac{1}{\varrho}\dfrac{dP}{dr}$

Near the star's surface $r = R, M_r = M$, so $\ddot{R} = -\dfrac{GM}{R^2} - \dfrac{1}{\varrho}\dfrac{dP}{dR}$

Free-fall means pressure $\ll$ gravity, so $\ddot{R} \approx -\dfrac{GM}{R^2}$

Assuming a constant acceleration $R = -\left(\ddot{R}/2\right)\tau_{\text{ff}}^2$, so

$$\tau_{\text{ff}} = \left(2R^3/GM\right)^{1/2} = \dfrac{1}{\left(\frac{2}{3}\pi G\overline{\rho}\right)^{1/2}} \approx 0.04\left(\dfrac{\rho_\odot}{\overline{\rho}}\right)^{1/2} \text{[d]}$$

# Stellar Pulsation

The star pulsates about the equilibrium configuration

→ same as dynamical timescale

$$\tau_{\text{pulsation}} \propto 1/\sqrt{\bar{\rho}}$$

# Propagation of Sound Speed (pressure wave)

Pressure induced perturbation,

$$R/\tau_{\text{ff}}^2 = -\frac{\ddot{R}}{2} = \frac{GM}{R^2} + \frac{1}{\varrho}\frac{dP}{dR} \approx \frac{1}{\varrho}\frac{dP}{dR} \approx \frac{1}{\varrho}\frac{P}{R}$$

so $\dfrac{R}{\tau_{\text{ff}}} \approx \sqrt{\dfrac{P}{\rho}} \approx c_s$ (sound speed) $\propto \sqrt{T}$ (for ideal gas)

$$\tau_s \approx \frac{R}{c_s}$$

In general, $\tau_{\text{dyn}} \approx \dfrac{1}{\sqrt{G\bar{\rho}}} \approx \dfrac{1.6\times10^{15}}{\sqrt{n}}$ [s] $= 1000\sqrt{\left(\dfrac{R}{R_\odot}\right)^3\left(\dfrac{M_\odot}{M}\right)}$ [S]

# Thermal Timescale

### Kelvin-Helmholtz timescale (radiation by gravitational contraction)

$$E_{\text{total}} = E_{\text{grav}} + \text{E}_{\text{thermal}} = \frac{1}{2} E_{\text{grav}} = -\frac{1}{2} \alpha \, G M^2 / R$$

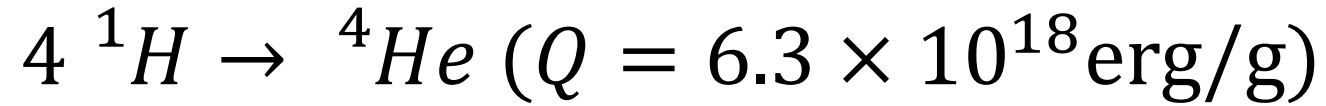This amount of energy is radiated away at a rate *L,* so timescale

$$\tau_{\text{KH}} = \frac{E_{\text{total}}}{L} = \frac{1}{2} \alpha \, G M^2 / R L$$

$$= 2 \times 10^7 \, M^2 / R L \quad [\text{yr}] \text{ in solar units}$$

$$\boxed{\tau_{\text{KH}} \approx 2 \times 10^7 \left( \frac{M}{M_\odot} \right)^2 \left( \frac{R_\odot}{R} \right) \left( \frac{L_\odot}{L} \right) [\text{yr}]}$$

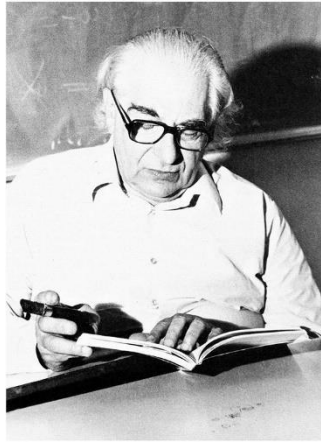| $M = 1\,\mathcal{M}_\odot, R = 1\,\text{pc}$ | $M = 1\,\mathcal{M}_\odot, R = 1\,\mathcal{R}_\odot$ |
| --- | --- |
| $\tau_{\text{dyn}} \approx 1.6 \times 10^7\,\text{yr}$ | $\tau_{\text{dyn}} \approx 1.6 \times 10^3\,\text{s} \approx 30\,\text{min}$ |
| $\tau_{\text{ther}} \approx 1\,\text{yr}$ | $\tau_{\text{ther}} \approx 3 \times 10^7\,\text{yr}$ |

# Nuclear Timescale

Time taken to radiate at a rate $L$ on nuclear energy

$$4 \, {}^1H \rightarrow \, {}^4He \; (Q = 6.3 \times 10^{18} \text{erg/g})$$

$$\tau_{\text{nuc}} = \frac{E_{\text{nuc}}}{L} = 6.3 \times 10^{18} \frac{M}{L}$$

$$\boxed{\tau_{\text{nuc}} \approx 10^{11} \left( \frac{M}{M_\odot} \right) \left( \frac{L_\odot}{L} \right) \; [\text{yr}]}$$

From the discussion above, $\tau_{\text{nuc}} \gg \tau_{\text{KH}} \gg \tau_{\text{dyn}}$

Mário Schönberg
(1914 Brazil – 1980)

Subrahmanyan Chandrasekhar
(1910 India – 1995 USA)

**The Schönberg-Chandrasekhar limit**
--- the maximum mass of a fusion-less
stellar core that can support against
gravitational collapse

# THE ASTROPHYSICAL JOURNAL

AN INTERNATIONAL REVIEW OF SPECTROSCOPY AND
ASTRONOMICAL PHYSICS

VOLUME 96        SEPTEMBER 1942        NUMBER 2

## ON THE EVOLUTION OF THE MAIN-SEQUENCE STARS

M. Śchönberg[1] AND S. Chandrasekhar

### ABSTRACT

The evolution of the stars on the main sequence consequent to the gradual burning of the hydrogen in the central regions is examined. It is shown that, as a result of the decrease in the hydrogen content in these regions, the convective core (normally present in a star) eventually gives place to an isothermal core. It is further shown that there is an upper limit ($\sim 10$ per cent) to the fraction of the total mass of hydrogen which can thus be exhausted. Some further remarks on what is to be expected beyond this point are also made.

$$\frac{M_c}{M} \approx 0.37 \left( \frac{\mu_e}{\mu_c} \right)^2 \quad (\sim 10\text{-}15\% \text{ in reality})$$

Take ionized H in env; pure He in core  $\mu = 1.34$
$\mu = 0.61$

$M_c \sim 8\text{-}9\% \, M$    $\mu_c \sim 2 \mu_e$

Beech 1988

141

An isothermal core cannot exceed ~10% of the total stellar mass, for otherwise the core cannot support the gravitational pressure of the envelope, and the core contracts.

No longer isothermal; $T$ increases; if $\gtrsim 10^8$ K, He is ignited.

The core determines the stellar evolution (fate); the envelope follows.

# Main-Sequence Lifetime of the Sun

**Energy Gained in a PP Chain**

- 4H → 1 He + neutrinos + energy
- Mass of 4 H = 6.693 x $10^{-27}$ kg
- Mass of 1 He = 6.645 x $10^{-27}$ kg
- **Mass deficit ➜ 0.048 × $10^{-27}$ kg** = 0.7%

$M_\odot \approx 2 \times 10^{33}$ [g]

$L_\odot \approx 4 \times 10^{33}$ [ergs/s]

**Fusion efficiency**

**Nuclear physics**

**Stellar physics**

$$\tau_\odot^{MS} \approx M_\odot \frac{(0.007)(0.1)\, c^2}{L_\odot} = 3.15 \times 10^{17} [s] = 10^{10} \text{ [yr]}$$

$$\text{Given } L_{MS}/L_\odot \approx (M/M_\odot)^{3.5} \rightarrow \tau^{MS} \approx 10^{10} (M_\odot/M)^{2.5} \text{ [yr]}$$

# Diffusion Timescale

Time taken for photons to walk out randomly from the stellar interior to eventual radiation from the surface

$$\sigma_{\text{Thomson}} = 6.6525 \times 10^{-25} \ [\text{cm}^2]$$

Thus, <u>mean free path</u> $\ell = 1/(\sigma_T n_e)$, where (all cgs units)
$\overline{n_e} \approx 10^{24}$ ($\bar{\rho}_{\odot} \approx 1.4$); $n_c \approx 10^{26}$ ($\rho_c \approx 150$). $\ell \approx [0.015 \mathinner{..} 1.5]$ cm

Take $\ell \approx 0.3$ cm, <u>mean-free time</u> $\tau = (\ell/c) \approx 10^{-11}$ s

Random walk, RMS distance after $N$ steps $d = \sqrt{N} \, \ell$.
Let $d = R_{\odot} \longrightarrow N \approx 5 \times 10^{22}$.
$\tau_{\text{diff}} = $ mean free time $\times$ steps $= \tau \, N \approx 10^4$ [yr]

Present Sun

$4.5 \times 10^9$ yr
$\rho_c = 158$ gm cm$^{-3}$
$T_c = 15.4 \times 10^6$ °K
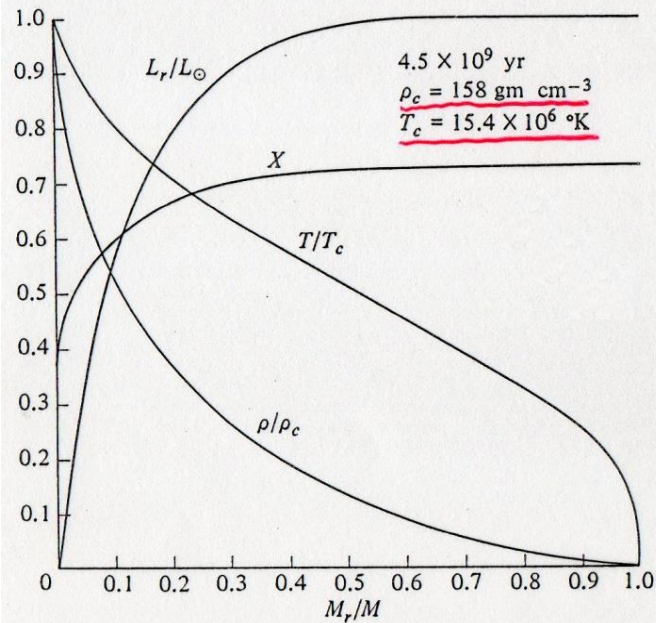
$L_r/L_\odot$

$X$

$T/T_c$

$\rho/\rho_c$

$M_r/M$

Fig. 7-11A  A Model Solar Interior. Density relative to the central density $\rho/\rho_c$, temperature relative to central temperature $T/T_c$, net luminosity relative to total luminosity $L_r/L_\odot$, and hydrogen abundance $X$ are shown as functions of fractional mass $M_r/M$. The chemical composition is $X = 0.730$, $Y = 0.245$, and $Z = 0.025$. The age is $4.5 \times 10^9$ years. [After S. Torres-Peimbert, E. Simpson, and R. K. Ulrich, 1969 (329).]

$X_c = 0.376$

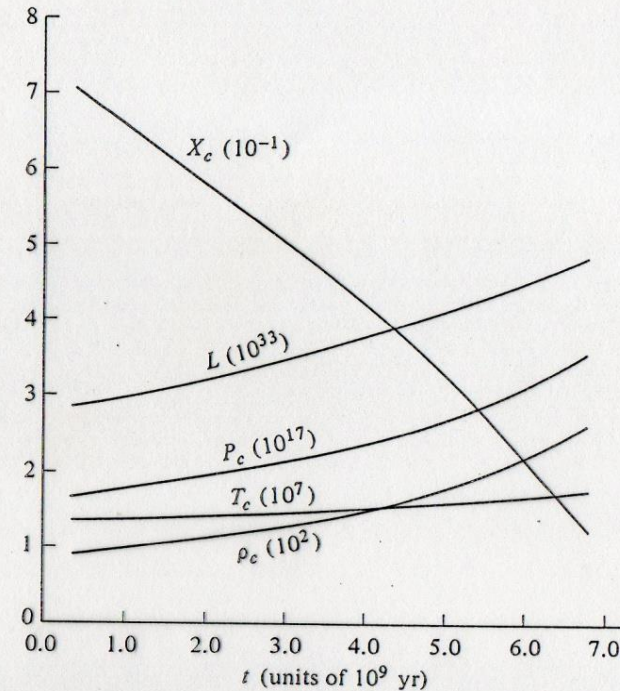At ZAMS, $X$ is homogeneous.

Sun on the main sequence

$X_c$ ($10^{-1}$)

$L$ ($10^{33}$)

$P_c$ ($10^{17}$)

$T_c$ ($10^7$)

$\rho_c$ ($10^2$)

$t$ (units of $10^9$ yr)

Fig. 7-11B  The Evolution of the Sun during 7 Billion Years. Total luminosity $L$ and central values of pressure $P_c$, temperature $T_c$, density $\rho_c$, and hydrogen abundance $X_c$ are shown as functions of time $t$, which is measured from the initial (homogeneous) state for which the composition is $X = 0.730$, $Y = 0.245$, and $Z = 0.025$. The power of ten by which each value must be multiplied is indicated in parentheses. The values of $P_c$, $\rho_c$, and $L$ are expressed in cgs units, and $T_c$ is expressed in degrees Kelvin. [After S. Torres-Peimbert, E. Simpson, and R. K. Ulrich, 1969 (329).]

$P_{deg} \sim 0.017\, P_{total}$ at ZAMS

0.075

$9.2 \times 10^9$ yr
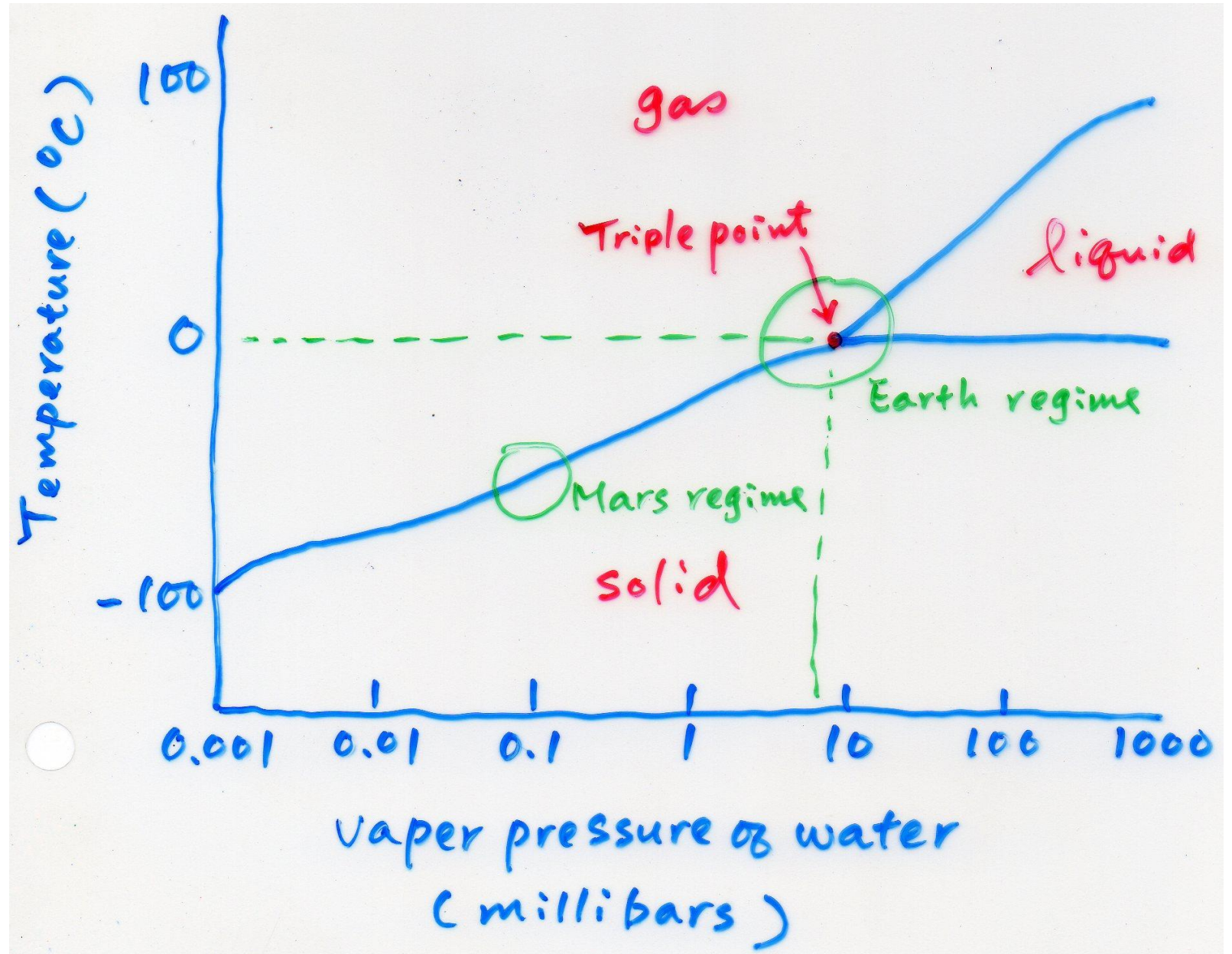
( Fig 7-10B )

145

# Phase Diagram of Water

$\rho - T$ diagram

$$P_{\text{ideal gas}} \propto \rho\, T / \mu$$

$$P^{NR}_{e,deg} = 1.00 \times 10^{13} \left(\frac{\rho}{\mu_e}\right)^{5/3} \ [\text{cgs}]$$

$$P^{ER}_{e,deg} = 1.24 \times 10^{15} \left(\frac{\rho}{\mu_e}\right)^{4/3} \ [\text{cgs}]$$

$$P_{\text{rad}} = \frac{1}{3}\, a\, T^4$$

Non-Relativistic, Non-Degenerate (i.e., ideal gas)

Non-Relativistic, Extremely Degenerate
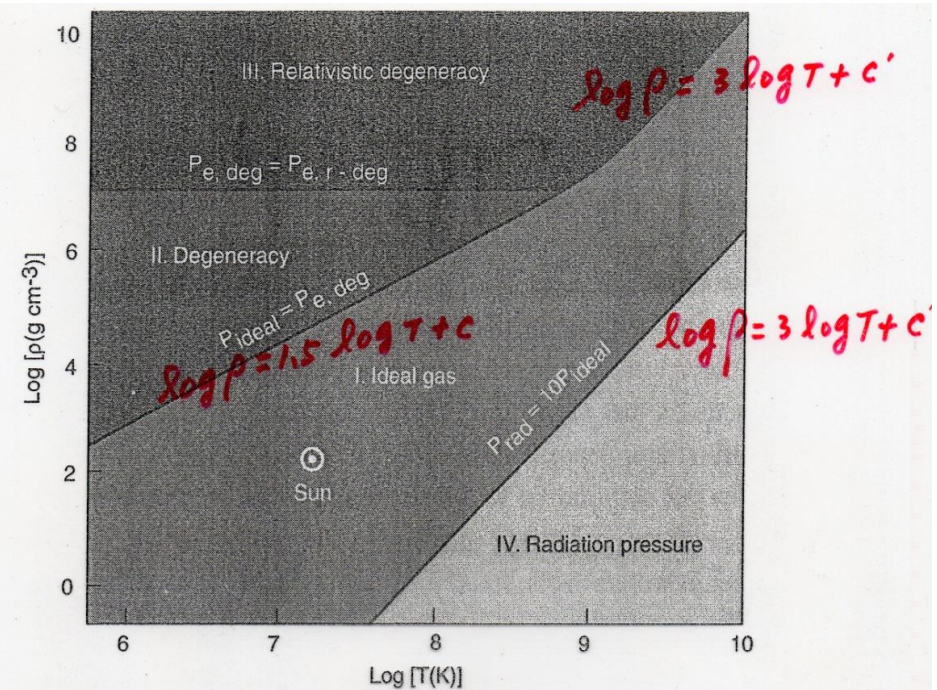
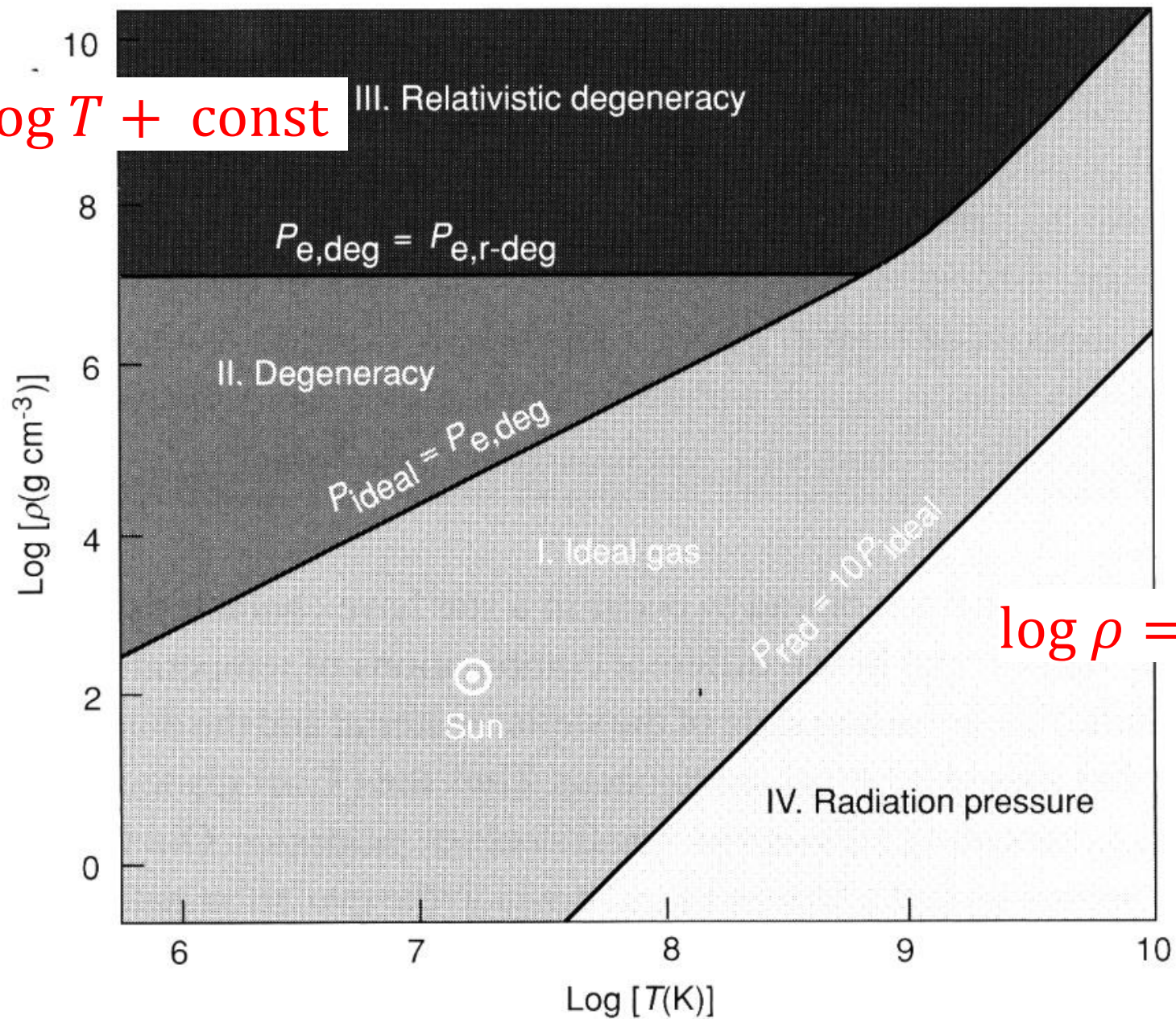Extremely Relativistic, Extremely Degenerate



Figure 7.1 Mapping of the temperature-density diagram according to the equation of state.

NR, ND   $P \sim \rho T$   $\left.\right\}$ $\log \rho = 1.5 \log T + \text{const.}$

NR, ED   $P \sim \rho^{5/3}$

ER, ED   $P \sim \rho^{4/3}$   $\left.\right\}$ $\log \rho = 3 \log T + \text{const}$
          $(\sim \rho T)$

$P_{rad}$ vs $P_{\text{ideal gas}}$   $P_{rad} \sim T^4$   $\left.\right\}$ $\log \rho = 3 \log T + \text{const}$
                    $P_{gas} \sim \rho T$

147

$\log \rho = 1.5 \log T + \text{const}$

$\log \rho = 3 \log T + \text{const}$

III. Relativistic degeneracy

$P_{e,deg} = P_{e,r\text{-}deg}$

II. Degeneracy

$P_{ideal} = P_{e,deg}$

I. Ideal gas

$P_{rad} = 10 P_{ideal}$

Sun

IV. Radiation pressure

$\log [\rho (\text{g cm}^{-3})]$

$\log [T(\text{K})]$

148
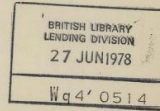
To recall Kelvin's classic phrase, there are two clouds obscuring the theory of the structure and mechanism of the stars. One is the persistent discrepancy in absolute amount between the astronomical opacity and the results of calculations based either on theoretical or experimental physics. The other is the failure of our efforts to reduce the behaviour of subatomic energy to anything approaching a consistent scheme. Whether these clouds will be dissipated without a fundamental revision of some of the beliefs and conclusions which we have here regarded as securely established, cannot be foreseen. The history of scientific progress teaches us to keep an open mind. I do not think we need feel greatly concerned as to whether these rude attempts to explore the interior of a star have brought us to anything like the final truth. We have learned something of the varied interests involved. We have seen how closely the manifestations of the greatest bodies in the universe are linked to those of the smallest. The partial results already obtained encourage us to think that we are not far from the right track. Especially do we realise that the transcendently high temperature in the interior of a star is not an obstacle to investigation but rather tends to smooth away difficulties. At terrestrial temperatures matter has complex properties which are likely to prove most difficult to unravel; but it is reasonable to hope that in a not too distant future we shall be competent to understand so simple a thing as a star.